

SHELL EFFECTS IN THE NUCLEAR  
DEFORMATION ENERGY

SHELL EFFECTS IN THE NUCLEAR  
DEFORMATION ENERGY

by

CARL K. ROSS, B.Sc., M.Sc.

A Thesis

Submitted to the Faculty of Graduate Studies  
in Partial Fulfilment of the Requirements  
for the Degree  
Doctor of Philosophy

McMaster University

July 1973

© Carl K. Ross 1974

DOCTOR OF PHILISOPHY (1973)  
(Physics)

McMASTER UNIVERSITY  
Hamilton, Ontario.

TITLE : Shell Effects in the Nuclear Deformation Energy

Author : Carl K. Ross, B.Sc., M.Sc.

SUPERVISOR : Dr. R. K. Bhaduri

NUMBER OF PAGES : vii, 117

SCOPE AND CONTENTS :

Although the Strutinsky method has been widely used in calculating the nuclear deformation energy, it contains various ambiguities which may affect the accuracy and reliability of the calculations. In particular, the smoothing procedure for extracting the smooth density of states used in calculating the shell correction to the deformation energy has no firm theoretical basis. As a means of testing this smoothing procedure, an alternative method for obtaining that part of the exact density of states which depends only on the overall features of the distribution of single-particle states is proposed. This approach utilizes a high temperature expansion of the exact single-particle partition function, and it is used to calculate the shell correction for three different spectra for which the partition function is known analytically at high temperatures. The shell corrections calculated by the partition function method are compared with the corresponding results from the Strutinsky method, and they are found

to be in reasonable agreement.

When the Strutinsky method is applied to potential wells of finite depth, the shell correction is found to be highly dependent on the parameters in the smoothing procedure. Lin suggested that this ambiguity might be removed by including the effects of the continuum resonances, but his calculations indicated that they are of little importance. The possible effects of the continuum on the smooth density of states are re-examined, and it is pointed out that resonances much higher in the continuum than those considered by Lin can influence the shell correction. When Lin's calculation is repeated including these higher resonances, a reasonably unique shell correction is obtained.

A third ambiguity in the Strutinsky method has been pointed out by Kelson and Shoshani, who suggest that it violates the conservation of angular momentum. They estimate that if the effects of angular momentum conservation are explicitly included, the fission barriers of superheavy nuclei may be lowered by as much as 2.5 MeV over existing calculations. An examination of the basis of the Strutinsky method shows however, that the correction as suggested by Kelson and Shoshani is inappropriate, and that for all practical purposes angular momentum conservation is properly included in the Strutinsky method.

The final chapter discusses the possible effects of shell structure in the deformation energy on the rotational

bands of deformed nuclei. A two-particle rotor is taken to be a rough approximation to a deformed rotating nucleus, and for an appropriate two-body potential the rotor is shown to display backbending behaviour similar to that observed for rare-earth nuclei. This indicates that centrifugal stretching may be an important mechanism in giving rise to backbending, and the possible effects of stretching in more realistic calculations is discussed.

## ACKNOWLEDGEMENTS

I wish to acknowledge the assistance of the following individuals and organizations who have contributed either directly or indirectly to the completion of this work:

My supervisor, Dr. R. K. Bhaduri, who was responsible for the overall direction of my studies as a graduate student, and who originated, and contributed directly to the work discussed in Chapters II and III;

Dr. C. S. Warke, with whom I collaborated during the summer of 1972. The work of Chapter IV was done during this time, and Dr. Warke's help with not only the basic ideas but also the technical details led to its rapid conclusion;

Dr. Y. Nogami, who suggested the problem discussed in Chapter V, and who helped with many of the numerical calculations;

My colleagues with whom I shared an office during the past four years. They have included Ernie MacFarlane, Keith Lassey, Pierre Grangé, Paul Curry and Byron Jennings, and have at various times both helped and hindered the work discussed in the following chapters;

Mrs. Hazel Coxall, who carefully and efficiently typed the original manuscript;

The National Research Council, and indirectly the Canadian taxpayers, who financed my four years as a graduate student at McMaster.

TABLE OF CONTENTS

	PAGE
CHAPTER I. INTRODUCTION	1
I.1 Review of Previous Work	1
I.2 Summary of Present Work	5
CHAPTER II PARTITION FUNCTION APPROACH TO SHELL CORRECTIONS	9
II.1 Outline of the Strutinsky Smoothing Procedure	9
II.2 Partition Function Method and Results	17
CHAPTER III CONTINUUM EFFECTS IN STRUTINSKY CALCULATIONS	33
III.1 Strutinsky Procedure for Finite Potentials	33
III.2 The Effect of Resonances in the Strutinsky Procedure	41
III.3 Other Modifications of the Strutinsky Procedure	50
CHAPTER IV ANGULAR MOMENTUM CONSERVATION IN THE STRUTINSKY METHOD	53
IV.1 Review of the Work of Kelson and Shoshani	53
IV.2 Re-examination of the Strutinsky Method	57

TABLE OF CONTENTS -- continued

	PAGE
CHAPTER IV. IV.3 Calculation of the Projection Correction	62
CHAPTER V. EFFECTS OF CENTRIFUGAL STRETCHING ON ROTATIONAL BANDS	72
V.1 Review of the Backbending Phenomenon	72
V.2 Backbending in a Simple Stretching Model	79
V.3 Possible Effects of More Compli- cated Stretching	93
APPENDIX A ELECTROMAGNETIC RADIATION IN A SMALL CUBIC CAVITY	100
APPENDIX B CONTINUUM CONTRIBUTIONS IN THE STRUTINSKY PROCEDURE	105
APPENDIX C THE NILSSON MODEL POTENTIAL	107
APPENDIX D DETAILS OF THE PAIRING CALCULATION	110
REFERENCES	112



## CHAPTER I

### INTRODUCTION

#### I.1 Review of Previous Work.

Because the atomic nucleus is a many-body system in which the constituent protons and neutrons are strongly interacting, calculations of nuclear structure based on first principles are very difficult. As a result, much of the present understanding of nuclear structure has come through the use of models of the nucleus, each of which contains some of the main features of the more complicated system. For example, the liquid drop model (LDM) assumes that the nucleus may behave to some extent like a charged liquid drop, and on this basis an expression for the nuclear binding energy as a function of mass number  $A$ , atomic number  $Z$ , and the nuclear shape may be derived (von Weizsacker 1935, Bethe 1936, Myers and Swiatecki 1966). The resulting expression gives a reasonably good fit to the experimental binding energies throughout the periodic table, and the LDM provides a natural explanation (Bohr and Wheeler 1939, Hill and Wheeler 1953) for the phenomenon of fission in which a heavy nucleus splits into two or more lighter fragments. On the other hand there remain small but systematic deviations in the fit to the binding energies which cannot be explained by the LDM, and calculations show that the LDM is not capable of

explaining the asymmetric mass distribution of the fission fragments. Both these discrepancies indicate that there are important aspects of nuclear structure which cannot be incorporated into the simple liquid drop model but which depend on the detailed motion of individual nucleons in the nucleus.

Another model which has had considerable success in correlating nuclear properties is one in which the individual nucleons are assumed to be moving independently of one another in some one-body potential well, similar to the motion of the atomic electrons in the Coulomb potential of the nucleus. This shell model, as it is called, has been used to predict the ground state spins of odd- $A$  nuclei, and to calculate the ground state deformations of deformed nuclei (Mottelson and Nilsson 1959). However, this model cannot give realistic estimates of the nuclear binding energy, and it has been found to be inadequate when used to calculate the change in the total energy with deformation (deformation energy) particularly at the large deformations encountered in the fission process (Nilsson et al. 1969). Even though the absolute value of the binding energy as calculated in the shell model is incorrect, the systematic deviations of the corresponding LDM expression from the measured values are closely related to closed shell configurations in the shell model. This suggests that it may be possible to combine the two models with the LDM giving the general behaviour of the binding energy as a function of  $A$ ,  $Z$  and shape, while the shell model is used to calculate the

deviations from the LDM result.

The first major attempt at calculating the effects of shell structure on the LDM was by Myers and Swiatecki (1966). By considering the effects of the grouping of single-particle states in a degenerate Fermi gas, they obtained a semi-empirical expression for the shell correction containing three arbitrary parameters which could be determined by fitting the experimental data. The resulting expression for the binding energy proved to be a considerable improvement over the corresponding expression for the LDM, and in particular it was able to reproduce the increased binding observed for closed shell nuclei as well as predicting finite deformations for nuclei away from closed shells. The most serious weakness of this approach is related to the deformation dependence of the shell correction, for Myers and Swiatecki assumed that for large deformations the distribution of single-particle states would become uniform, and shell effects disappear. As a result, their expression for the binding energy contained an arbitrary damping factor to guarantee that for large deformations the shell correction would go to zero, although it was soon recognized that grouping of the single particle states may persist even for very large deformations (Strutinsky 1967, 1968). Myers and Swiatecki (1967) later generalized the deformation dependence of their shell correction to take account of this fact, but their method of calculating the shell correction has largely been replaced by a method proposed by Strutinsky

(1967, 1968).

The main advantage of the Strutinsky method over that of Myers and Swiatecki is that the shell correction can be obtained for any single particle spectrum, and no assumptions need to be made as to the deformation dependence of the shell correction. As in the Myers and Swiatecki method, the shell correction is given by the difference between a sum over the energies of the occupied single-particle states, and a corresponding sum for a smooth distribution of single-particle states in energy space. This smooth distribution is calculated according to a prescription given by Strutinsky, and as will be discussed later, this prescription is somewhat arbitrary in that it depends on two nonphysical smoothing parameters. However, these are reasonably well determined, at least for the case of infinite potential wells.

When the Strutinsky method was applied to the calculation of fission barriers of heavy nuclei (Nilsson et al. 1969, Bolsterli et al. 1972, Brack et al. 1972) it was found to provide a basis for explaining diverse phenomena associated with the fission process, including the existence of short-lived fission isomers (Bjornholm and Strutinsky 1969, Clark 1971). Moller (1970) and Gotz et al. (1972) have also used it to calculate the ground state deformations of rare earth nuclei, and they find that the predicted deformations are in close agreement with the values obtained experimentally.

On the other hand, various ambiguities and

uncertainties regarding the Strutinsky method have recently been pointed out, and the accuracy and reliability of the method has not yet been firmly established. Lin (1970) has noted that when the Strutinsky smoothing procedure is applied to the single-particle spectrum resulting from a finite one-body potential the (resulting shell correction is very sensitive to the two smoothing parameters mentioned earlier. Sheline et al. (1972) found that for nuclei in the zirconium region, the deformation energy calculated by the Strutinsky method does not have the properties expected from the observed energy levels and transition probabilities, and they speculate that the discrepancies may be due to inadequacies in either the Strutinsky method or the liquid drop formula. Finally, Bassichis et al. (1973) have done a model calculation using the constrained Hartree-Fock method to calculate the shell correction as a function of deformation, and they find that the corresponding results obtained from the Strutinsky method disagree by 25% on the average.

## I.2 Summary of Present Work.

One of the more serious weaknesses of the Strutinsky method is the empirical smoothing procedure used to extract a uniform density of states from a discrete spectrum. Because the shell correction depends sensitively on this uniform density of states, it is desirable to have a smoothing procedure

for which the accuracy and range of validity is reasonably well understood, and which can be used as a check on the Strutinsky prescription. The second chapter discusses the statistical mechanics of a single particle in an infinite potential well, and shows how a density of states which depends only on the gross features of the energy distribution of single-particle states can be obtained by making a semiclassical expansion of the exact single-particle partition function. Because this approach requires that the partition function be known analytically for high temperatures, it can only be applied in a few special cases. However, the shell correction obtained for these cases using this partition function approach is found to agree very well with the corresponding results from the Strutinsky method.

The third chapter discusses the calculation of shell corrections for finite potential wells using the Strutinsky method. The work of Lin (1970) is reviewed, and his method of including the effect of the continuum in the Strutinsky smoothing procedure is outlined. It is shown that if this method is to be successful, resonances which lie very high in the continuum must be included, and Lin's calculations are repeated, showing that even for a finite potential well it is possible to obtain a value for the shell correction which is independent of the Strutinsky smoothing parameters. The inclusion of the continuum effects make the shell correction calculations impractically lengthy, and various

other techniques which have recently been used for calculating the shell correction for finite potential wells are discussed.

The basis of the Strutinsky method is the Hartree-Fock approximation, but the Hartree-Fock ground state for a deformed even-even nucleus does not correspond to a state of good angular momentum. The effect on the deformation energy of projecting a state of zero angular momentum from the Hartree-Fock ground state has recently been considered by Kelson and Shoshani (1972). They conclude that the effects of angular momentum conservation on the fission barriers of actinide nuclei are negligible, but that the fission barriers of superheavy nuclei may be lowered by as much as 2.5 MeV. It is shown in the fourth chapter that within the context of the Strutinsky method, the calculation reported by Kelson and Shoshani is incorrect, and that when done properly, the effects of angular momentum conservation on the deformation energy are negligible for all nuclei.

The fifth chapter discusses the role of the deformation energy in giving rise to the recently observed "backbending" behavior in rare-earth nuclei (Johnson et al. 1972). A two-particle rotor is taken as a rough approximation to a deformed rotating nucleus, and the energy levels of this system are obtained for various forms of the two-body potential. A potential with two minima is shown to give the backbending behavior characteristic of nuclei in the

rare-earth region, and this indicates that centrifugal stretching may be an important mechanism contributing to the observed backbending. The deformation energy surfaces of rare-earth nuclei are examined to determine what the nature of this stretching may be, and a prolate-to-oblate shape transition is suggested as one possibility.



## CHAPTER II

### PARTITION FUNCTION APPROACH TO SHELL CORRECTIONS

#### II.1 Outline of the Strutinsky Smoothing Procedure.

The nuclear deformation energy for a nuclide specified by atomic number  $Z$  and neutron number  $N$  is defined as the change in the total energy as a function of the nuclear shape, and in principle it can be calculated once the two-body nucleon-nucleon interaction is specified. However, even in the Hartree-Fock approximation such calculations would be extremely difficult for heavy and superheavy nuclei, and more practical approaches for obtaining the deformation energy are required. The Strutinsky method as originally proposed (Strutinsky 1967, 1968) was based on the Hartree-Fock approximation, and the total energy  $E(N, Z, \alpha)$  written as

$$E(N, Z, \alpha) = E_{\text{HF}}(N, Z, \alpha), \quad (1)$$

where  $\alpha$  is some set of parameters specifying the nuclear deformation. If  $\bar{E}_{\text{HF}}(N, Z, \alpha)$  denotes that part of the Hartree-Fock energy which is a smoothly varying function of  $N$ ,  $Z$  and  $\alpha$ , then eq. (1) can be rewritten as

$$E = \bar{E}_{\text{HF}} + (E_{\text{HF}} - \bar{E}_{\text{HF}}), \quad (2)$$

where each term is a function of  $N$ ,  $Z$  and  $\alpha$ . The advantage of this approach is that  $(E_{\text{HF}} - \bar{E}_{\text{HF}})$  can be written approximately as (Strutinsky 1968)

$$E_{\text{HF}} - \bar{E}_{\text{HF}} = E_{\text{sp}}^{n,p} - \bar{E}_{\text{sp}}^{n,p}, \quad (3)$$

where

$$E_{\text{sp}}^{n,p} = \sum_{i(n)} \epsilon_i + \sum_{i(p)} \epsilon_i, \quad (4)$$

and  $\bar{E}_{\text{sp}}^{n,p}$  is the smoothly varying part of  $E_{\text{sp}}^{n,p}$ . The single-particle energies in eq. (4) are to be taken from some realistic one-body potential such as the Nilsson model, and the sums are over all occupied neutron (n) or proton (p) single-particle energies. In order to further simplify eq. (2), Strutinsky assumed that the smoothly varying part of the Hartree-Fock energy is approximately equal to the semi-empirical liquid drop energy so that

$$E_{\text{LD}} = \bar{E}_{\text{HF}}. \quad (5)$$

Combining eqs. (2), (3) and (5) gives

$$E = E_{\text{LD}} + \delta E^{n,p}, \quad (6)$$

where the shell correction  $\delta E^{n,p}$  is given by

$$\delta E^{n,p} = E_{\text{sp}}^{n,p} - \bar{E}_{\text{sp}}^{n,p}. \quad (7)$$

The accuracy of eq. (5) will be discussed in Chapter IV, but the present chapter is concerned with the calculation of  $\bar{E}_{\text{sp}}^{n,p}$ , both by the Strutinsky smoothing procedure, and by an alternative method derived from statistical mechanics. Eq. (4) shows that  $E_{\text{sp}}^{n,p}$  can be split into two terms as

$$E_{\text{sp}}^{n,p} = E_{\text{sp}}^n + E_{\text{sp}}^p, \quad (8)$$

where the first term involves a sum only over neutron states, and the second only over proton states. Since  $E_{sp}^n$  and  $E_{sp}^p$  have the same form, the smoothing procedure will be identical for both, and so the following discussion will consider only the neutrons explicitly. For simplicity the superscript  $n$  will also be dropped.

The calculation of  $\bar{E}_{sp}$  might at first sight be thought to involve the averaging of  $E_{sp}$  over a wide range of values of  $N$ ,  $Z$  and  $a$ . However, the reason for the structure in  $E_{sp}$  is that the single-particle states of a one-body potential are not uniformly distributed as a function of energy, but tend to be grouped together into shells. For example, fig. 1 shows the shell structure for the spherical harmonic oscillator potential, for which each shell contains  $(n+1)(n+2)$  single-particle states, where  $n$  is the principal quantum number, and there are no states between shells. By recognizing the relation between variations in  $E_{sp}$  and the presence of shells in the single-particle spectrum, Strutinsky was able to formulate a method for calculating  $\bar{E}_{sp}$  for a given  $N$ ,  $Z$  and  $a$ , thus greatly simplifying the shell correction calculations.

The basis of the Strutinsky procedure for calculating  $\bar{E}_{sp}$  is a smooth density of states  $\bar{g}(e)$ , the properties of which may be obtained by first considering the exact density of states  $g(e)$  given by

$$g(e) = \sum_i \delta(e - \epsilon_i) \quad (9)$$

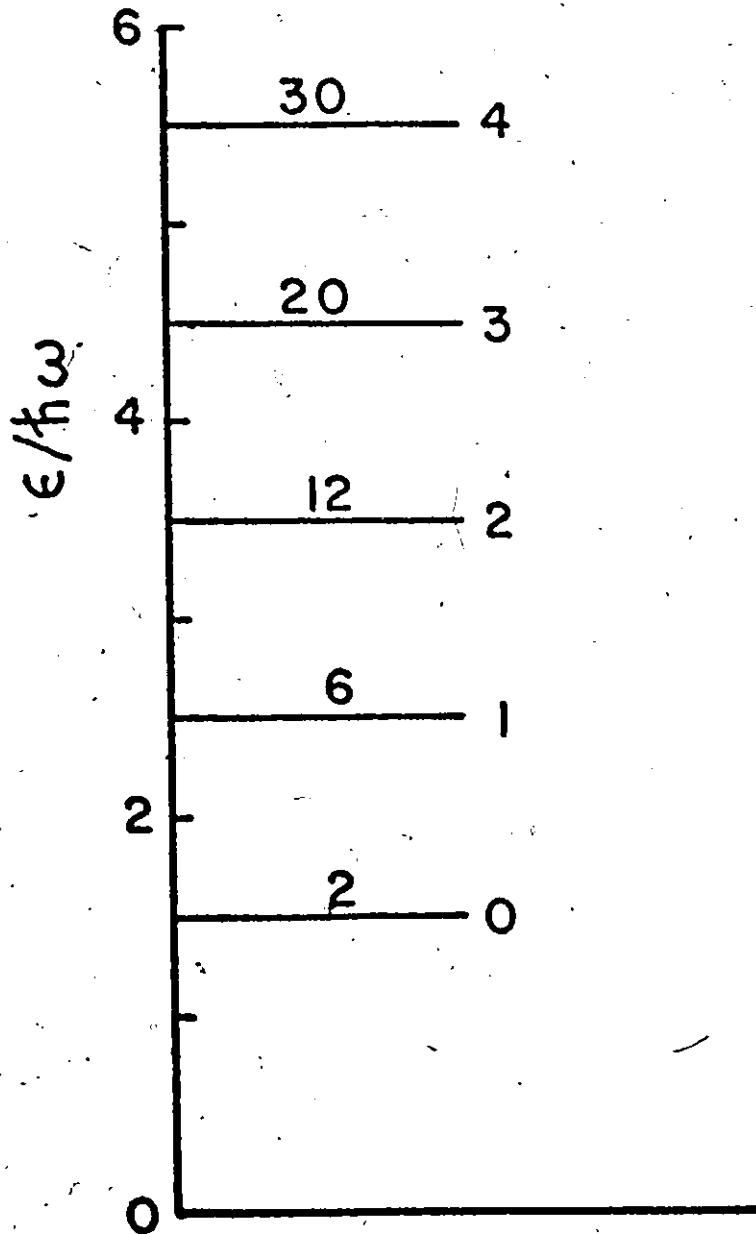


Fig. 1 The first few energy levels of the spherical harmonic oscillator potential. The number to the right of each level is the principal quantum number  $n$ , while the degeneracy  $(n+1)(n+2)$  is shown above each level.

where the sum is over all single-particle states. The number of states in an energy interval of width  $2\Delta$  about energy  $\epsilon$  is given by

$$n(\epsilon) = \int_{\epsilon-\Delta}^{\epsilon+\Delta} g(\epsilon') d\epsilon' \quad , \quad (10)$$

and if  $\Delta$  is taken to be much smaller than the major shell spacing, it is clear that  $n(\epsilon)$  will be a rapidly varying function of  $\epsilon$ . The basic property of  $\bar{g}(\epsilon)$  is that it should be such that the long-range variations in  $n(\epsilon)$  are preserved, but the short-range fluctuations due to shell structure are smoothed out. This criterion does not in itself specify how  $\bar{g}(\epsilon)$  is to be calculated, and the prescription proposed by Strutinsky utilizes the identity

$$\delta(x) = \lim_{\gamma \rightarrow 0} \frac{1}{\gamma\sqrt{\pi}} \exp(-x^2/\gamma^2) \quad , \quad (11)$$

to rewrite  $g(\epsilon)$  as a sum of Gaussians. It is then argued that for finite  $\gamma$ , the resulting expression will give a smooth density of states, and so  $\bar{g}(\epsilon)$  is to a first approximation

$$\bar{g}(\epsilon) = \frac{1}{\gamma\sqrt{\pi}} \sum_i \exp(-(\epsilon - \epsilon_i)^2/\gamma^2) \quad . \quad (12)$$

Then in terms of  $\bar{g}(\epsilon)$ ,

$$\bar{E}_{sp} = \int_{-\infty}^{\infty} \epsilon \bar{g}(\epsilon) d\epsilon \quad , \quad (13)$$

and

$$N = \int_{-\infty}^{\bar{\lambda}} \bar{g}(\epsilon) d\epsilon, \quad (14)$$

where  $\bar{\lambda}$  is the Fermi energy corresponding to the last filled level in the smooth distribution of states.

Unfortunately, the shell correction obtained using eq. (12) is found to depend sensitively on the value of  $\gamma$ , and this is not satisfactory, since except for the requirement that  $\gamma$  be of the order of the major shell spacing, it is arbitrary. Strutinsky argued that the reason for this  $\gamma$ -dependence can be related to the fact that eq. (12) is not consistent in the sense that

$$\bar{g}(\epsilon) \neq \frac{1}{\gamma\sqrt{\pi}} \int_{-\infty}^{\infty} \bar{g}(\epsilon') \exp(-(\epsilon-\epsilon')^2/\gamma^2) d\epsilon', \quad (15)$$

unless  $\bar{g}(\epsilon)$  is a constant, or proportional to  $\epsilon'$ . In order to correct this deficiency, a curvature function was introduced (Strutinsky 1967, 1968; Nilsson et al. 1969) such that eq. (12) would be consistent if  $\bar{g}(\epsilon)$  could be expressed as a polynomial of order  $(2k+1)$  or less. The resulting expression for  $\bar{g}(\epsilon)$  is

$$\bar{g}(\epsilon) = \frac{1}{\gamma\sqrt{\pi}} \sum_{l=0}^{2k} \exp(-u_1^2) f_{2k}(u_1), \quad (16)$$

where  $u_i = (\epsilon - \epsilon_i)/\gamma$ , and  $f_{2k}(u_i)$  is the curvature function of order  $K \equiv 2k$ . In terms of Hermite polynomials,  $f_{2k}(u_i)$  may be written as

$$f_{2k}(u_i) = \sum_{\ell=0}^{2k} c_{\ell} H_{\ell}(u_i) \quad (17)$$

where

$$c_{\ell} = \begin{cases} \frac{(-1)^{\ell/2}}{2^{\ell} (\ell/2)!} & \ell \text{ even} \\ 0 & \ell \text{ odd} \end{cases} \quad (18)$$

and this is equivalent to

$$f_{2k}(u_i) = L_k^{1/2}(u_i^2) \quad (19)$$

where  $L_k^{1/2}$  is an associated Laguerre polynomial. When  $\delta E$  is now calculated using eq. (16), it is found to be independent of  $\gamma$  and  $K$  over a considerable range, and so a unique value for the shell correction can be obtained. In order to illustrate the  $\gamma$  and  $K$  dependence of  $\delta E$ , it was calculated for various values of  $\gamma$  and  $K$  for 70 neutrons in the harmonic oscillator spectrum of fig. 1, and the results are shown in fig. 2. The importance of the curvature correction in reducing

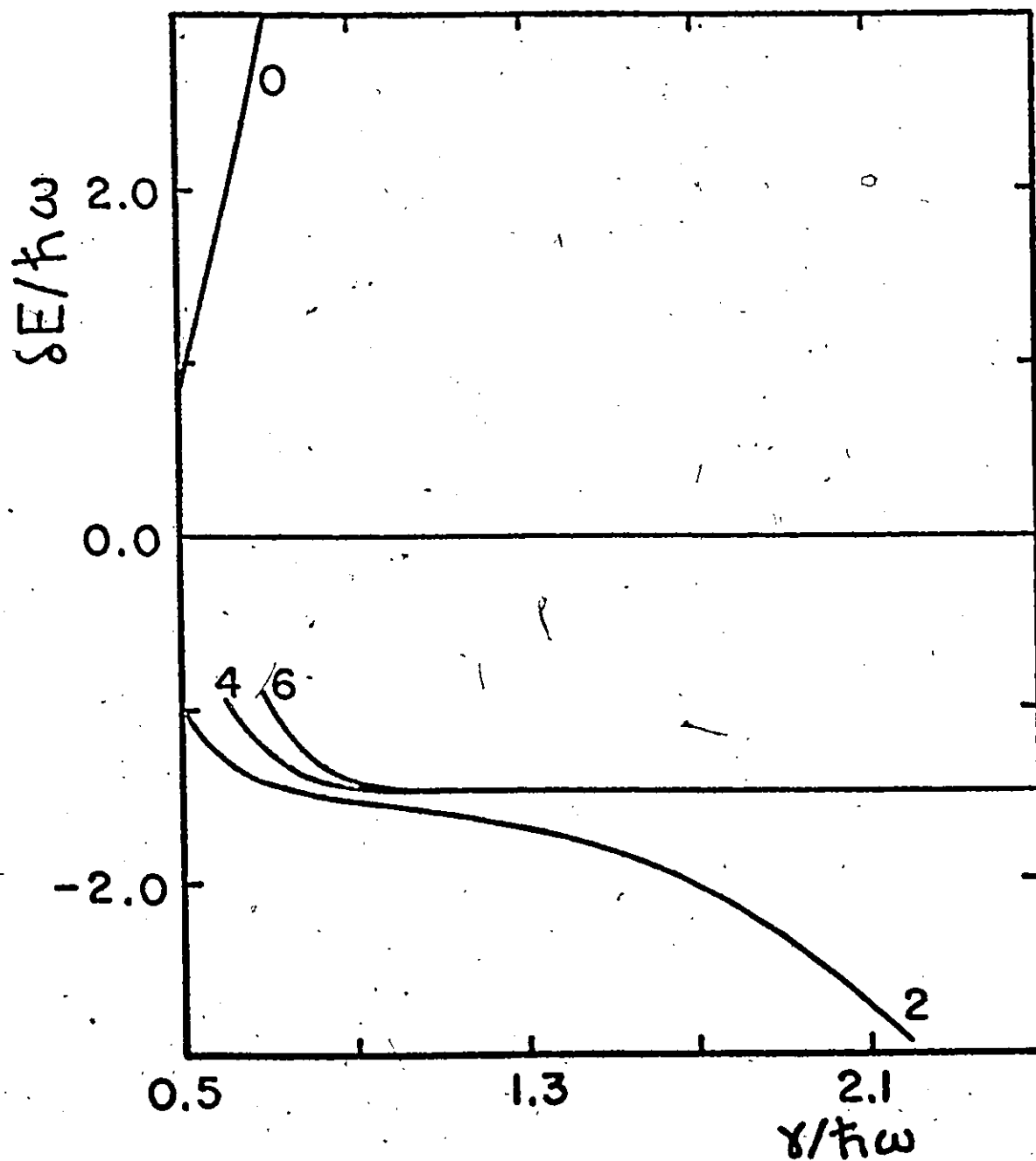


Fig. 2 Strutinsky shell correction for 70 particles in the spherical harmonic oscillator potential. The shell correction is shown as a function of the smoothing width  $\gamma$  for curvature orders from 0 to 6.



the  $\gamma$  dependence of  $\delta E$  is clear from this figure, and for  $K \geq 4$  the shell correction is virtually independent of  $\gamma$  for  $\gamma > 1 \hbar\omega$  where  $\omega$  is the oscillator frequency.

Although the Strutinsky smoothing procedure has been widely used for calculating shell corrections, it is nevertheless an empirical approach in which eq. (16) gives one possible prescription for calculating  $\bar{g}(\epsilon)$ . Since the shell correction is typically only about 0.5% of the total energy, it is very sensitive to  $\bar{g}(\epsilon)$ , and even the small contributions to  $\bar{g}(\epsilon)$  from energies below the bottom of the potential well have important effects on  $\delta E$ . In order to obtain an independent check on the Strutinsky procedure, an alternative method for removing the effects of shell structure in the density of states was formulated, and is described in the next section.

## II.2 Partition Function Method and Results.

The single-particle partition function for a particle in a one-body potential with eigenvalues  $\epsilon_i$  is given by

$$Z(\beta) = \sum_i e^{-\beta \epsilon_i}, \quad (20)$$

where  $\beta = 1/kT$ ,  $T$  is the absolute temperature and the sum is over all single-particle states. Using eq. (9) for  $g(\epsilon)$ ,  $Z(\beta)$  may be rewritten as

$$Z(\beta) = \frac{1}{\beta} \left\{ \beta \int_{-\infty}^{\infty} g(\epsilon) e^{-\beta \epsilon} d\epsilon \right\}, \quad (21)$$

where the quantity in brackets is the two-sided Laplace transform (van der Pol and Bremmer 1955, p.18) of the exact density of states. Eq. (21) shows that  $g(\epsilon)$  may be obtained by taking the Laplace inverse of  $\beta Z(\beta)$ , and this suggests that by making an appropriate expansion of  $Z(\beta)$ , a similar equation might be used to obtain a density of states which depends only on the gross features of the distribution of single-particle energies.

In the sum over single-particle energies given by eq. (20), the contributions of the various terms decrease as  $\epsilon_i$  increases, and the contribution of any two adjacent terms can be written as

$$e^{-\beta \epsilon_i} [1 + e^{-\beta d}]$$

where  $d = \epsilon_{i+1} - \epsilon_i$ . The relative importance of these two terms is a function of the product  $\beta d$ , and in the limit of  $\beta d \rightarrow \infty$  the contribution of the term in  $\epsilon_{i+1}$  is negligible, while in the other extreme of  $\beta d = 0$ , both terms contribute equally. The level spacing  $d$  can vary from zero up to the maximum possible shell spacing  $d_m$ , and so for fixed  $\beta$ , the contribution of the term in  $\epsilon_{i+1}$  depends on the energy difference between  $\epsilon_i$  and  $\epsilon_{i+1}$ . However, for  $kT \gg d_m$ ,  $\beta d \approx 0$  for all values of  $d$  and this indicates that for small  $\beta$ ,  $Z(\beta)$  will be rather insensitive to variations in the spacing of adjacent energy levels. Then by taking the

exact partition function and expanding it about  $\beta = 0$ , it should be possible to extract those terms which are independent of the detailed shell structure in the energy level spectrum, and define a corresponding density of states as

$$Z_{sc}(\beta) = \frac{1}{\beta} \left\{ \beta \int_{-\infty}^{\infty} g_{sc}(\epsilon) e^{-\beta \epsilon} d\epsilon \right\} . \quad (22)$$

The subscript sc in eq. (22) is used to indicate that the small  $\beta$  expansion of the exact partition function gives a semiclassical approximation to  $Z(\beta)$ , in which the leading term is the classical result (Huang 1963, p.213).

Before eq. (22) can be used to calculate  $g_{sc}(\epsilon)$ , some criterion must be established for determining the number of terms to be included in the semiclassical expansion of  $Z(\beta)$ . At first sight, it might be thought that all terms in  $Z_{sc}(\beta)$  which give rise to smooth, non-singular contributions in  $g_{sc}(\epsilon)$  should be included, but certain delta function terms, although singular in nature, have been found to make important contributions to the shell correction. Perhaps the most serious weakness of the partition function approach is that no simple method which is applicable to all single-particle spectra, has been found for truncating the high temperature expansion of  $Z(\beta)$ , and each spectrum must be considered separately.

Some of the difficulties which arise are illustrated by considering the spectrum of the one-dimensional harmonic

oscillator in which each level can accommodate only one particle. The energy levels are given by

$$\epsilon_n = (n+0.5)\hbar\omega \quad , \quad (23)$$

where  $\omega$  is the oscillator frequency, and so the exact partition function is

$$Z(\beta) = \sum_{n=0}^{\infty} \exp(-\beta(n+0.5)\hbar\omega) = \frac{1}{2} \operatorname{csch}(\beta\hbar\omega/2) \quad . \quad (24)$$

Expanding  $Z(\beta)$  about  $\beta=0$  gives (Abramowitz and Stegun 1965, p.85)

$$Z_{SC}(\beta) = \frac{1}{\beta(\hbar\omega)} - \frac{1}{24} \beta(\hbar\omega) + \frac{7}{5760} \beta^3(\hbar\omega)^3 + \dots \quad , \quad (25)$$

from which  $g_{SC}(\epsilon)$  is found to be (van der Pol and Bremmer 1955, p.383)

$$g_{SC}(\epsilon) = \frac{\theta(\epsilon)}{(\hbar\omega)} - \frac{\delta'(\epsilon)}{24}(\hbar\omega) + \frac{7}{5760} \delta^{(3)}(\epsilon)(\hbar\omega)^3 + \dots \quad . \quad (26)$$

In eq. (26) the step function  $\theta(\epsilon)$  is defined such that  $\theta(\epsilon)=1$  for  $\epsilon > 0$ , while  $\theta(\epsilon) = 0$  for  $\epsilon < 0$ , and  $\delta^{(n)}(\epsilon)$  denotes the  $n^{\text{th}}$  derivative of the delta function. Using the relation

$$\int_{-\infty}^{\infty} f(\epsilon) \delta^{(n)}(\epsilon) d\epsilon = (-1)^n f^{(n)}(0) \quad , \quad (27)$$

for any function  $f(\epsilon)$ , it is clear that any terms in  $g_{SC}(\epsilon)$

involving second or higher order derivatives of the delta function make no contribution to either eq. (13) or (14) and so no contribution to  $\delta E$ . However, the term involving  $\delta'(\epsilon)$  can make a contribution to the shell correction, and if it is included,  $\bar{\lambda}$  and  $\bar{E}_{sp}$  are given by

$$N = \bar{\lambda}/(\hbar\omega) ,$$

and

$$\bar{E}_{sp} = \left[ \frac{1}{2} \left( \frac{\bar{\lambda}}{\hbar\omega} \right)^2 + \frac{1}{24} \right] (\hbar\omega) = \left[ \frac{N^2}{2} + \frac{1}{24} \right] (\hbar\omega) . \quad (28)$$

The exact energy is

$$E_{sp} = \sum_{n=0}^{N-1} (n+0.5)\hbar\omega = \frac{N^2}{2}(\hbar\omega) . \quad (29)$$

and so the shell correction is given by

$$\delta E = -(\hbar\omega)/24 . \quad (30)$$

On the other hand, if the  $\delta'(\epsilon)$  term in  $g_{sc}(\epsilon)$  is dropped, the shell correction is found to be exactly zero, and since  $E_{sp}$  can be written as a smooth function of  $N$  [eq. (29)] it might be expected that this is the correct result. However, a Strutinsky calculation for the same spectrum shows that in this method the shell correction is equal to  $-(\hbar\omega)/24$  to at least four significant figures, and it is not clear whether this should be considered as a spurious contribution in the Strutinsky method, or as an indication that the  $\delta'(\epsilon)$  term should be included in eq. (26). In the following work, any terms involving delta functions or derivatives of delta

functions have been included in calculating the shell correction, and it is always found that their inclusion improves the agreement with the results from the Strutinsky procedure.

Three different single-particle spectra will now be discussed, and the shell correction calculated by the partition function method and compared with the corresponding results from the Strutinsky procedure. In two of the cases considered, higher order terms in the expansion of  $Z(\beta)$  give rise to derivatives of delta functions in  $g_{sc}(\epsilon)$  and the series can be truncated as for the one-dimensional oscillator. However, the cubic box spectrum presents special difficulties, and the number of terms to be included in  $Z_{sc}(\beta)$  has to be obtained by other considerations. Finally, Appendix A contains an application of the partition function method to black-body radiation in a small cubic cavity, and corrections to Planck's radiation law and the Stefan-Boltzmann law due to the finite size of the cavity are derived.

a) Infinite harmonic oscillator.

In this case, the single-particle spectrum is given by

$$\epsilon_n = (n+1.5)\hbar\omega, \quad (31)$$

where  $n(n=0,1,\dots)$  is the principal quantum number, and  $\omega$  the oscillator frequency. Each harmonic oscillator level can accommodate  $(n+1)(n+2)$  neutrons (or protons) and so

$$Z(\beta) = e^{-1.5\beta\hbar\omega} \sum_{n=0}^{\infty} (n+1)(n+2)e^{-\beta n \hbar\omega},$$

which can easily be summed to give

$$Z(\beta) = \frac{1}{4} \operatorname{csch}^3(\beta\hbar\omega/2) \quad (32)$$

The semiclassical approximation to  $Z(\beta)$  may be obtained by expanding eq. (32) about  $\beta=0$  (Abramowitz and Stegun 1965, p.85) with the result that

$$Z_{\text{sc}}(\beta) = \frac{2}{(\beta\hbar\omega)^3} - \frac{1}{4(\beta\hbar\omega)} + \frac{17}{960}(\beta\hbar\omega) + \dots \quad (33)$$

According to Eq. (22),  $g_{\text{sc}}(\epsilon)$  is given by the Laplace inverse of  $\beta Z_{\text{sc}}(\beta)$ , so that (van der Pol and Bremmer 1955, p.383)

$$g_{\text{sc}}(\epsilon) = \left[ \frac{\epsilon^2}{(\hbar\omega)^3} - \frac{1}{4(\hbar\omega)} \right] \theta(\epsilon) + \frac{17}{960}(\hbar\omega)\delta'(\epsilon) + \dots \quad (34)$$

The next term in  $g_{\text{sc}}(\epsilon)$  will be proportional to  $\delta^{(3)}(\epsilon)$ , and as pointed out earlier, it or higher order terms will not contribute to  $\delta E$ .

Fig. 3 compares the Strutinsky density of states calculated with  $\gamma = 1.2\hbar\omega$  and a sixth order curvature function with  $g_{\text{sc}}(\epsilon)$  as given by eq. (34) for  $\epsilon \leq 1.5\hbar\omega$ . For higher energies the two results are essentially identical, but in the vicinity of  $\epsilon=0$  they are quite different, and in particular the Strutinsky density of states is nonzero for  $\epsilon < 0$ , in contrast to the partition function result.

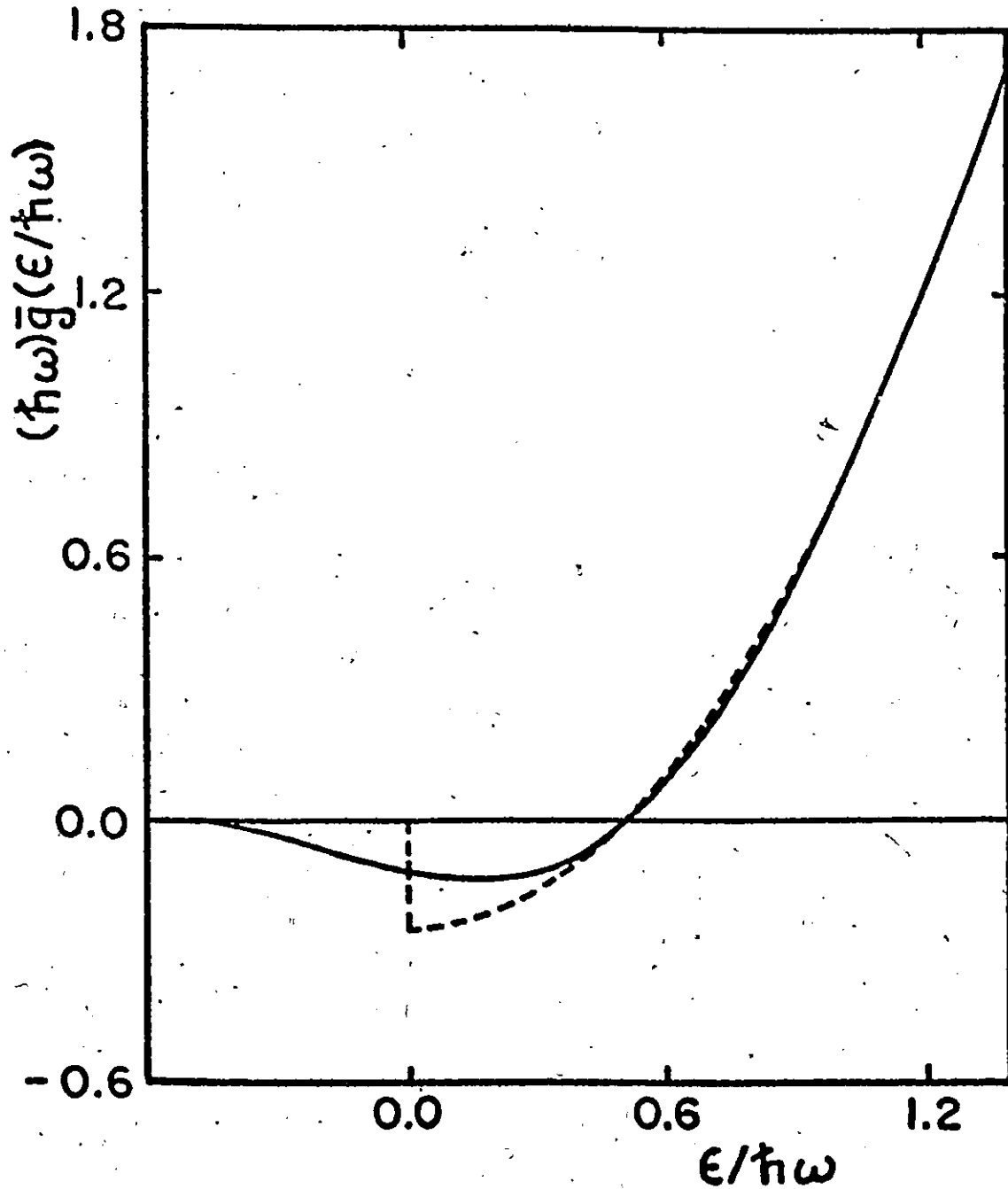


Fig. 3 Comparison of the density of states for the spherical harmonic oscillator potential calculated by the Strutinsky method (solid line) and the partition function method (dashed line). The Strutinsky calculation was performed with  $\gamma=1.2 \hbar\omega$  and a sixth order curvature correction.



Using  $g_{sc}(\epsilon)$  as given by eq. (34) in eqs. (13) and (14) the Fermi energy is found to be given by the solution of

$$\left(\frac{\bar{\lambda}}{\hbar\omega}\right)^3 - \frac{3}{4}\left(\frac{\bar{\lambda}}{\hbar\omega}\right) - 3N = 0 \quad (35)$$

where  $N$  is the particle number, and  $\bar{E}_{sp}$  is given by

$$\bar{E}_{sp} = \frac{1}{4} \left[ \left(\frac{\bar{\lambda}}{\hbar\omega}\right)^4 - \frac{1}{2}\left(\frac{\bar{\lambda}}{\hbar\omega}\right)^2 - \frac{17}{240} \right] (\hbar\omega) \quad (36)$$

The shell correction was calculated using eqs. (35) and (36) for a series of  $N$  values from 40 to 200, and the results are shown in fig. 4, where  $\hbar\omega$  has been taken to be  $\hbar\omega = 41/(2N)^{1/3}$ . A corresponding calculation of  $\delta E$  by the Strutinsky method gave results which for all practical purposes are identical to those shown in fig. 4, and agreement to about four significant figures was obtained throughout the range of  $N$  considered.

b) Cubic box.

In this case the energy levels are given by

$$\epsilon_{uvw} = \frac{\hbar^2 \pi^2}{2mL^2} (u^2 + v^2 + w^2) \quad (37)$$

where  $u$ ,  $v$  and  $w$  are integers running from one to infinity,  $L$  is the length of the box, and  $m$  the particle mass. The partition function becomes

$$Z(\beta) = 2 \left[ \sum_{n=1}^{\infty} \exp(-c\beta n^2) \right]^3 \quad (38)$$

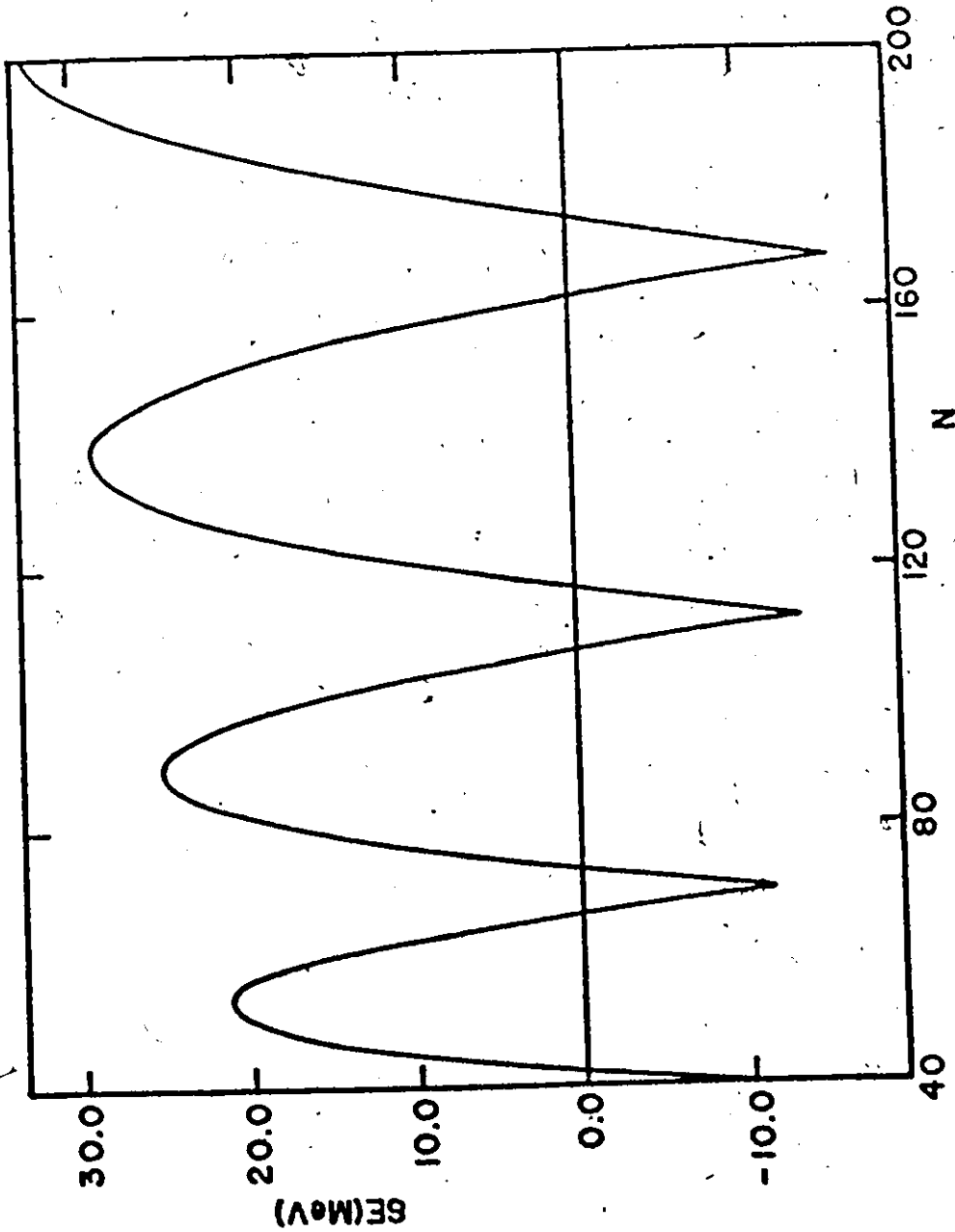


Fig. 4 Shell correction calculated by the partition function method for various numbers of particles in the spherical harmonic oscillator potential. Although  $\delta E$  is only defined for even integer values of  $N$ , the discrete points have been joined by a smooth curve. The corresponding results from the Strutinsky method are indistinguishable on this scale.

where the factor of 2 accounts for the two-fold degeneracy of each single-particle level, and  $c = \hbar^2 \pi^2 / 2mL^2$ . The sum in eq. (38) cannot be done analytically, but an expansion for small  $\beta$  can be obtained using the identity (van der Pol and Bremmer 1955, p.236)

$$\sum_{n=1}^{\infty} \exp(-\beta cn^2) = \frac{1}{2} \left[ \left( \frac{\pi}{c} \right)^{1/2} \frac{1}{\beta^{1/2}} - 1 + 2 \left( \frac{\pi}{c} \right)^{1/2} \frac{1}{\beta^{1/2}} \sum_{n=1}^{\infty} \exp(-\pi^2 n^2 / \beta c) \right] \quad (39)$$

For small  $\beta$ , the terms in the sum on the right-hand side decrease very rapidly with  $n$ , so that

$$Z_{sc}(\beta) = \frac{1}{4} \left( \frac{\pi}{c} \right)^{3/2} \frac{1}{\beta^{3/2}} - \frac{3}{4} \left( \frac{\pi}{c} \right) \frac{1}{\beta} + \frac{3}{4} \left( \frac{\pi}{c} \right)^{1/2} \frac{1}{\beta^{1/2}} + \frac{3}{4} \left( \frac{\pi}{c} \right)^{3/2} \frac{1}{\beta^{3/2}} \exp(-\pi^2 / \beta c) + \dots \quad (40)$$

and taking the term-by-term Laplace inverse of  $\beta Z_{sc}(\beta)$  gives

$$g_{sc}(\epsilon) = \left[ \frac{\pi}{2} \left( \frac{\epsilon}{c} \right)^{1/2} - \frac{3\pi}{4} + \frac{3}{4} \left( \frac{\epsilon}{c} \right)^{1/2} \right] \frac{\theta(\epsilon)}{c} - \frac{\delta(\epsilon)}{4} + \frac{3}{4c} \sin \left[ 2\pi \left( \frac{\epsilon}{c} \right)^{1/2} \right] \theta(\epsilon) + \dots \quad (41)$$

Unlike  $g_{sc}(\epsilon)$  for the harmonic oscillator, the higher order terms in  $g_{sc}(\epsilon)$  for the cubic box are not proportional to

derivatives of the delta function, and so the number of terms to be included in eq. (41) is not as clear-cut. However, beyond the fourth term, the contributions to  $g_{sc}(\epsilon)$  are oscillatory, and will lead to corresponding contributions in  $\bar{\lambda}$  and  $\bar{E}_{sp}$  which are rapidly varying functions of  $N$ . Since  $\bar{E}_{sp}$  should be a smooth function of particle number, it is surmised that these sinusoidal terms in  $g_{sc}(\epsilon)$  correspond to shell structure in the exact density of states, and so should not be included in  $\bar{E}_{sp}$ . For this reason, the expansion given by eq. (41) is truncated beyond the delta function term.

The first three terms of eq. (41) were obtained earlier (Hill and Wheeler 1953) by counting the number of states in a given element of energy space, and this calculation serves as an independent check on the method used here for obtaining  $g_{sc}(\epsilon)$ . The first three terms may be interpreted as the volume, surface and curvature contributions to the density of states, and they give rise to similar contributions in  $\bar{E}_{sp}$ . It is worth noting that the term in  $1/\sqrt{\epsilon}$  leads to a divergence in  $g_{sc}(\epsilon)$  for small  $\epsilon$ , and so the density of states obtained from the Strutinsky method will be very different than the result given by eq. (41) for energies near zero.

In using eq. (41) to calculate the shell correction, the mass  $m$  was taken to be the neutron mass, so that

$$\hbar^2/2m = 20.7219 \text{ MeV-fm}^2, \quad (42)$$

and  $L$  was chosen such that  $N/L^3 = \rho_n$ , where  $\rho_n$  is the neutron density. Taking  $\rho_n$  to be one-half of the total density gives (Bethe 1971)

$$L = 2.274 N^{1/3} \text{ fm} ,$$

and the shell correction obtained using these parameters in eq. (41) is shown by the solid line in fig. 5 for particle numbers from 40 to 200. When the Strutinsky method is applied to the level spectrum for the cubic box, the shell correction is found to be  $\gamma$ -dependent, particularly for values of  $N$  less than 80. However, by taking  $\delta E$  from the region of  $\gamma$  in which it is reasonably  $\gamma$ -independent ( $\gamma \approx 8c$ ) and using a sixth order curvature correction, the results shown by the dashed line in fig. 5 are obtained. Qualitatively the shell correction obtained by the two methods is very similar, and the agreement is to within 2 MeV throughout the range of  $N$  considered. The reason for the  $\gamma$ -dependence of the Strutinsky result for small values of  $N$  is probably due to the fact that for the cubic box  $\bar{g}(\epsilon)$  cannot be accurately approximated by a polynomial, particularly near  $\epsilon=0$ , and so the consistency condition is no longer accurately satisfied.

c) Quasirotational spectrum.

Consider the spectrum given by

$$\epsilon_n = (n+0.5)^2 ,$$

(43)

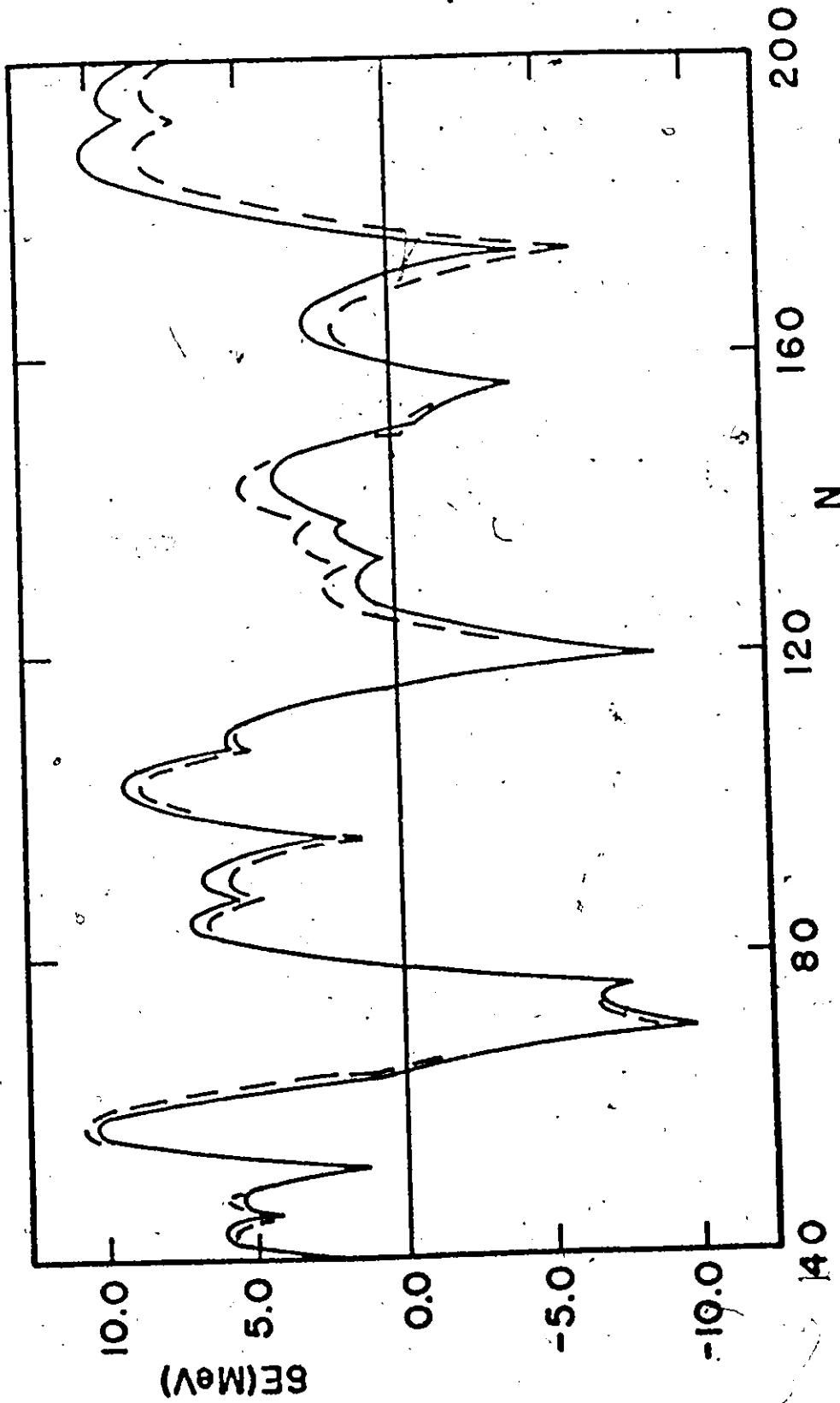


Fig. 5 Shell correction calculated by the partition function method (solid line) and by the Strutinsky method (dashed line) for various numbers of particles in the cubic box potential. The parameters used in the Strutinsky calculation are discussed in the text.

where each level can hold  $2(2n+1)$  particles, and  $n$  runs from zero to infinity. The partition function is given by

$$Z(\beta) = 2 \sum_{n=0}^{\infty} (2n+1) \exp(-(n+0.5)^2 \beta) ,$$

which can be expanded for small  $\beta$  using the Euler-Maclaurin summation formula (Abramowitz and Stegun 1965, p.16):

$$Z_{SC}(\beta) = \frac{2}{\beta} + \frac{1}{6} + \frac{7}{240} \beta + \dots \quad (44)$$

Taking the Laplace inverse of  $\beta Z_{SC}(\beta)$  gives for the smooth density of states

$$g_{SC}(\epsilon) = 2\theta(\epsilon) + \frac{\delta(\epsilon)}{6} + \frac{7}{240} \delta'(\epsilon) + \dots \quad (45)$$

with the result that

$$\bar{\lambda} = 0.5(N-1/6) ,$$

and

$$\bar{E}_{sp} = \bar{\lambda}^2 - \frac{7}{240} = N^2 - \frac{N}{12} - \frac{1}{45} .$$

In this case, the shell corrections calculated by the two different methods were compared for only a few values of  $N$ , but reasonable agreement between the two methods was again obtained.

Since the publication of the work discussed in this section (Bhaduri and Ross 1971), another method has been proposed for the calculation of shell corrections (Ramamurthy and Kapoor 1972). It is based on the high temperature behavior of the thermodynamic properties of the many-particle system, and assumes that for high temperatures shell effects no longer influence quantities such as the nuclear entropy. The method has been applied by Ramamurthy and Kapoor (1972) and Bengtsson (1972) to realistic single-particle spectra and close agreement with the corresponding results from the Strutinsky procedure was obtained. This approach has the advantage that it can be applied to an arbitrary level spectrum, unlike the method discussed in this section which requires that the single-particle partition function be known analytically for small  $\beta$ . However, it is considerably more difficult to use than the Strutinsky method, and the main importance of these different approaches to the calculation of the shell correction is that they provide an independent check on the Strutinsky smoothing procedure.

The equivalence of the Strutinsky method and the partition function approach has been shown numerically for a few simple cases in this chapter. However, the equivalence of the two approaches has recently been proved analytically (Jennings 1973), and the proof indicates that for most infinite single-particle potentials the Strutinsky method can reliably be used to calculate the shell correction.



## CHAPTER III

### CONTINUUM EFFECTS IN STRUTINSKY CALCULATIONS

#### III.1 Strutinsky Procedure for Finite Potentials.

The work of the last chapter indicates that the Strutinsky method can reliably be used for calculating the shell correction provided the one-body potential well is infinitely deep. However, Lin (1970) pointed out that if the potential is finite in depth, then the shell correction calculated by the Strutinsky procedure becomes dependent on  $\gamma$  and the curvature order, and it is no longer possible to obtain a unique value of  $\delta E$ . One reason why the Strutinsky procedure might be expected to break down for finite potentials can be seen by examining eq. (II.16), which involves a sum over all single-particle states. Despite the fact that the contributions of states lying above (or below) the energy  $\epsilon$  are damped out by the Gaussian smoothing, there is nevertheless a large energy interval about  $\epsilon$  from which states can contribute significantly. In fact, numerical calculations show that all states  $\epsilon_i$  satisfying  $|\epsilon - \epsilon_i|/\gamma < 3.5$  must be included in Strutinsky calculations for infinite potential wells. For the case of 70 particles in the infinite harmonic oscillator potential where the Fermi energy is approximately  $5.5 \hbar\omega$  (see fig. 1) this means that for  $\gamma = 1.2 \hbar\omega$ , all levels below about  $10 \hbar\omega$  must be included in calculating  $\delta E$ , and even

more levels are required for larger values of  $\gamma$ . Such high-lying states are generally not available for realistic finite potential wells, and in the case of the neutrons in  $\text{Pb}^{208}$  for example, the edge of the continuum lies only about  $1 \hbar\omega$  above the Fermi energy. Because of this upper cut-off on the bound state energies it is not surprising that the Strutinsky method as originally proposed is incapable of giving a unique result for the shell correction.

In order to examine the importance of high-lying levels in the Strutinsky method, consider the spherical Nilsson model potential (Nilsson 1955, Gustafson et al. 1967) for which the energy levels are given by

$$\begin{aligned} \epsilon_{j=l+1/2} &= (2n+l+3/2) - \kappa(N) l - \kappa(N) \mu_0 [l(l+1) - N(N+3)/2] , \\ \epsilon_{j=l-1/2} &= (2n+l+3/2) + \kappa(N) (l+1) - \kappa(N) \mu_0 [l(l+1) - N(N+3)/2] , \end{aligned} \quad (1)$$

where the energy is expressed in units of  $\hbar\omega$ . In eq. (1),  $n$  ( $n=0,1,\dots$ ) is the radial quantum number,  $l$  ( $l=0,1,\dots$ ) is the orbital angular momentum,  $j$  is the total angular momentum and  $N$  is the principal quantum number given by  $N=2n+l$ . The parameters  $\kappa(N)$  and  $\mu_0$  have been taken from the work of Seeger (1967) and for neutrons are given by

$$\mu_0 = 0.308 , \quad \kappa(N) = 0.21 [(N+1)(N+2)/2]^{-1/3} ,$$

while  $\hbar\omega$  has been taken to be  $\hbar\omega = 41/A^{1/3}$  (Roy and Nigam 1967, p.233),

which is approximately 6.92 MeV for  $^{208}\text{Pb}$ . The Fermi energy for the 126 neutrons in  $^{208}\text{Pb}$  corresponds to the  $2p_{1/2}$  level, and a few of the nearby Nilsson model levels are shown in the right-hand column of fig. 6. The zero of energy in this figure has been chosen such that the measured neutron removal energy corresponds approximately to the binding energy of the  $2p_{1/2}$  level.

The Strutinsky shell correction for 126 neutrons occupying the energy levels given by eq. (1) is shown in fig. 7 as a function of  $\gamma$  for various values of the curvature order. In this calculation, all levels which contribute significantly to the sum in eq. (II.16) have been included, which for  $\gamma=1.2 \hbar\omega$  means all levels below  $3.2 \hbar\omega$  ( $\approx 22$  MeV) while for  $\gamma=2.4 \hbar\omega$  the corresponding cutoff is approximately  $7.4 \hbar\omega$  ( $\approx 51$  MeV). (Note that all energies are now measured with respect to the zero of energy shown in fig. 6). For curvature orders larger than 2 and  $\gamma > 1.2 \hbar\omega$ , the shell correction is seen to be virtually independent of  $\gamma$  and the curvature order, and so a unique value of  $\delta E$  can be obtained. However, when the same spectrum is truncated beyond the  $2d_{3/2}$  level, the results shown in fig. 8 are obtained. The shell correction is now a strong function of  $\gamma$  and the curvature order, and apart from the fact that the fourth-order minimum corresponds approximately to the shell correction obtained in fig. 7, there is no obvious way of determining  $\delta E$ .

The Strutinsky shell correction for a finite potential

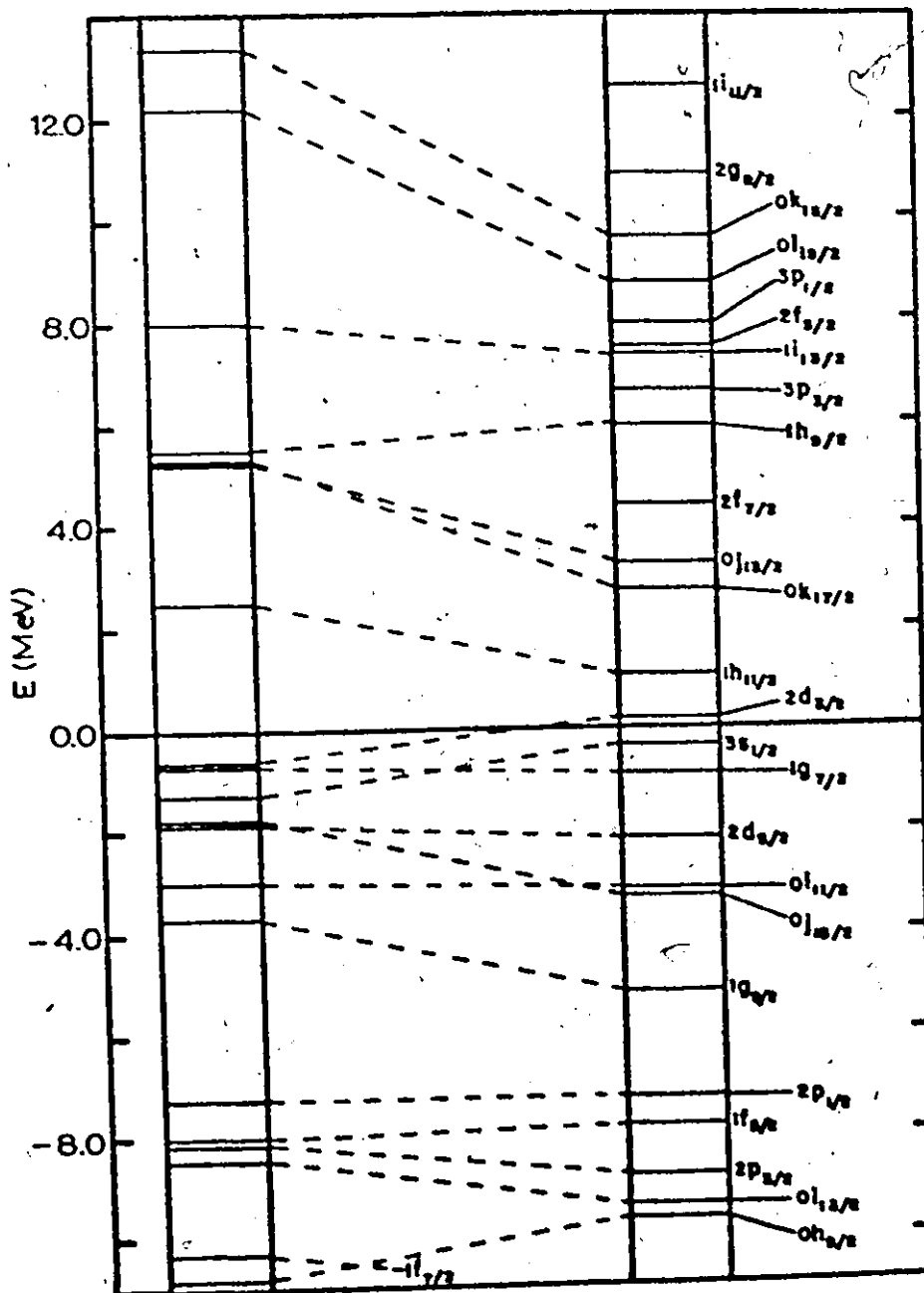


Fig. 6 Comparison of the single-particle spectra for the neutrons in  $^{208}\text{Pb}$  obtained using a Woods-Saxon potential (left-hand spectrum) and an infinite Nilsson potential (right-hand spectrum). The levels lying above zero energy in the Woods-Saxon spectrum correspond to peaks in the function  $\Delta g(\epsilon)$  defined by eq. (III.6), and are associated with continuum resonances.

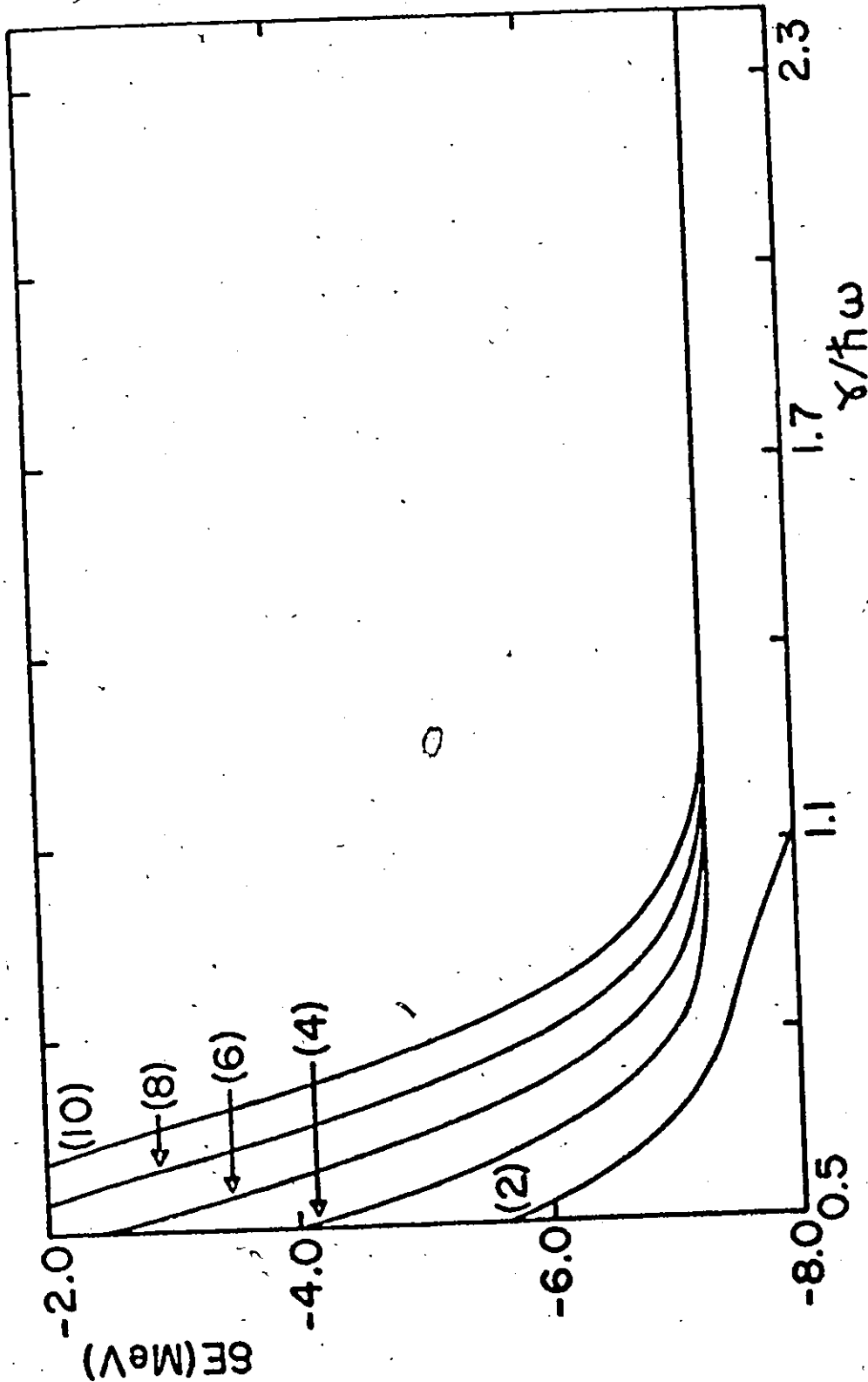


Fig. 7 Strutinsky shell correction in MeV for the neutrons in  $^{208}\text{Pb}$  as a function of  $\gamma$  for the Nilsson spectrum defined in eq. (III.1). Here  $\gamma$  is expressed in units of  $\hbar\omega$  ( $\hbar\omega = 6.92$  MeV) and the shell correction is shown for various curvature functions.

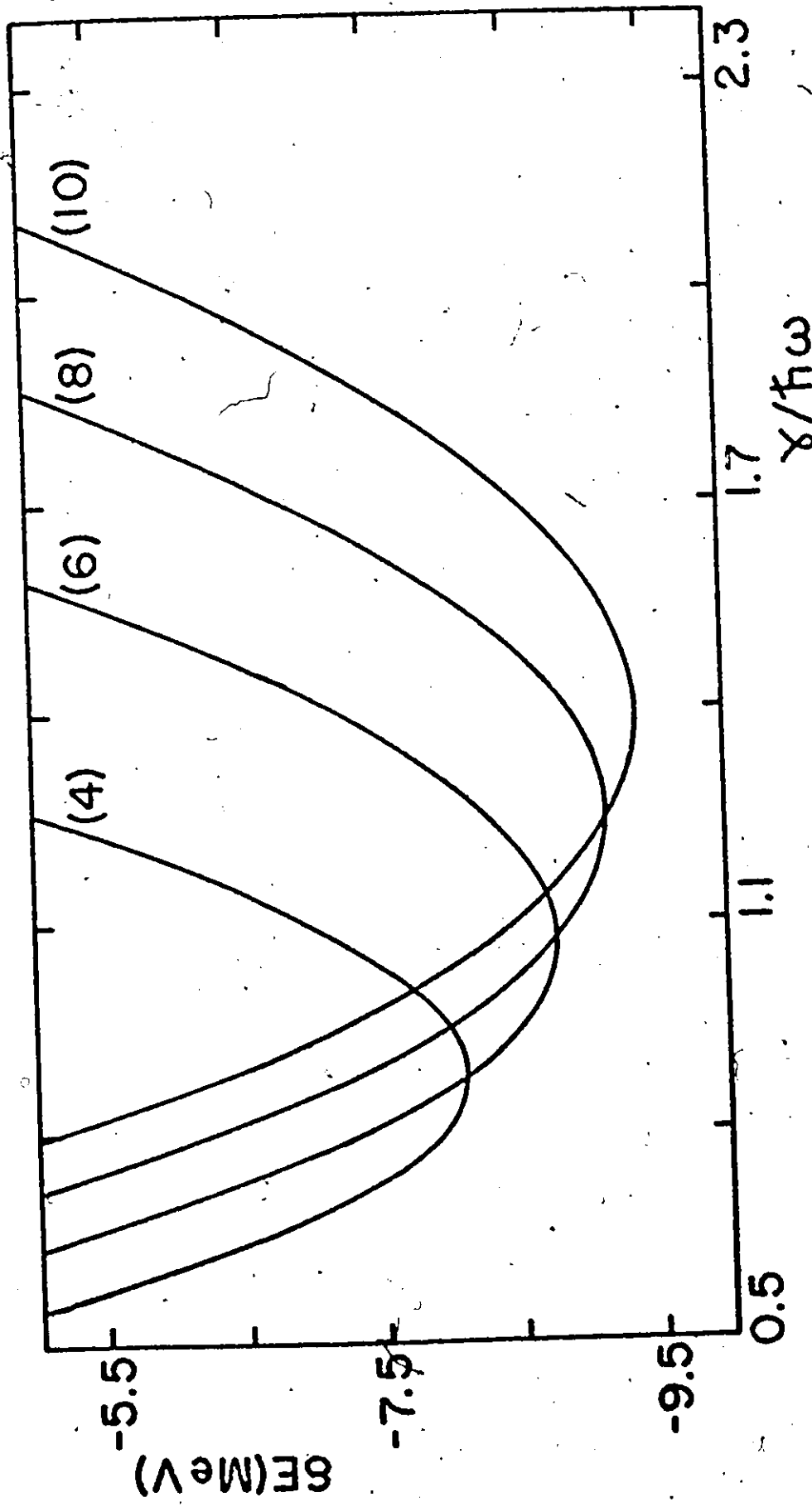


Fig. 8 Same as fig. 7, but with the Nilsson spectrum truncated after the  $2d_{3/2}$  level.

should behave similarly to that obtained for the truncated Nilsson spectrum, and in order to verify this, the shell correction was calculated for a spherical Woods-Saxon potential. The potential is given by (Blomqvist and Wahlborn 1960)

$$V(r) = -V_0 f(r) + \frac{\lambda}{2} \left( \frac{\hbar}{mc} \right)^2 V_0 \frac{1}{r} \frac{df(r)}{dr} \quad (\underline{2})$$

where

$$f(r) = [1 + \exp((r-R)/a)]^{-1} ,$$

and the parameters for the neutrons in  $^{208}\text{Pb}$  are

$$\begin{aligned} V_0 &= 44 \text{ MeV} , & \lambda &= 32 , \\ R &= 7.52 \text{ fm} , & a &= 0.67 \text{ fm} , \\ \hbar^2/2m &= 20.7219 \text{ MeV-fm}^2 , & \hbar/mc &= 0.21 \text{ fm} . \end{aligned} \quad (\underline{3})$$

The bound state eigenvalues and eigenfunctions were obtained by numerical integration of the Schrodinger equation using the Noumerov method (Blatt 1967) and a few of the single-particle levels near the Fermi energy are shown in the left-hand column of fig. 6. The shell correction calculated using the energy levels of  $V(r)$  is shown in fig. 9 for 126 neutrons and as expected the results are qualitatively similar to those shown in fig. 8 for the truncated Nilsson spectrum. The results obtained by Lin (1970) for a slightly different potential are also similar to those presented in fig. 9, and so it is

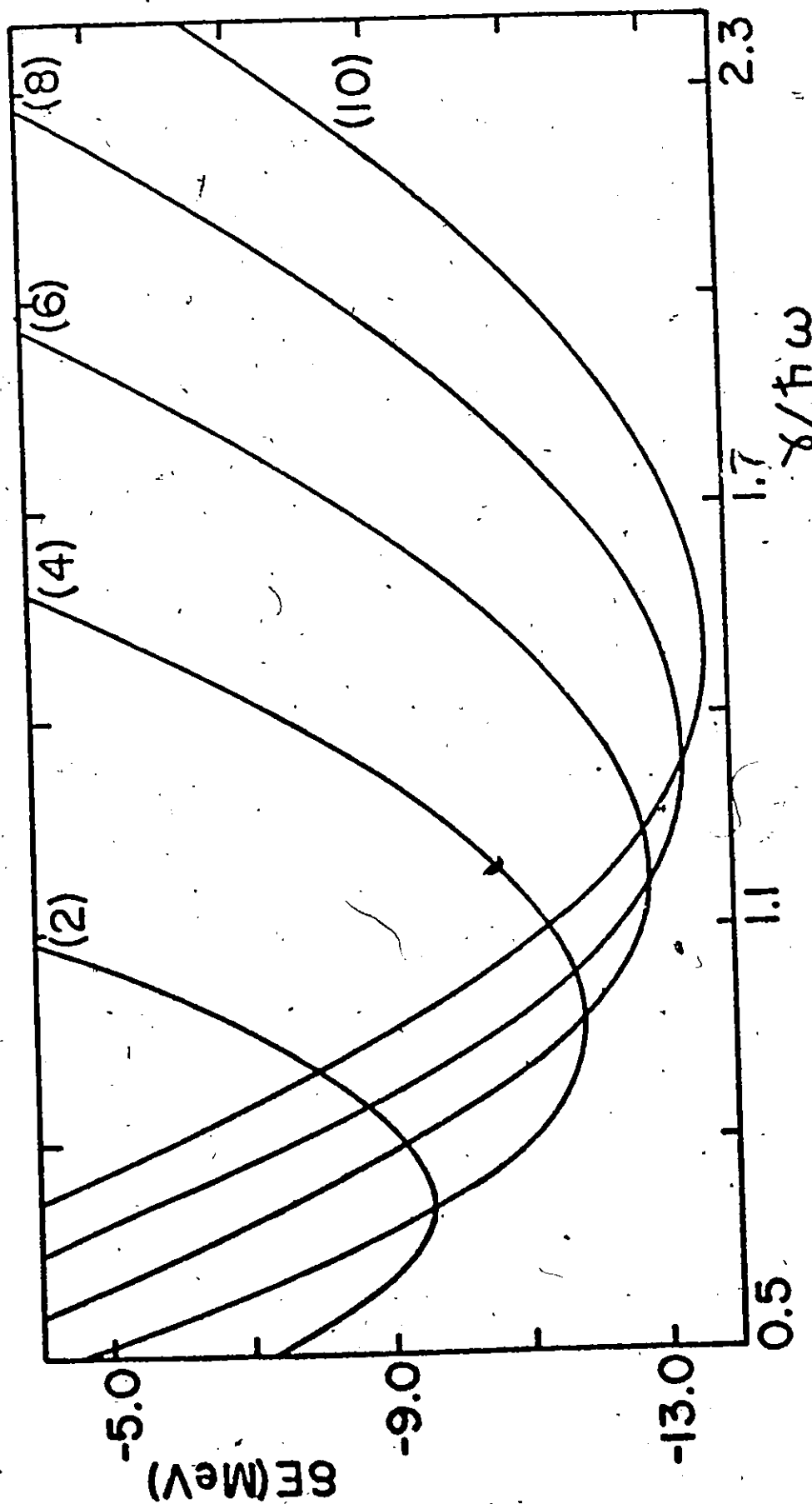


Fig. 9 Strutinsky shell correction in MeV for the neutrons in  $^{208}\text{Pb}$  as a function of  $\gamma$  for the Woods-Saxon potential defined by eq. (III.2), ignoring continuum effects. Here  $\gamma$  is expressed in units of  $\hbar\omega$  ( $\hbar\omega=6.92$  MeV) and the shell correction is shown for various curvature functions.



clear that if only the bound states are considered, the Strutinsky method cannot be reliably used to calculate the shell correction for finite potential wells.

After recognizing this difficulty, Lin (1970) suggested that if the Strutinsky method is to be applied to finite potentials, then the effects of continuum resonances should also be included in calculating  $\bar{g}(\epsilon)$ . By considering all resonances up to 20 MeV for  $^{208}\text{Pb}$ , he showed that the shell correction remained dependent on  $\gamma$  and the curvature order, and thus concluded that continuum effects were not capable of removing the ambiguities in the Strutinsky smoothing procedure. However, the discussion earlier in this section of the shell correction for the Nilsson model showed that levels much higher than 20 MeV can contribute to the shell correction, and for  $\gamma=2.4 \hbar\omega$ , levels as high as 50 MeV may be important. This indicates that Lin's calculations should be accurate for values of  $\gamma$  in the vicinity of  $\gamma=1 \hbar\omega$ , but that for larger values of  $\gamma$  higher resonances may seriously alter his results. In the next section it is shown how the continuum resonances affect the calculation of the shell correction, and Lin's calculations are repeated, including the high-energy resonances.

### III.2. The Effect of Resonances in the Strutinsky Procedure.

As a basis for discussing the effect of a potential on the continuum density of states, consider a single particle of

mass  $m$  in a large spherical box of volume  $V$ . According to a theorem due to Weyl, and discussed by Balian and Bloch (1970), the leading term in the density of states for a particle in a box is independent of the shape of the box. Then using the result obtained in Chapter II for the cubic box [eq. (II.41)] the leading term in the density of states is

$$g_0(\epsilon) = \frac{V}{2\pi^2} \left( \frac{2m}{\hbar^2} \right)^{3/2} \sqrt{\epsilon} \quad (4)$$

where the subscript indicates that this is the lowest order term, and the only one which remains as the volume  $V$  goes to infinity. If a one-body potential of finite depth is now introduced at the centre of this spherical box, the density of states as given by eq. (4) will be modified due to the presence of the potential, and this modification was first considered by Beth and Uhlenbeck (1937). If the one-body potential is spin independent, the correction to eq. (4) is (Huang 1963, p.311)

$$\Delta g(\epsilon) = \frac{2}{\pi} \sum_{\ell=0}^{\infty} (2\ell+1) \frac{d\delta_{\ell}(\epsilon)}{d\epsilon} \quad (5)$$

where  $\delta_{\ell}(\epsilon)$  is the phase shift for energy  $\epsilon$  of the  $\ell^{\text{th}}$  partial wave, and the factor of two arises from spin degeneracy. For the more usual situation in which the one-body potential contains a spin-orbit interaction, the phase shifts will be different for each  $\ell$  and  $j$  so that  $\Delta g(\epsilon)$  becomes (Lin 1970, Ross

and Bhaduri 1972)

$$\Delta g(\epsilon) = \frac{1}{\pi} \sum_{j=1/2}^{\infty} (2j+1) \sum_{\ell=j-1/2}^{\ell=j+1/2} \frac{d\delta_{\ell,j}(\epsilon)}{d\epsilon} \quad (6)$$

Depending on the one-body potential, the phase shift  $\delta_{\ell,j}(\epsilon)$  may change rapidly by  $\pi$  radians over a small energy interval, thus giving rise to a continuum resonance, and a corresponding peak in  $\Delta g(\epsilon)$ . Lin proposed that these rapid variations in  $\Delta g(\epsilon)$  should be included on a similar footing as the discrete levels when using the Strutinsky smoothing procedure, so that  $\bar{g}(\epsilon)$  would become

$$\bar{g}(\epsilon) = \frac{1}{\gamma\sqrt{\pi}} \sum_{\substack{\text{bound} \\ \text{states } i}} \exp(-u_i^2) L_k^{1/2}(u_i^2) + \frac{1}{\gamma\sqrt{\pi}} \int_0^{\infty} \Delta g(\epsilon') \exp(-u'^2) \times L_k^{1/2}(u'^2) d\epsilon' \quad (7)$$

where  $u_i = (\epsilon - \epsilon_i)/\gamma$  and  $u' = (\epsilon - \epsilon')/\gamma$ .

There is no strong justification for including the effects of the continuum resonances in  $\bar{g}(\epsilon)$ , and Strutinsky (1972) has pointed out that there is no completeness requirement on the sum over single-particle energies in eq. (II.16). However, as the depth of the one-body potential increases, the resonances will drop below zero energy and become bound states, and in this sense they may contain information on the variation of the level density with energy.

Lin used eq. (7) in his calculations to determine the effect of the continuum resonances on the shell correction, but as was pointed out earlier, he took account of only those resonances lying below 20 MeV. In order to determine whether higher energy resonances can alter his results, particularly for larger values of  $\gamma$ , the shell correction was calculated using eq. (7) for two slightly different potentials. The calculations including the resonances are technically much more difficult than those involving only the discrete levels, and some of the details are given in Appendix B. In particular, the phase shifts must be calculated to high energy, and the position and shape of each resonance carefully determined. Near the resonances, the phase shifts were obtained by numerical integration of the Schrodinger equation (Blatt 1967), while for energies greater than 20 MeV and far removed from the resonances, the WKB method was used (Messiah 1965, p.410).

The first potential considered is that given by eq. (2) for the neutrons in  $^{208}\text{Pb}$ , and a few of the bound states near the Fermi energy are shown in the left-hand column of fig. 6. The phase shifts for energies between 0 MeV and 20 MeV are shown in fig. 10 for the states given by  $j=l+1/2$ , where  $l$  lies between 0 and 10. Some of the resonances are seen to be sharp and well-defined, and their positions are shown in fig. 6 along with the bound-state energies. The dashed lines indicate the close correspondence between the continuum resonances and discrete Nilsson levels, thus giving

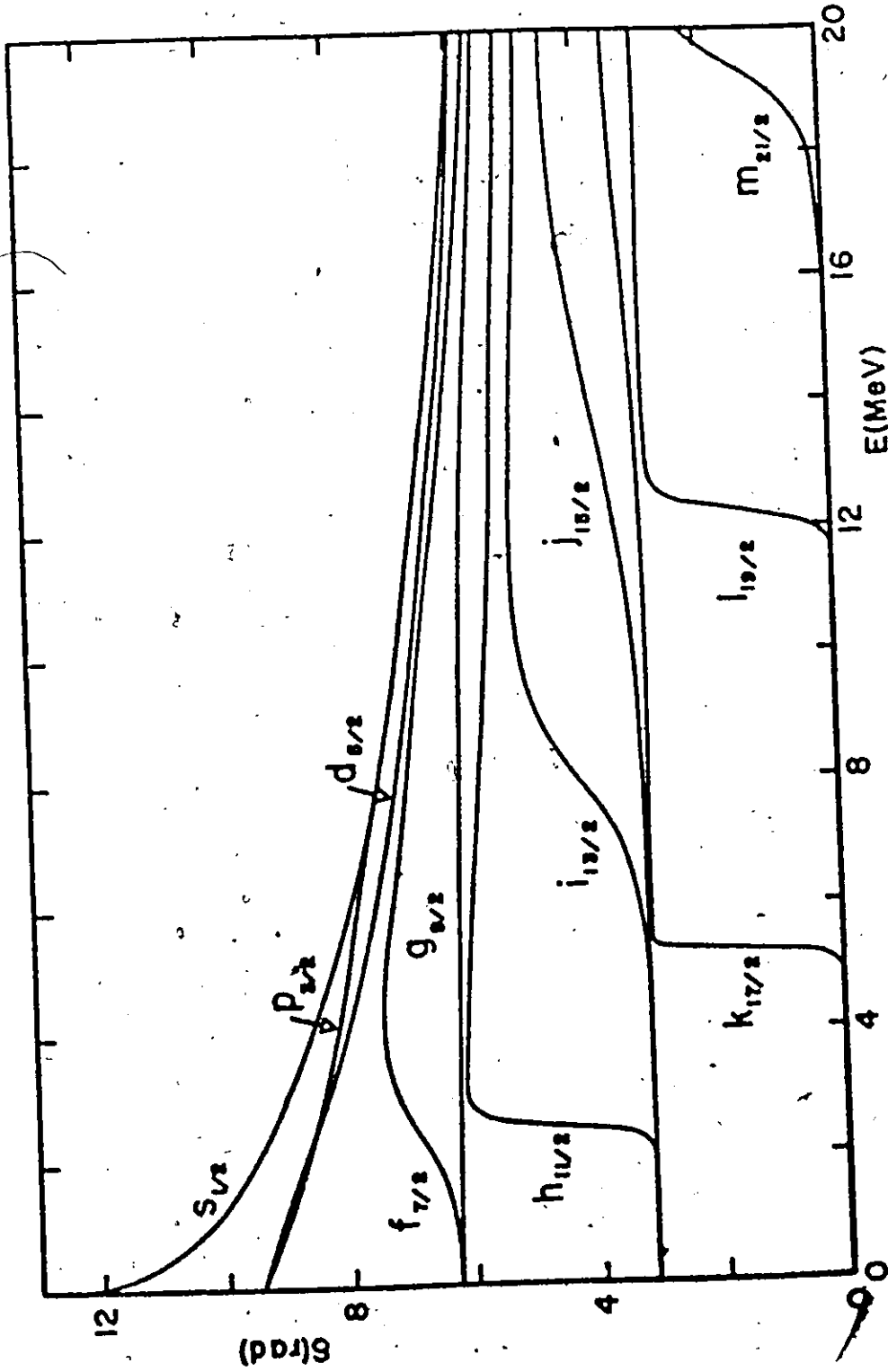


Fig. 10 The phase shift  $\delta_{lj}$  as a function of energy for the Woods-Saxon potential given by eqs. (III.2) and (III.3). Only the states with  $j=l+1/2$  and  $l \leq 10$  are shown. 45

further credence to Lin's suggestion that the effects of the resonances should be included in  $\bar{g}(\epsilon)$ .

The discussion in the first section of this chapter indicated that for values of  $\gamma$  in the vicinity of  $\gamma = 2.5 \hbar\omega$ , resonances at least as high as 50 MeV could contribute to the shell correction, and in order to ensure convergence when calculating  $\bar{g}(\epsilon)$ , the phase shifts were obtained for energies up to 100 MeV. A rough estimate of  $l_m$ , the maximum value of  $l$  for which the corresponding state will have a significant phase shift, can be obtained by using the classical relation

$$l_m = \left( \frac{2m}{\hbar^2} \right)^{1/2} \sqrt{\epsilon} R ,$$

where  $R$  is the radius of the one-body potential. Taking  $R$  from eq. (3), and  $\epsilon$  to be 100 MeV gives  $l_m \approx 17$ , and so the phase shifts were computed for all states with  $l$  less than 20.

The shell correction obtained by including the effects of the continuum resonances is shown in fig. 11, and should be contrasted with fig. 9, which included only the contributions of the bound states. The  $\gamma$  and order dependence of  $\delta E$  has been greatly reduced, and the uncertainty between the sixth- and tenth-order results is only about 0.3 MeV. The dashed line is the result of a calculation including only the resonances below 20 MeV, and it is clear that the resonances at higher energies play an important role for values of  $\gamma$  greater than about  $1.2 \hbar\omega$ .

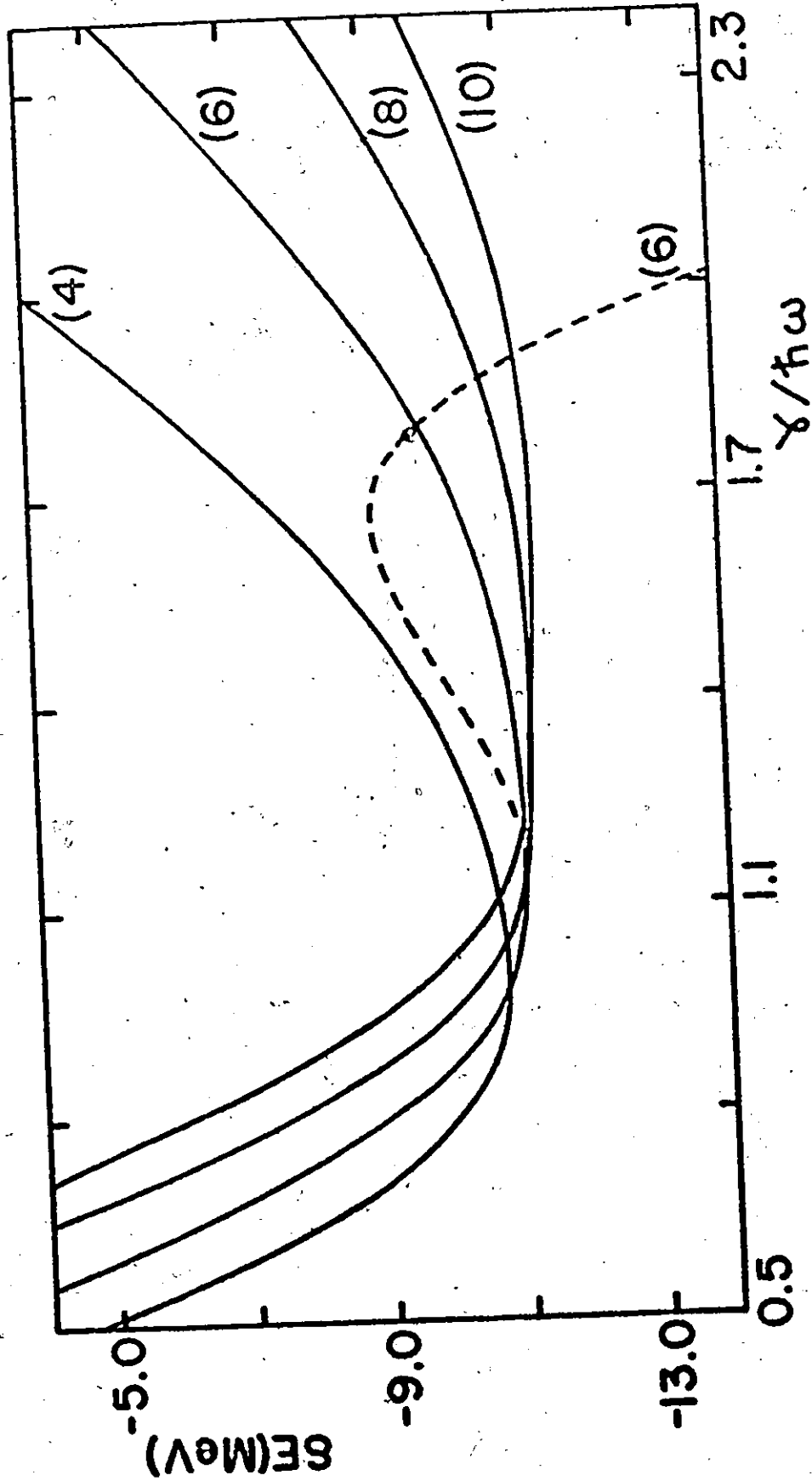


Fig. 11 Same as fig. 9, but including continuum effects. The dashed line is the result of a sixth-order calculation, but with the continuum effects truncated beyond  $2.89 \hbar\omega$  ( $\approx 20$  MeV).

In order to check that these results do not depend on the particular potential used, the parameters in the Woods-Saxon potential given by eq. (2) were changed to those thought appropriate for the 184 neutrons in the superheavy nucleus  $A=298$  (Sobiczewski et al. 1971). The parameter set referred to as "variant I" by Sobiczewski et al. has

$$V_0 = 43 \text{ MeV} , \quad R = 8.48 \text{ fm} , \quad (8)$$

with the other parameters remaining as given in eq. (3). Since  $\hbar\omega$  is smaller for this nucleus (6.14 MeV) than for  $^{208}\text{Pb}$ , the cut-off on the energy was taken to be 90 MeV rather than 100 MeV, and the maximum values of  $l$  considered were  $l=19$  for states with  $j=l+1/2$  and  $l=18$  for those with  $j=l-1/2$ . Fig. 12 shows the effect of including the resonances in  $\delta E$ , and as in fig. 11 for  $^{208}\text{Pb}$ , a reasonably unique value for the shell correction can be obtained. The dashed line shows the effect of truncating the continuum contributions at 60 MeV, and indicates that most of the contributions to  $\delta E$  come from below this energy.

Although the inclusion of the continuum resonances in the Strutinsky smoothing procedure gives rise to a shell correction which is reasonably independent of  $\gamma$  and the curvature order, it greatly complicates the calculation of  $\delta E$ . For the spherically symmetric potentials discussed in this section, the phase shifts have to be computed to very high energies,



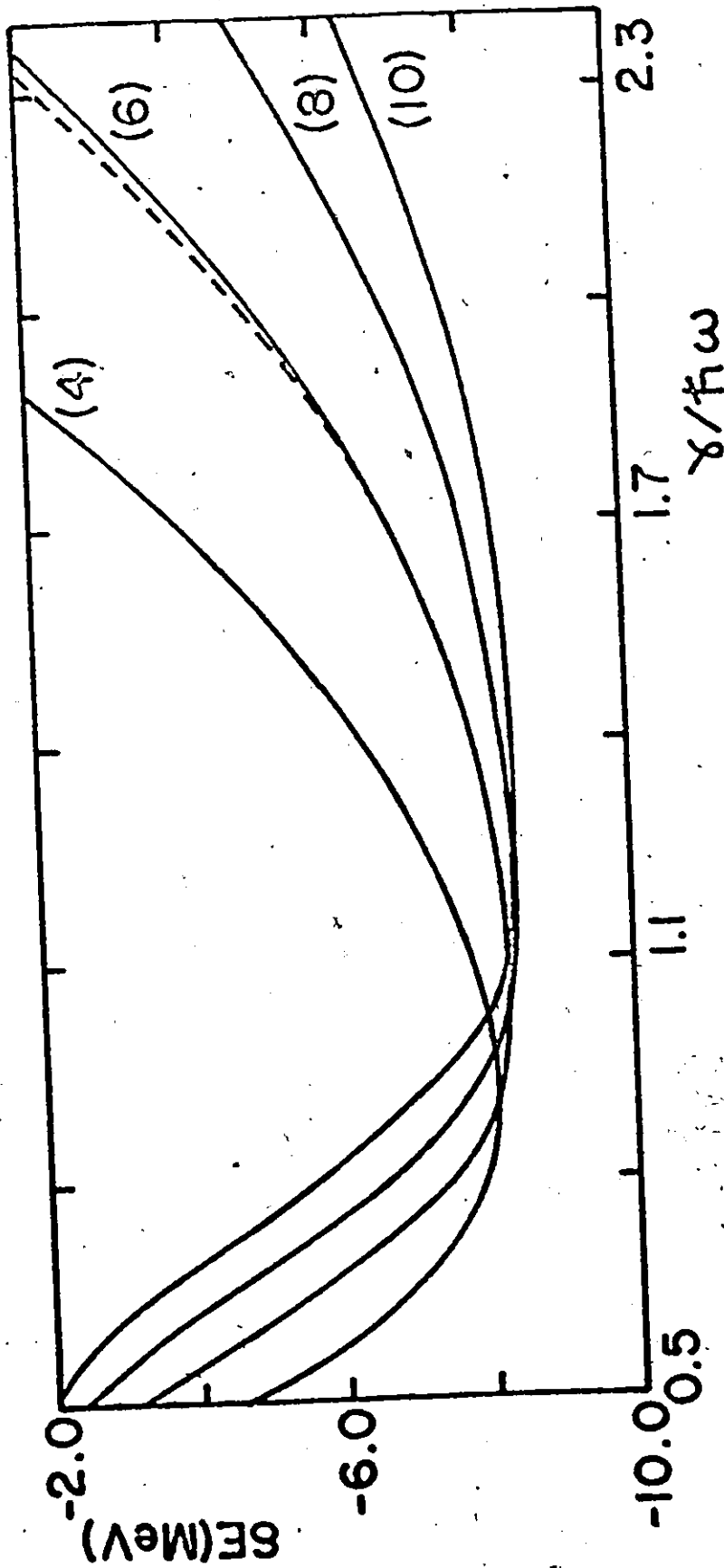


Fig. 12 Same as fig. 11, but for the 184 neutrons in the superheavy nuclide with  $A=298$ .  
 The dashed line shows the effect of truncating the continuum contribution at  $10\hbar\omega$   
 ( $\approx 60$  MeV) for the sixth order calculation ( $1\hbar\omega=6.14$  MeV).

and for deformed potentials the calculations may be even more difficult, since the phase shift is no longer a useful concept, and eq. (6) for  $\Delta g(\epsilon)$  would have to be modified. Because of these difficulties, and because there is no firm theoretical justification for including the continuum resonances in the Strutinsky smoothing procedure, various other approaches have been adopted for calculating the shell correction for finite potentials.

### III.3 Other Modifications of the Strutinsky Procedure.

It has been suggested (Brack et al. 1972) that the shell correction for finite potentials can be obtained from the Strutinsky method by imposing the condition

$$\frac{\partial(\delta E)}{\partial \gamma} = 0, \quad (9)$$

but this is clearly not sufficient, since figs. 8 and 9 show that the solution of eq. (9) also depends on the curvature order. In some of the calculations involving Woods-Saxon potentials this condition has apparently been supplemented by applying eq. (9) to the fourth-order calculation (Pauli 1971). A comparison of figs. 7 and 8 indicates that this may be a reasonable approximation, although the error involved is about 0.8 MeV.

Extensive shell correction calculations for finite

potential wells have recently been reported by Bolsterli et al. (1972). They use a matrix diagonalization method to solve for the eigenvalues of the one-body potential, and besides giving the bound state energies, this procedure gives rise to spurious states lying above zero energy. Bolsterli et al. argue that these states should be included in the Strutinsky procedure, and show that their inclusion gives a reasonably unique shell correction. Since the physical significance of these unbound states is not clear, this is not a very satisfactory procedure, and it depends on the fact that the eigenvalues are obtained by matrix diagonalization. These spurious states would not arise if a finite-difference method were used for integrating the Schrodinger equation, and so the shell correction becomes dependent on the numerical technique used for calculating the eigenvalues.

Finally, Bunatian et al. (1972) have recently suggested that the smoothing procedure, and in particular the curvature function, may be modified so that only the bound state energies are required. Although this will perhaps prove to be the most satisfactory approach, it has not yet been used in calculations involving realistic potential wells, and so its accuracy and reliability remain to be tested.

The work of this chapter indicates that at the present time, there are many uncertainties regarding the application of the Strutinsky method to finite potential wells. As a result, it is not clear that there is any advantage in using

a finite, rather than an infinite, potential in shell correction calculations, despite the fact that the single-particle energies for a finite potential well may be slightly more realistic.

CHAPTER IV  
ANGULAR MOMENTUM CONSERVATION IN THE  
STRUTINSKY METHOD

IV.1 Review of the Work of Kelson and Shoshani.

The initial success of the Strutinsky method (Strutinsky 1967, 1968) as a means of obtaining the nuclear deformation energy has led to a wide variety of calculations using different single-particle potentials, and studying different aspects of the deformation energy surface. For example, Nilsson et al. (1969) performed extensive calculations based on the Nilsson model potential, and their work confirmed that the deformation energy may display more than one minimum as a function of deformation. In addition, their calculations provided further evidence that the stabilizing influences of shell closures may lead to stable superheavy nuclei in the vicinity of  $Z = 110$  and  $N = 180$ . More recently, similar calculations have also been performed using finite potential wells (Bolsterli et al. 1972, Brack et al. 1972) which qualitatively confirm the results of Nilsson et al., and extensive estimates of the decay properties of superheavy elements have been made (Fiset and Nix 1972, Nix 1972). However, Kelson and Shoshani (1972) have suggested that angular momentum conservation has not been properly incorporated in these shell correction calculations, and they estimate that its correct

inclusion would lead to fission barriers for superheavy nuclei which are lower than present calculations indicate by as much as 2.5 MeV. Such a large change in the fission barrier height would lead to a drastic reduction in the half-lives for these superheavy elements, and the objective of the present chapter is to show that within the context of the Strutinsky method, the correction to the fission barrier due to angular momentum conservation is much less than predicted by Kelson and Shoshani (KS).

The work of KS is based on the Hartree-Fock approximation, in which the total energy for a nucleus specified by  $N$ ,  $Z$  and deformation  $\alpha$  is given by

$$E_{\text{HF}}(\alpha) = \langle \phi_{\text{HF}}(\alpha) | H | \phi_{\text{HF}}(\alpha) \rangle \quad (1)$$

where  $H$  is the many-body Hamiltonian, and  $\phi_{\text{HF}}(\alpha)$  the Hartree-Fock determinantal wavefunction. The nuclear deformation energy can in principle be obtained by calculating  $E_{\text{HF}}(\alpha)$  as a function of  $\alpha$ , and the fission barrier height is given by

$$E_{\text{bh}} = E_{\text{HF}}(\alpha_{\text{sp}}) - E_{\text{HF}}(\alpha_{\text{gs}}) \quad (2)$$

where the subscripts  $\text{sp}$  and  $\text{gs}$  specify respectively the saddle point and ground state deformations. However, KS point out that for an even-even nucleus, the ground state has angular momentum  $J = 0$ , while the Hartree-Fock wave function does not

in general correspond to a state of good J, and so it is important to project out the J=0 component of  $\phi_{HF}(\alpha)$  when calculating the deformation energy. For a state of J=0, the total energy will be given by

$$E_0(\alpha) = E_{HF}(\alpha) + \Delta_0(\alpha) \quad , \quad (3)$$

where the notation of Ripka (1968) has been used to denote the projection correction, and so the corrected fission barrier height becomes

$$\begin{aligned} E'_{bh} &= E_0(\alpha_{sp}) - E_0(\alpha_{gs}) \\ &= E_{bh} + (\Delta_0(\alpha_{sp}) - \Delta_0(\alpha_{gs})) \quad . \quad (4) \end{aligned}$$

KS consider the quantity in parentheses in eq. (4) as the correction to be applied to existing fission barrier calculations, and they estimate that it may be as large as -2.5 MeV for some superheavy nuclei.

In order to calculate  $\Delta_0(\alpha)$ , KS consider a well-deformed nucleus for which the intrinsic and rotational motion can be approximately separated, and the Hamiltonian written as

$$H = H_{int} + H_{rot} \quad . \quad (5)$$

The rotational part of H is given by

$$H_{\text{rot}} = \frac{\hbar^2}{2\mathcal{I}} J^2, \quad (6)$$

where  $\mathcal{I}$  is the moment of inertia, while  $H_{\text{int}}$  describes the motion of the nucleons in a coordinate system rotating with angular velocity  $\omega = \hbar\sqrt{J(J+1)}/\mathcal{I}$  about an axis perpendicular to the nuclear symmetry axis. The Hartree-Fock determinantal wave function can always be expanded in terms of states of good angular momentum as

$$\phi_{\text{HF}}(\alpha) = \sum_J a_J \phi_J(\alpha), \quad (7)$$

where the sum is only over even  $J$ , and the expansion coefficients satisfy the normalization requirement

$$\sum_J |a_J|^2 = 1. \quad (8)$$

The Hartree-Fock energy becomes

$$E_{\text{HF}}(\alpha) = \sum_J |a_J|^2 \langle \phi_J(\alpha) | H | \phi_J(\alpha) \rangle, \quad (9)$$

and to the extent that eq. (5) is valid, this may be rewritten as

$$E_{\text{HF}}(\alpha) = E_0(\alpha) + \frac{\hbar^2}{2\mathcal{I}} \sum_J |a_J|^2 J(J+1). \quad (10)$$



On comparing eqs. (3) and (10),  $\Delta_0(\alpha)$  is seen to be

$$\Delta_0(\alpha) = -\frac{\hbar^2}{2\mathcal{I}} \langle \phi_{\text{HF}}(\alpha) | \underline{J}^2 | \phi_{\text{HF}}(\alpha) \rangle \quad (11)$$

and by further approximating  $\phi_{\text{HF}}(\alpha)$  by Nilsson model wave functions, KS are able to use eq. (11) to estimate the effect of angular momentum conservation on the fission barrier.

Although the projection correction as proposed by KS should be applied to calculations of the deformation energy based on Hartree-Fock theory, most recent calculations have been based on the Strutinsky method. KS assume that the effects of angular momentum conservation are the same for both methods, and in this way they conclude that the fission barriers of superheavy nuclei may be lowered by as much as 2.5 MeV over existing calculations. In the next section the basis of the Strutinsky method will be examined in some detail, and the effects of angular momentum conservation explicitly included. It will be shown that the effect is much smaller than that suggested by KS, and probably lies within present uncertainties in the Strutinsky smoothing procedure.

#### IV.2 Re-examination of the Strutinsky Method.

In Chapter II, the main emphasis was on the Strutinsky smoothing procedure, and the brief discussion of the foundation of the Strutinsky method itself was based on the

Hartree-Fock approximation. However, the shell correction is only a small fraction of the total energy, and if realistic calculations of the nuclear deformation energy are to be performed, the effects of the short-range pairing correlations must also be taken into account. The generalization of the Hartree-Fock approximation to include pairing effects is known as the Hartree-Bogolyubov approximation (Baranger 1961, Valatin 1961, Rowe 1970, p.205) and in this approach the ground state wave function has the form

$$|\phi\rangle = \prod_{\mu>0} (u_{\mu} + v_{\mu} a_{\mu}^{\dagger} a_{\bar{\mu}}^{\dagger}) | \rangle . \quad (12)$$

In eq. (12),  $| \rangle$  denotes the vacuum state, and  $a_{\mu}^{\dagger}$  and  $a_{\bar{\mu}}^{\dagger}$  are creation operators which create particles in the single-particle states  $|\mu\rangle$  and  $|\bar{\mu}\rangle$ , where  $|\bar{\mu}\rangle$  is the time-reversed state of  $|\mu\rangle$ . The parameters  $u_{\mu}$  and  $v_{\mu}$ , as well as the single-particle basis specified by  $\mu$ , are obtained by minimizing

$$E_{HB}(\alpha) = \langle \phi(\alpha) | H | \phi(\alpha) \rangle , \quad (13)$$

where  $\alpha$  specifies the deformation. However,  $|\phi(\alpha)\rangle$  is not in general a state of good angular momentum, and just as in the Hartree-Fock approximation it is necessary to project out the  $J=0$  component before calculating the ground state energy  $E_0(\alpha)$  (Onishi and Yoshida 1966, Gunye and Khadkikar 1970,

Góeke et al. 1972). In analogy with eq. (3),  $E_0(\alpha)$  may be written as

$$E_0(\alpha) = E_{HB}(\alpha) + \Delta_0(\alpha) \quad , \quad (14)$$

and under the same assumptions which led to eq. (11),  $\Delta_0(\alpha)$  is given by

$$\Delta_0(\alpha) = \frac{\hbar^2}{2g} \langle \phi(\alpha) | \mathbb{J}^2 | \phi(\alpha) \rangle \quad . \quad (15)$$

Although the same notation has been used in sect. 1 for the ground state energy and projection correction calculated in the Hartree-Fock approximation, no confusion should arise since the discussion in the remainder of this chapter will always refer to these quantities as given by eqs. (14) and (15).

Given a two-body interaction, eq. (14) could in principle be used to calculate the nuclear deformation energy. However, for heavy nuclei the calculations would be technically very difficult, and in the Strutinsky method  $E_{HB}(\alpha)$  is first simplified slightly by writing

$$E_{HB}(\alpha) \approx E_{HF}(\alpha) + E_{pc}(\alpha) \quad , \quad (16)$$

where  $E_{pc}(\alpha)$  is the pairing correlation energy (Nilsson et al. 1969, Bolsterli et al. 1972) obtained using the single-particle

energies from the Hartree-Fock calculation. The use of eq. (16) means that the short-range pairing interaction can no longer influence the choice of single-particle states, and some of the self-consistency inherent in the Hartree-Bogolyubov method has been lost. Satpathy et al. (1969) have pointed out that the use of eq. (16) for  $E_{HB}(\alpha)$  rather than eq. (13) may introduce considerable error, but they make no detailed comparison of the two approaches. To some extent, the lack of self-consistency in eq. (16) may be partially counteracted by the fact that the strength of the pairing interaction can be chosen empirically, while in eq. (13) no such freedom exists.

On combining eqs. (14) and (16), the ground state energy as a function of  $N$ ,  $Z$  and  $\alpha$  becomes

$$E_0 = E_{HF} + E_{pc} + \Delta_0 \quad , \quad (17)$$

where the explicit deformation dependence is no longer indicated. The basic idea of the Strutinsky method is to extract that part of  $E_0$  which is a smoothly varying function of  $N$ ,  $Z$  and  $\alpha$  and identify it with the energy calculated using the liquid drop model. This means that

$$E_{LD} = \bar{E}_{HF} + \bar{E}_{pc} + \bar{\Delta}_0 \quad , \quad (18)$$

where the bar is used to denote the smoothly varying part of each quantity. A serious weakness of the Strutinsky method is

that a precise definition of  $\bar{E}_0$  in terms of  $N$ ,  $Z$  and  $\alpha$  has never been formulated, and so the validity of eq. (18) cannot be directly verified. However, by using eq. (18),  $E_0$  may be written as

$$E_0 = E_{LD} + (E_{HF} - \bar{E}_{HF}) + (E_{pc} - \bar{E}_{pc}) + (\Delta_0 - \bar{\Delta}_0) \quad (19)$$

and Strutinsky was further able to show (Strutinsky 1968) that

$$E_{HF} - \bar{E}_{HF} = E_{sp}^{n,p} - \bar{E}_{sp}^{n,p} = \delta E \quad (20)$$

where  $E_{sp}^{n,p}$  has been defined in eq. (II.4). By introducing

$$\delta E_{pc} = E_{pc} - \bar{E}_{pc} \quad (21)$$

and

$$\delta \Delta_0 = \Delta_0 - \bar{\Delta}_0 \quad (22)$$

eq. (19) can be finally written as

$$E_0 = E_{LD} + \delta E + \delta E_{pc} + \delta \Delta_0 \quad (23)$$

Previous applications of the Strutinsky method have neglected  $\Delta_0$  in eq. (17) and taken  $E_{LD}$  to be

$$E_{LD} = \bar{E}_{HF} + \bar{E}_{pc} \quad (24)$$

so that  $E_0$  is given by eq. (23) but without the term  $\delta\Delta_0$ . The correction to  $E_0$  due projection effects as given by KS is equivalent to introducing  $\Delta_0$  in eq. (17), but keeping eq. (24) for  $E_{LD}$ , so that

$$\delta\Delta_0(KS) = \Delta_0 \quad (25)$$

However,  $E_{LD}$  is a semiempirical expression for the energy which has been obtained by fitting the experimental ground state masses and fission barriers (Myers and Swiatecki 1966), and as such represents the energy of a state with good J. For this reason,  $E_{LD}$  should be identified with the smoothed energy corresponding to a state of good angular momentum, and so eq. (18) and not eq. (24) should be used for  $E_{LD}$ . On comparing eqs. (22) and (25) it is clear that  $\delta\Delta_0$  will be much smaller than  $\delta\Delta_0(KS)$ , since  $\delta\Delta_0$  depends only on the shell structure in  $\Delta_0$ , and not on  $\Delta_0$  itself. A more quantitative estimate of  $\delta\Delta_0$  based on eq. (15) will now be undertaken with Nilsson model wave functions and single-particle energies replacing the corresponding Hartree-Fock quantities.

#### IV.3 Calculation of the Projection Correction.

The calculation of  $\delta\Delta_0$ , the effect of angular momentum conservation on the deformation energy, requires that the projection correction  $\Delta_0$  be known as a function of N, Z and

$\alpha$ . Eq. (15) defines  $\Delta_0$  in terms of  $\langle J^2 \rangle$  and  $\mathcal{I}$ , and although the calculation of  $\langle J^2 \rangle$  is straightforward, there are various approaches which might be used for calculating  $\mathcal{I}$ . KS use a scaling law based on the rigid rotor and hydrodynamic limits of the moment of inertia in order to calculate  $\mathcal{I}$  for any deformation  $\alpha$  in terms of a fixed deformation  $\alpha_0$ . This method has the advantage that the moment of inertia fits the experimental data at one deformation, but has the serious disadvantage that the scaling law is a smooth function of  $N$ ,  $Z$  and  $\alpha$ , and so any shell structure in  $\mathcal{I}$  is suppressed. However,  $\delta\Delta_0$  will be very sensitive to the effects of shell structure in both  $\langle J^2 \rangle$  and  $\mathcal{I}$ , and it is important to use a method for calculating the moment of inertia which includes these single-particle effects. The approach that will be used here is based on the Inglis cranking model (Inglis 1954) including pairing effects, and it has been applied with considerable success to the rare-earth nuclei (Nathan and Nilsson 1965). More recently, the cranking model has also been used to calculate the moments of inertia of fission isomers in the actinide region (Sobiczewski et al. 1973) and the results are consistent with the measured properties of both the ground state minimum and the highly deformed secondary minimum.

The Nilsson model hamiltonian used for generating the single-particle wave functions, and energies required in the pairing calculation was taken from the work of Seeger (1967),

and is discussed in some detail in Appendix C. The eigenfunctions and eigenvalues are obtained by diagonalizing this Hamiltonian in a spherical harmonic oscillator basis, and only quadrupole deformations are considered. Once the single-particle energies are known, the pairing calculation must be done so that the occupation and nonoccupation probabilities  $v_{\mu}^2$  and  $u_{\mu}^2$  appearing in eq. (12) can be obtained. The parameters used in these calculations were taken from Nilsson et. al. (1969) and these parameters, as well as the method used for solving the pairing equations for the Fermi energy  $\lambda$  and the gap parameter  $\Delta$  are discussed in Appendix D. Given  $\lambda$  and  $\Delta$ ,  $v_{\mu}^2$  and  $u_{\mu}^2$  can be obtained from

$$v_{\mu}^2 = \frac{1}{2} \left\{ 1 - \frac{\epsilon_{\mu} - \lambda}{\xi_{\mu}} \right\} \quad (26)$$

and

$$u_{\mu}^2 = \frac{1}{2} \left\{ 1 + \frac{\epsilon_{\mu} - \lambda}{\xi_{\mu}} \right\} \quad (27)$$

where the quasiparticle energy  $\xi_{\mu}$  is given by

$$\xi_{\mu} = [(\epsilon_{\mu} - \lambda)^2 + \Delta^2]^{1/2} \quad (28)$$

The evaluation of  $\langle \underline{J}^2 \rangle$  may be carried out by first writing

$$\underline{J}^2 = \underline{J}_n^2 + 2 \underline{J}_p \cdot \underline{J}_n + \underline{J}_n^2 \quad (29)$$



where  $\underline{J}_n$  and  $\underline{J}_p$  denote respectively the total angular momentum of the neutrons and protons. Since only neutron-neutron and proton-proton pairing is considered, the ground state wave function  $|\phi\rangle$  can be written as

$$|\phi\rangle = |\phi_n\rangle |\phi_p\rangle, \quad (30)$$

and for axially symmetric nuclei,

$$J_z^{n(p)} |\phi_{n(p)}\rangle = 0. \quad (31)$$

Using eqs. (30) and (31),  $\langle \underline{J}^2 \rangle$  becomes

$$\langle \underline{J}^2 \rangle = \langle \underline{J}^2 \rangle_n + \langle \underline{J}^2 \rangle_p, \quad (32)$$

and so the contributions of the neutrons and protons to  $\langle \underline{J}^2 \rangle$  can be calculated separately. For either neutrons or protons,

$$\underline{J}^2 = \sum_l \underline{j}_l^2 + \sum_{\substack{l,m \\ l \neq m}} \underline{j}_l \cdot \underline{j}_m, \quad (33)$$

where the sums are over all neutrons or protons, and in terms of single-particle quantities  $\langle \underline{J}^2 \rangle_{n(p)}$  is given by (Ross and Warke 1973)

$$\begin{aligned}
\langle \underline{J}^2 \rangle_{n(p)} = & 2 \sum_{\mu > 0} \langle \mu | j^2 | \mu \rangle v_{\mu}^2 + 2 \sum_{\mu, \nu > 0} [\langle \mu \nu | j_1 j_2 | \mu \nu - \nu \mu \rangle \\
& + \langle \mu \bar{\nu} | j_1 j_2 | \mu \bar{\nu} - \bar{\nu} \mu \rangle] v_{\mu}^2 v_{\nu}^2 + 2 \sum_{\mu, \nu > 0} \langle \mu \mu | j_1 j_2 | \nu \bar{\nu} - \bar{\nu} \nu \rangle v_{\mu} u_{\mu} v_{\nu} u_{\nu}. \quad (34)
\end{aligned}$$

The total  $\langle \underline{J}^2 \rangle$ , as well as  $\langle \underline{J}_n^2 \rangle$  and  $\langle \underline{J}_p^2 \rangle$ , for the nuclide  $^{256}\text{No}$  are shown as a function of deformation  $\epsilon$  in fig. 13. They are seen to be rapidly increasing functions of deformation, but show no pronounced shell structure effects.

The moment of inertia is given quite generally by

(Rowe 1970, p.126)

$$\mathcal{I} = 2 \sum_{i \neq 0} \frac{|\langle i | J_x | 0 \rangle|^2}{\omega_i - \omega_0}, \quad (35)$$

where  $|0\rangle$  denotes the ground state,  $|i\rangle$  is any intermediate state, and  $\omega_0$  and  $\omega_i$  are the corresponding eigenvalues. For the nuclear model under consideration in this section,  $|0\rangle$  corresponds to  $|\phi\rangle$ , the quasi-particle vacuum, while  $|i\rangle$  is any state corresponding to a two-quasi-particle excitation. As for  $\langle \underline{J}^2 \rangle$ ,  $\mathcal{I}$  can be separated as

$$\mathcal{I} = \mathcal{I}_n + \mathcal{I}_p, \quad (36)$$

where (Sobiczewski et al. 1973)

$$\mathcal{I}_{n(p)} = 2 \sum_{\mu, \nu > 0} \frac{[|\langle \mu | j_x | \nu \rangle|^2 + |\langle \mu | j_x | \bar{\nu} \rangle|^2]}{\epsilon_{\mu} + \epsilon_{\nu}} (v_{\mu} u_{\nu} - v_{\nu} u_{\mu})^2. \quad (37)$$

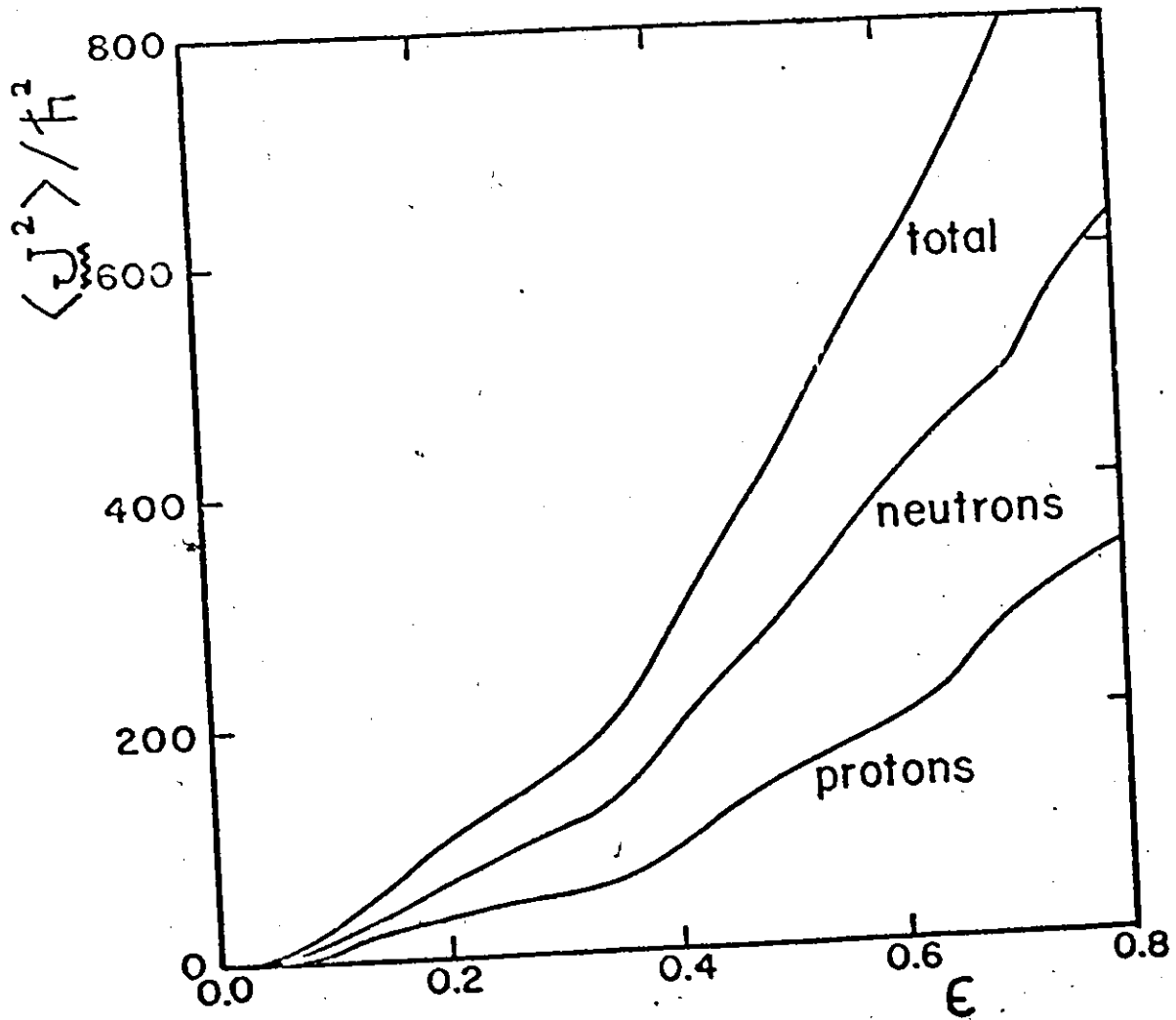


Fig. 13 Expectation value of  $J^2$  (in units of  $\hbar^2$ ) including pairing effects, as a function of the quadrupole deformation  $\epsilon$  for  $^{256}\text{No}$ . The separate contributions of the neutrons and protons to  $\langle J^2 \rangle$  are also shown.

The quantum numbers which are represented by the indices  $\mu$  and  $\nu$  are given in Appendix C, and the sums in eq. (37) (and eq. (34)) are over all the single-particle levels from the lowest in the potential well to the last included in the pairing calculation (Appendix D). Fig. 14 shows  $\mathcal{J}$ ,  $\mathcal{J}_n$  and  $\mathcal{J}_p$  as a function of deformation for the nuclide  $^{256}\text{No}$ , and the pronounced shell structure effects which are present indicate that the main contributions to  $\delta\Delta_0$  will come from these rapid variations in  $\mathcal{J}$ .

The projection correction  $\Delta_0$  is shown as a function of deformation for  $^{256}\text{No}$  in fig. 15a and for the super-heavy nuclide  $^{290}\text{110}$  in fig. 15b. Since eq. (15) for  $\Delta_0$  assumes a well-defined rotational spectrum, it is not expected to be valid for small deformations, and  $\Delta_0$  has not been shown for  $\epsilon < 0.2$ . In order to estimate  $\delta\Delta_0$  [eq. (22)] some method must be found for extracting that part of  $\Delta_0$  which is a smoothly varying function of  $N$ ,  $Z$  and  $\epsilon$ . Since  $\Delta_0$  depends not only on the single-particle energies but also on the wave functions, the smoothing procedure of Strutinsky cannot be used. However, the hydrodynamic model of Bohr (1952) suggests that both  $\langle \underline{J}^2 \rangle$  and  $\mathcal{J}$  can be written in the form  $CA^a \epsilon^b$  where  $A$  is the mass number, and  $C$ ,  $a$  and  $b$  are constants which will be different for  $\langle \underline{J}^2 \rangle$  and  $\mathcal{J}$ . Because the hydrodynamic model concerns itself only with gross nuclear properties, and does not include the detailed effects of single-particle motion, the values of  $\langle \underline{J}^2 \rangle$  and  $\mathcal{J}$

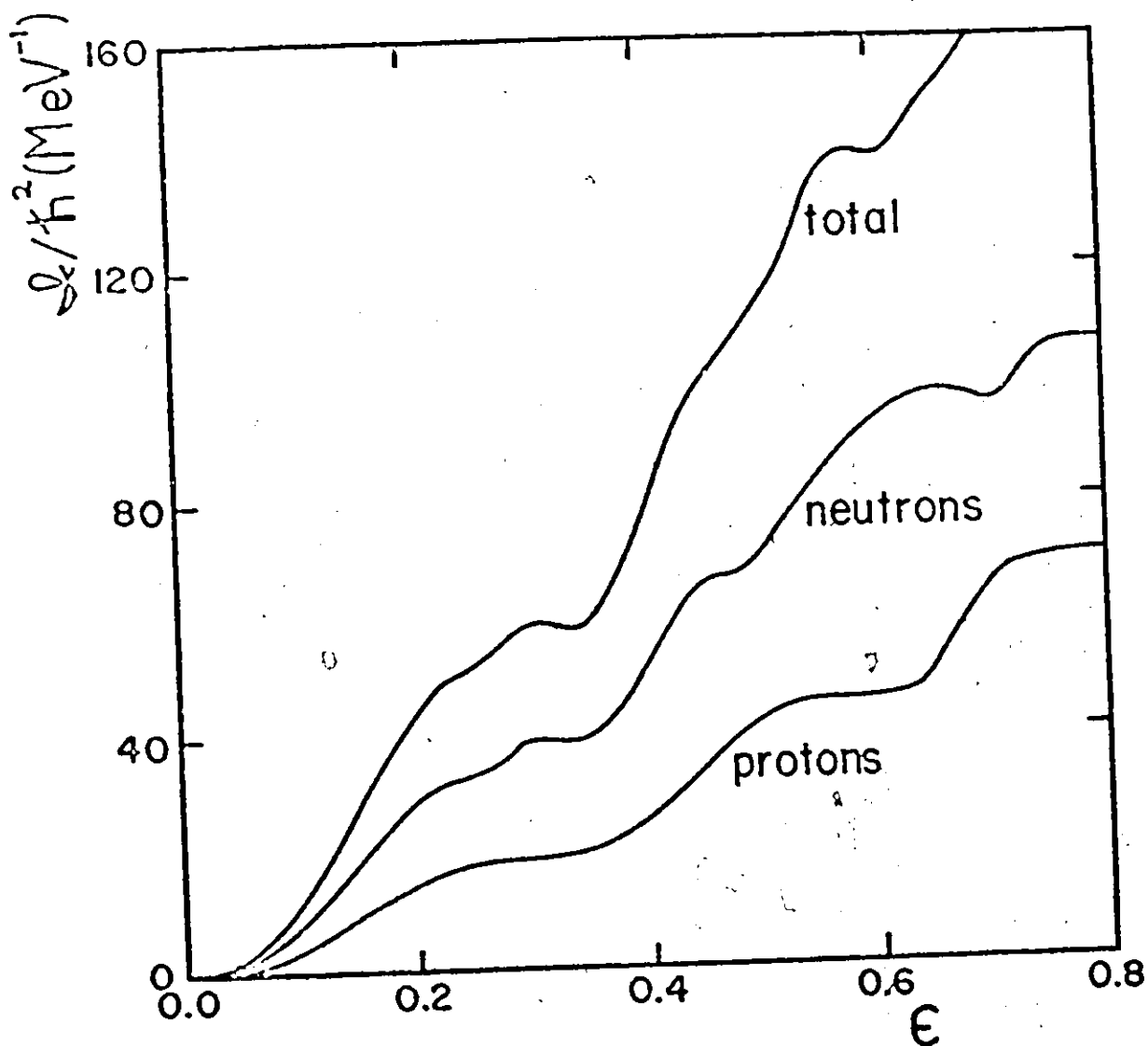


Fig. 14 Moment of inertia as a function of the quadrupole deformation  $\epsilon$  for  $^{256}\text{No}$ . The cranking model including pairing effects was used to calculate  $J$ , and the separate contributions of the neutrons and protons are also shown.

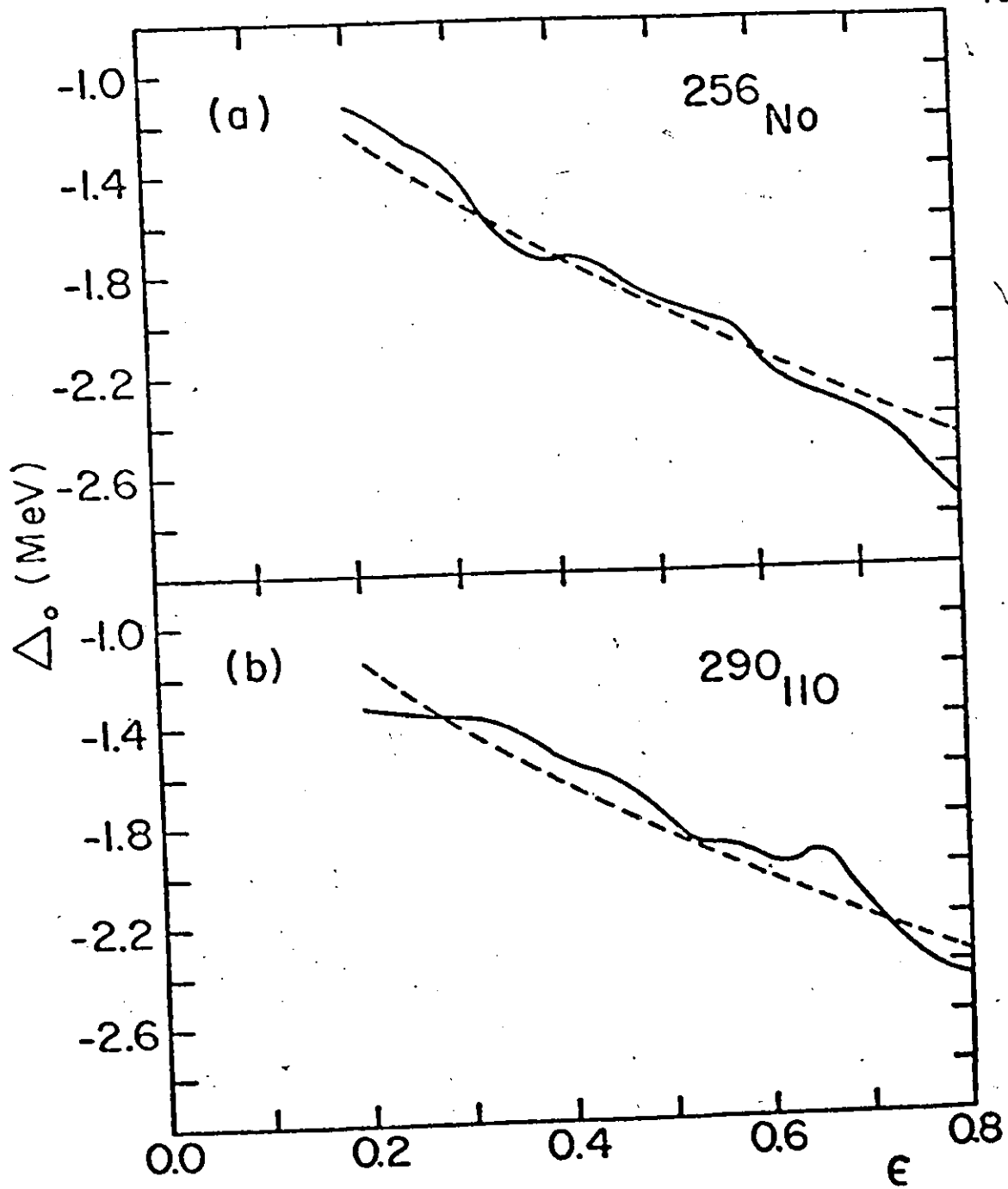


Fig. 15 The projection correction  $\Delta_0$  (solid line) and its smooth part  $\bar{\Delta}_0$  (dashed line) for a)  $^{256}\text{No}$  and b) the superheavy nucleus with  $Z=110$  and  $N=180$ .

extracted from it can be used to estimate  $\bar{\Delta}_0$ . The constants C, a and b were obtained by doing a least squares fit to  $\langle \underline{J}^2 \rangle$  and  $\mathcal{J}$  for five nuclei with values of A between 210 and 306 ( $^{210}\text{Po}$ ,  $^{232}\text{Th}$ ,  $^{256}\text{No}$ ,  $^{290}_{110}$  and  $^{306}_{118}$ ) and seven values of  $\epsilon$  (for each A) between 0.2 and 0.8. The results of the fitting are for

$$\langle \underline{J}^2 \rangle / \hbar^2 : C = 0.568, \quad a = 1.42, \quad b = 1.82, \quad (38)$$

and for

$$\mathcal{J} / \hbar^2 : C = 1.07 \cdot 10^{-2} \text{ MeV}^{-1}, \quad a = 1.83, \quad b = 1.31, \quad (39)$$

so that

$$\bar{\Delta}_0 = -26.2 A^{-0.41} \epsilon^{0.51} \text{ MeV} . \quad (40)$$

The dashed lines in fig. 15 show  $\bar{\Delta}_0$  as a function of deformation for  $^{256}\text{No}$  and  $^{290}_{110}$  and  $\delta\Delta_0$  may be obtained as the difference between the solid and dashed lines. It is seen to be everywhere less than 200 keV, and as such is a negligible contribution to  $E_0(\epsilon)$ . In fact, Bolsterli et al. (1972) estimate that there is an uncertainty of about 500 keV in their calculations of the shell correction  $\delta E$ , and so  $\delta\Delta_0$  is unimportant compared to the present ambiguities in the Strutinsky smoothing procedure.

CHAPTER V  
EFFECTS OF CENTRIFUGAL STRETCHING ON  
ROTATIONAL BANDS

V.1 Review of the Backbending Phenomenon.

One of the most characteristic features of the rare-earth nuclei ( $150 < A < 190$ ) is the existence of well-defined rotational bands. These bands are similar to those expected for a rigid rotor, and to a first approximation can be described by

$$E_J = \frac{\hbar^2}{2I} J(J+1) \quad , \quad (1)$$

where  $I$ , the moment of inertia, is constant. However, significant deviations from eq. (1) often occur, particularly at higher values of  $J$ , and attempts have been made to generalize eq. (1) as

$$E_J = AJ(J+1) + B[J(J+1)]^2 + \dots \quad , \quad (2)$$

where  $A$ ,  $B$ , ... are adjustable parameters. Although eq. (2) is an improvement over eq. (1), the convergence of this expansion has been found to be rather poor (Stephens et al. 1964), and alternative methods of parameterizing  $E_J$  have been proposed. In particular, Harris (1965) has generalized the



cranking model to obtain an expansion of  $E_J$  of the form

$$E_J = \alpha\omega^2 + \beta\omega^4 + \dots \quad (3)$$

where  $\omega$ , the angular velocity, is related to  $J$  and  $E_J$  through

$$\frac{dE_J}{d\omega} = \hbar\omega \frac{d[J(J+1)]^{1/2}}{d\omega} \quad (4)$$

For a given number of parameters, eq. (3) is found to give a considerably better fit to the experimental data than eq. (2) (Johnson and Szymanski 1973), although the reason for this is not well understood. Closely related to the Harris model is the variable moment of inertia (VMI) model of Mariscotti et al. (1969) in which the energy levels are described by a two-parameter formula of the form

$$E_J = \frac{1}{2} C (\mathcal{J} - \mathcal{J}_0)^2 + \frac{\hbar^2 J(J+1)}{2\mathcal{J}} \quad (5)$$

where  $C$  and  $\mathcal{J}_0$  are parameters, and  $\mathcal{J}$  is determined by the condition

$$\frac{\partial E_J}{\partial \mathcal{J}} = 0 \quad (6)$$

Eq. (5) has been shown by Mariscotti et al. (1969) to be equivalent to the two-parameter Harris formula, and this VMI model has been successfully applied to the rotational bands in a

wide range of rare-earth nuclei.

Although minor deviations from the spectrum of a rigid rotor have been observed in the rotational bands of rare-earth nuclei for some time, more recent measurements have shown that very large discrepancies may occur for high-lying levels. Working with the ground state band of  $^{162}\text{Er}$ , Johnson et al. (1972) were the first to observe a sudden change in the character of the band near  $J=14$ , and their measurements suggested that the nuclear moment of inertia may increase dramatically over a range of about four units of  $J$ . Similar results have now been obtained for a wide range of rare-earth nuclei, and recent measurements are summarized by Johnson and Szymanski (1973).

The analysis of these measurements is commonly discussed in terms of a plot of  $2\mathcal{I}/\hbar^2$  versus  $(\hbar\omega)^2$ , where  $\omega$  is related to  $J$  through

$$\omega = \hbar\sqrt{J'(J'+1)}/\mathcal{I}, \quad (7)$$

where  $J'$  is considered to be a continuous variable. In order to relate  $\omega$  and  $\mathcal{I}$  to the experimental energy levels, eqs. (5) and (6) are used to give (Johnson and Szymanski 1973)

$$\hbar\omega = 2\sqrt{J'(J'+1)} \left[ \frac{dE_{J'}}{dJ'(J'+1)} \right], \quad (8)$$

and once  $\hbar\omega$  is known,  $2\mathcal{L}/\hbar^2$  can be determined from eq. (7)

as

$$\frac{2\mathcal{L}}{\hbar^2} = \left[ \frac{dE_{J'}}{dJ'(J'+1)} \right]^{-1} \quad (9)$$

Since  $E_{J'}$  is only known at integer values of  $J'$ , the derivatives in eq. (8) and (9) must be approximated in terms of finite differences, and this is done by assuming that the local variation of  $E_{J'}$  with  $J'(J'+1)$  is quadratic. Then for the transition  $J$  to  $J-2$ , the derivatives will be exact for

$$J'(J'+1) = \sqrt{J^2 - J + 1} \quad , \quad (10)$$

and so

$$(\hbar\omega)^2 = 4(J^2 - J + 1) \left[ \frac{E_J - E_{J-2}}{4J-2} \right]^2 \quad , \quad (11)$$

and

$$\frac{2\mathcal{L}}{\hbar^2} = \left[ \frac{4J-2}{E_J - E_{J-2}} \right] \quad . \quad (12)$$

Fig. 16a shows  $2\mathcal{L}/\hbar^2$  versus  $(\hbar\omega)^2$  for the ground state band of  $^{162}\text{Er}$  (Johnson and Szymanski 1973) and each point obtained from eq. (11) and (12) is for simplicity labeled by

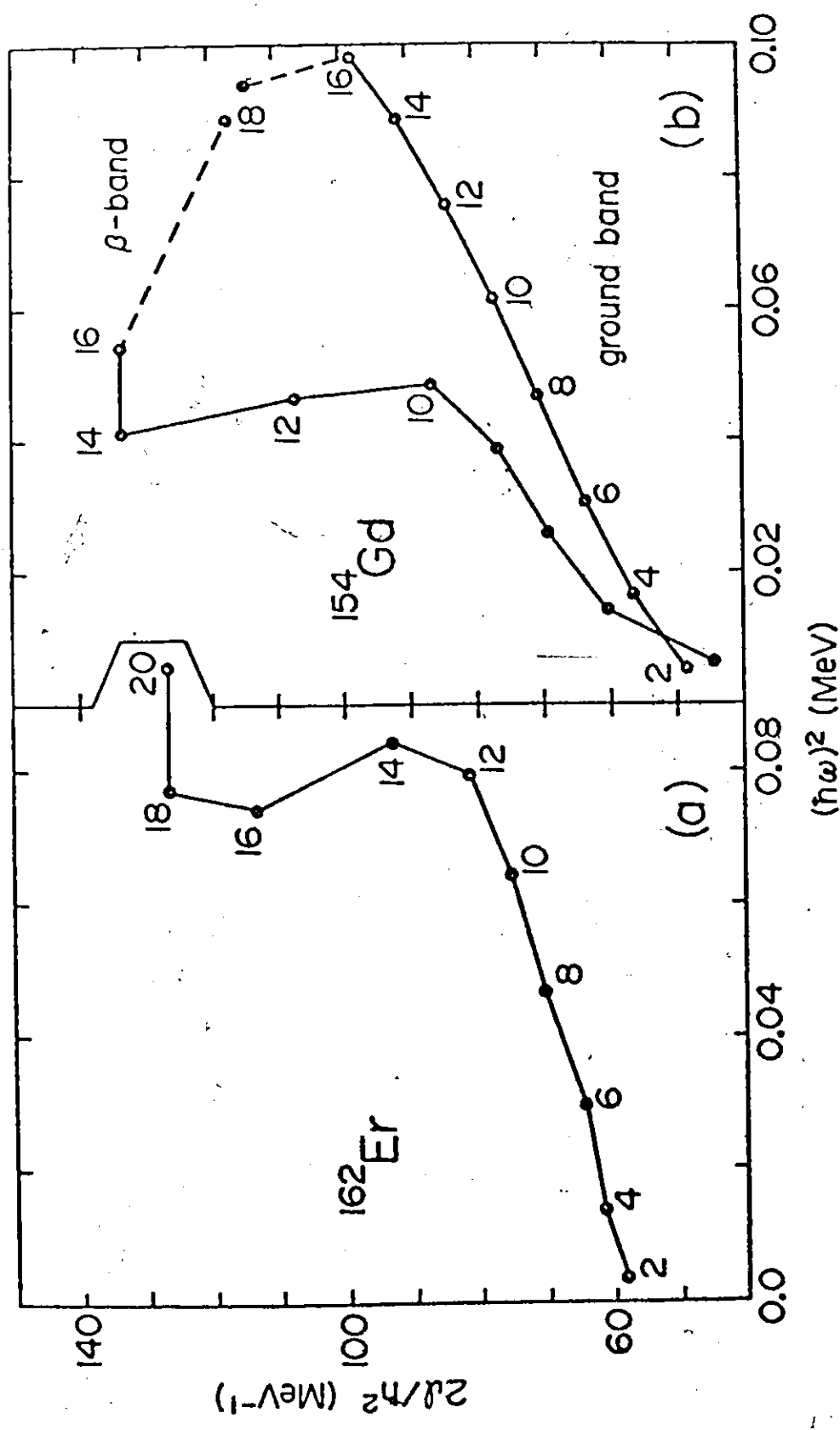


Fig. 16  $2\epsilon/\hbar^2$  versus  $(\hbar\omega)^2$  for a) the ground state band of  $^{162}\text{Er}$  and b) the ground state band and  $\beta$ -band of  $^{154}\text{Gd}$ . The number labeling each point is the corresponding angular momentum, and the dashed lines indicate that the data for  $I=18$  of  $^{154}\text{Gd}$  are still tentative.



the corresponding value of  $J$ , and not  $J'$  as given by eq. (10). Measurements have also been performed (Ward et al. 1973a) Khoo et al. 1973) for both the ground state band and  $\beta$ -band of  $^{154}\text{Gd}$ , and these results are shown in fig. 16b. The term "backbending" has come to be used for those regions of fig. 16 in which  $(\hbar\omega)^2$  decreases as  $2\mathcal{J}/\hbar^2$  increases, while "downbending" refers to the regions in which  $(\hbar\omega)^2$  increases as  $2\mathcal{J}/\hbar^2$  decreases.

The possibility of a sudden increase in the moment of inertia at large values of  $J$  was first suggested by Mottelson and Valatin (1960). They pointed out that the Coriolis force tends to counteract the short-range pairing correlations, and that for sufficiently large values of  $J$  it may destroy them completely. If this is the case, there will exist a critical value of  $J$  at which the nucleus will undergo a phase transition from the superfluid to the normal state, and the gap parameter  $\Delta$  will go to zero. Because of the dependence of the moment of inertia on the gap parameter (Rowe 1970, p.127), a sudden decrease in  $\Delta$  would lead to a corresponding increase in  $\mathcal{J}$ , and to the observed backbending behaviour.

A large number of calculations on the backbending phenomenon have been reported, and all except one utilize the CAP effect of Mottelson and Valatin. The only exception is the band-crossing model of Stephens and Simon (1972) in which the sudden change in the moment of inertia is attributed to a crossing of the zero-quasiparticle ground state

band and a two-quasiparticle rotational band with a larger moment of inertia at some critical value of  $J$ . Although this model is able to at least qualitatively explain the observed backbending and downbending behaviour, Damgaard and Faessler (1973) have pointed out that if the CAP effect is included in this model, backbending occurs for values of  $(\hbar\omega)^2$  much smaller than observed experimentally.

Many of the calculations involving the CAP effect have been based on schematic models, and consider only the changes in the pairing correlations as the angular momentum increases (Sorensen 1971, Krumlinde and Szymanski 1971, Vallieres et al. 1972). However, various models have been proposed which also allow for the possibility of centrifugal stretching (Bes et al. 1968, Krumlinde 1968, Krumlinde 1971) and more recently, calculations based on Hartree-Bogolyubov theory which allow for changes in both the pairing correlations and the nuclear shape have been attempted (Kumar 1972, Faessler et al. 1973, Goeke et al. 1973). The basic result of these more realistic calculations is that centrifugal stretching plays only a minor role in the observed backbending behaviour, and that the main effect comes from a sudden decrease in the neutron pairing gap. On the other hand, for some nuclei the deformation energy can show considerable structure as a function of deformation (Kumar and Baranger 1968, Nilsson et al. 1969, Gotz et al. 1972) and it might be expected that for these cases stretching

effects could be very important.

In order to investigate the possible effects of stretching on the moment of inertia, a simple model consisting of two particles of equal mass interacting through a potential  $V(r)$  was constructed. For this two-particle rotor the energy levels can be obtained exactly, and the form of  $V(r)$  varied in order to determine what features it must have in order to give rise to backbending and downbending. In the next section, the governor model of Trainor and Gupta (1971) is used to indicate that a two-particle rotor may be considered as a first approximation to a deformed rotating nucleus, and the mass and equilibrium separation are estimated using this model. Besides showing that for an appropriate choice of  $V(r)$  backbending and downbending can be obtained, the reduced transition probabilities in the ground state band are calculated and compared with the predictions of the rigid rotor model.

The possible effects of stretching in more realistic calculations is examined qualitatively in the final section, and it is suggested that a prolate-to-oblate shape transition at high excitation energies is one form of stretching which could lead to backbending.

## V.2 Backbending in a Simple Stretching Model.

The governor model of Trainor and Gupta (1971) assumes

that for a deformed rotating nucleus, there exists a rotationally invariant core which does not participate in the rotational motion, and that only the mass outside this core contributes to the rotational energy. Assuming that any centrifugal stretching which may take place is controlled by harmonic restoring forces, this model is able to give reasonably good fits to the energy levels of the ground state band of rare-earth nuclei for  $I \leq 14$ . The size of the rotationally invariant core decreases as the angular momentum increases, although this variation is generally less than 8% from the ground state to the state with  $I=14$ . To the extent that the size of the core remains constant, and the mass outside the core can be approximated by two point masses separated by a distance of about twice the nuclear radius, the governor model can be further approximated as a two-particle rotor. The mass and equilibrium separation of the two-particle system can then be estimated using the ground state moment of inertia combined with the core size obtained empirically by Trainor and Gupta.

The mass and equilibrium size of the rotor will be estimated using the data for  $^{162}\text{Er}$ , although similar results would be obtained for any nuclei in this region. The size of the rotationally invariant core varies from about 140 nucleons for the ground state of  $^{162}\text{Er}$  to 132 nucleons for the state with  $I=14$ , and so the "average" size of the core is 136 nucleons. This means that roughly 26 nucleons are



actively participating in the rotational motion, and so the reduced mass of the rotor is  $\mu=6.5$  nucleon masses.

As a result,

$$\hbar^2/2\mu \approx 3.2 \text{ MeV-fm}^2, \quad (13)$$

and this value has been used in all of the present calculations. For the ground state band of  $^{162}\text{Er}$ ,  $2\mathcal{J}_0/\hbar^2$  is approximately  $59 \text{ MeV}^{-1}$  (see fig. 16a), and using

$$\mathcal{J}_0 = \mu r_0^2 \quad (14)$$

gives the equilibrium size of the rotor to be  $r_0 \approx 14 \text{ fm}$ .

The form of the two-body interaction  $V(r)$  is largely arbitrary, and the principal motivation of the present work was to determine if it is possible to obtain backbending for any reasonable form of  $V(r)$ . However, shell correction calculations based on the Strutinsky method (Nilsson et al. 1969) indicate that at least for actinide nuclei the deformation energy may display two (or more) minima as a function of deformation. Similar calculations (Gotz et al. 1972) show that some rare-earth nuclei, particularly those near the Pt region may also have a secondary minimum in the deformation energy for prolate deformations considerably larger than the ground state minimum. In order to determine how a secondary minimum might affect the spectrum of a deformed

nucleus,  $V(r)$  was constructed from three matching parabolas as

$$V(r) = \begin{cases} a_2(r-r_0)^2 & r < m_1 \\ b_2(r-r_1)^2 + b_0 & m_1 < r < m_2 \\ c_2(r-r_2)^2 + c_0 & r > m_2 \end{cases} \quad (15)$$

When the parameters  $r_0$ ,  $r_1$ ,  $r_2$ ,  $b_0$ ,  $c_0$  and  $a_2$  are given, the matching radii  $m_1$  and  $m_2$  and the curvatures  $b_2$  and  $c_2$  are determined by the requirement that the three parabolas and their first derivatives are continuous at  $m_1$  and  $m_2$ . For the potential denoted by  $P_1$  and shown in fig. 17 the parameters are

$$\begin{aligned} r_0 &= 14 \text{ fm}, & b_0 &= 1.75 \text{ MeV}, & a_2 &= 0.1 \text{ MeV-fm}^{-2}, \\ r_1 &= 19 \text{ fm}, & c_0 &= 1.1 \text{ MeV}, \\ r_2 &= 21 \text{ fm}, \end{aligned} \quad (16)$$

while for potential  $P_2$  shown in the same figure they are

$$\begin{aligned} r_0 &= 13 \text{ fm}, & b_0 &= 2.35 \text{ MeV}, & a_2 &= 0.1 \text{ MeV-fm}^{-2}, \\ r_1 &= 19 \text{ fm}, & c_0 &= 1.8 \text{ MeV}, \\ r_2 &= 21 \text{ fm}. \end{aligned} \quad (17)$$

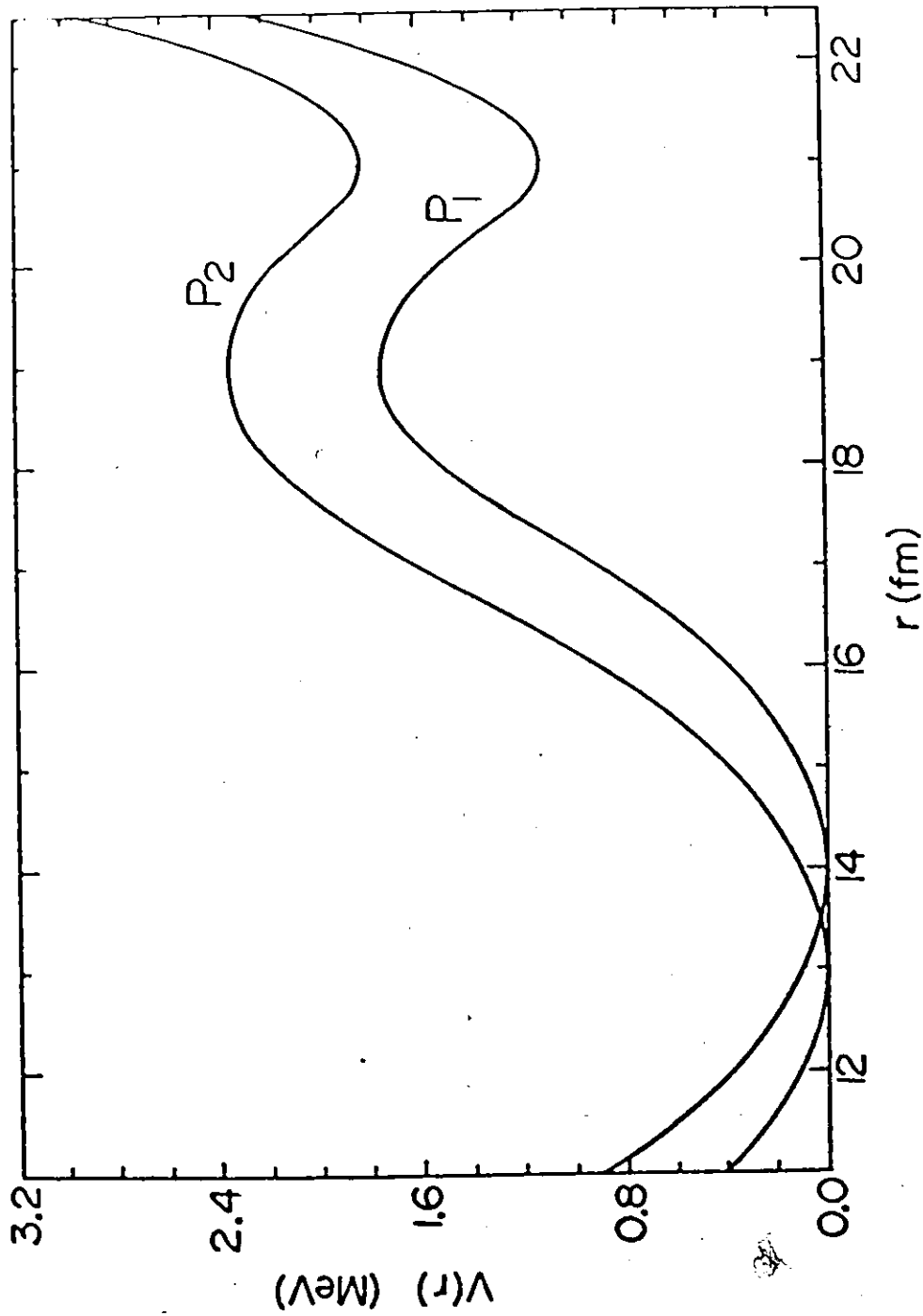


Fig. 17 The potentials  $P_1$  and  $P_2$  formed from three matching parabolas, and used in calculating the spectrum of the two-particle rotor.

Once the potential  $V(r)$  is specified, the Schrodinger equation for the two-body system may be solved numerically, and the same method used in Chapter III has been applied here. The energy levels may be classified according to the radial quantum number  $n(n=0,1,\dots)$  and the angular momentum  $J(J=0,2,\dots)$  where for a given  $J$  the energy increases with increasing  $n$ . In the terminology used to describe the experimental spectra of deformed nuclei, the energy levels corresponding to  $n=0$  belong to the ground state band while those with  $n=1$  are members of the  $\beta$ -band.

The energy levels as a function of  $J$  for potentials  $P_1$  and  $P_2$  are shown in fig. 18, and the corresponding plot of  $2\mathcal{E}/\hbar^2$  versus  $(\hbar\omega)^2$  for the ground state band and  $\beta$ -band of potential  $P_1$  is shown in fig. 19. On comparing fig. 19 with fig. 16a, it is seen that the backbending in the ground state band has been reproduced rather well. None of the levels in the  $\beta$ -band of  $^{162}\text{Er}$  have been identified as yet, but fig. 16b shows that the  $\beta$ -band of  $^{154}\text{Gd}$  exhibits backbending at  $J=10$ . By choosing parameters for the two-body potential corresponding to  $P_2$ , the results shown in fig. 20 for  $2\mathcal{E}/\hbar^2$  versus  $(\hbar\omega)^2$  were obtained. This figure shows that the rotor model is qualitatively able to reproduce the backbending and downbending in the  $\beta$ -band as well as the backbending in the ground state band.

The basic reason for the sudden increase in the moment of inertia of the ground state band at a particular value of

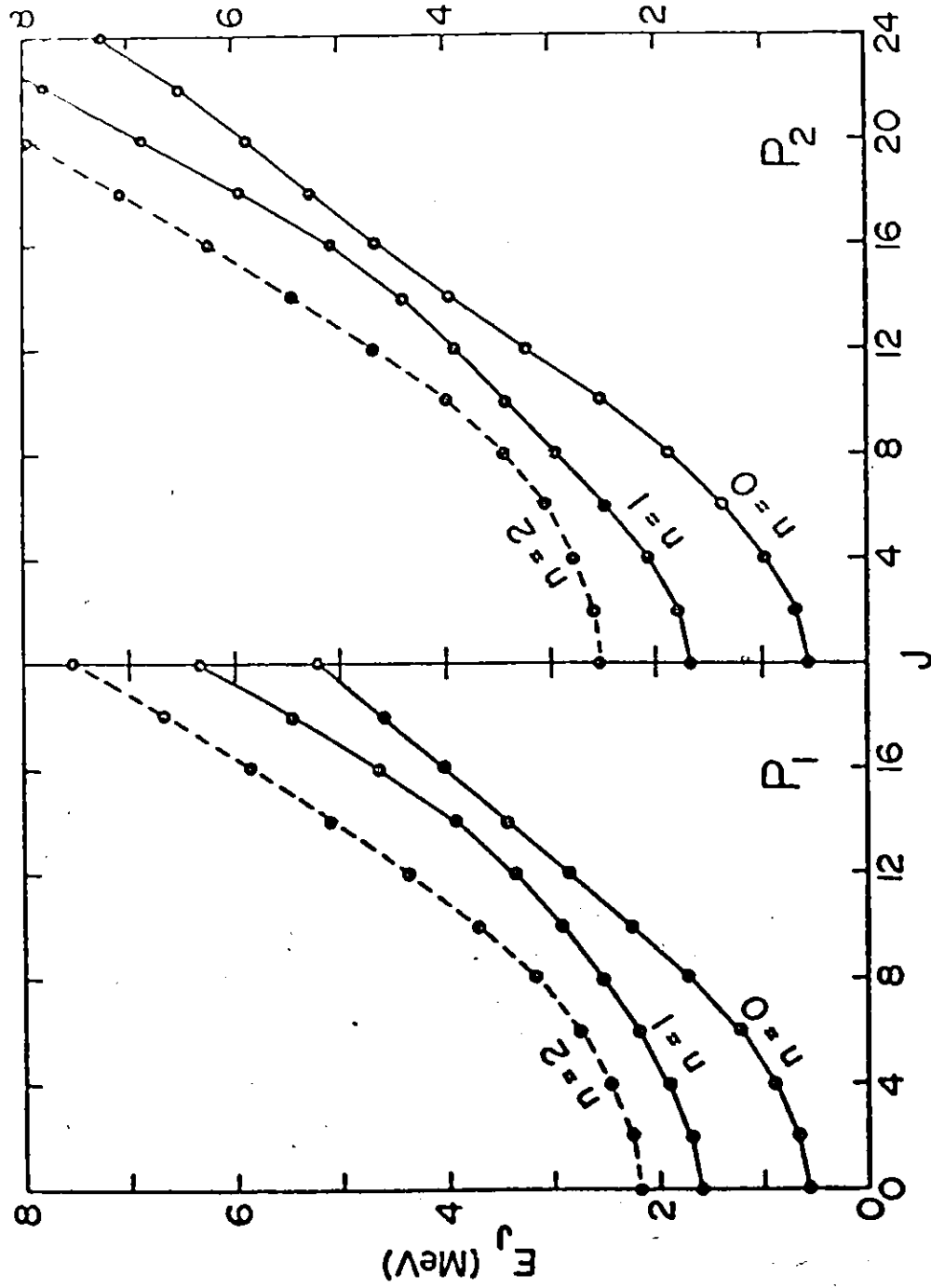


Fig. 18 Energy levels as a function of angular momentum for potentials  $P_1$  and  $P_2$ . The radial quantum number is shown for each band. The figure clearly illustrates the anomalous features of the ground state band and  $\beta$ -band which give rise to backbending and downbending.

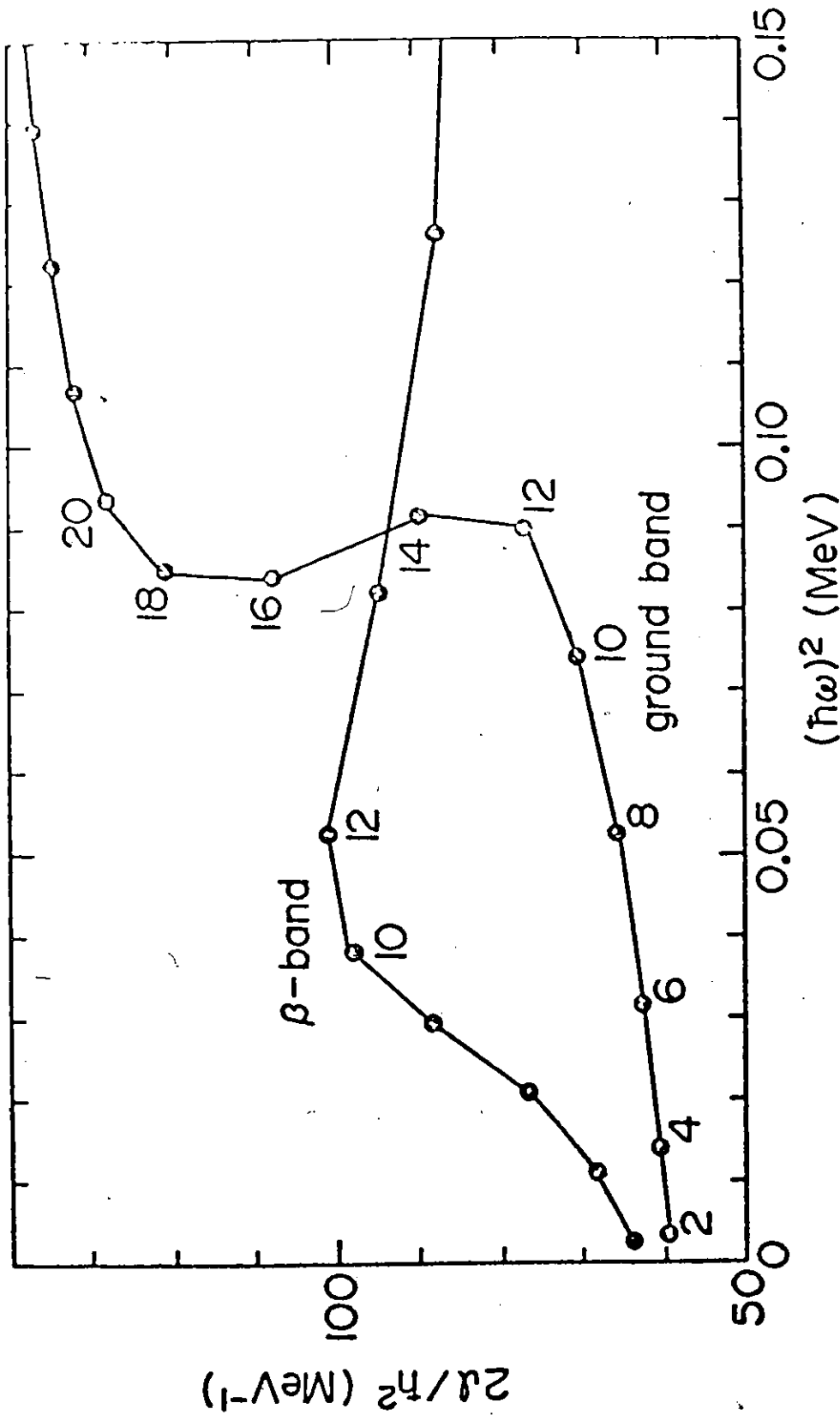


Fig. 19  $2I/h^2$  versus  $(\hbar\omega)^2$  for the ground state band and  $\beta$ -band of potential  $P_1$ . Each point has been labeled with its corresponding angular momentum, and the points for different  $J$  have been joined by straight lines.

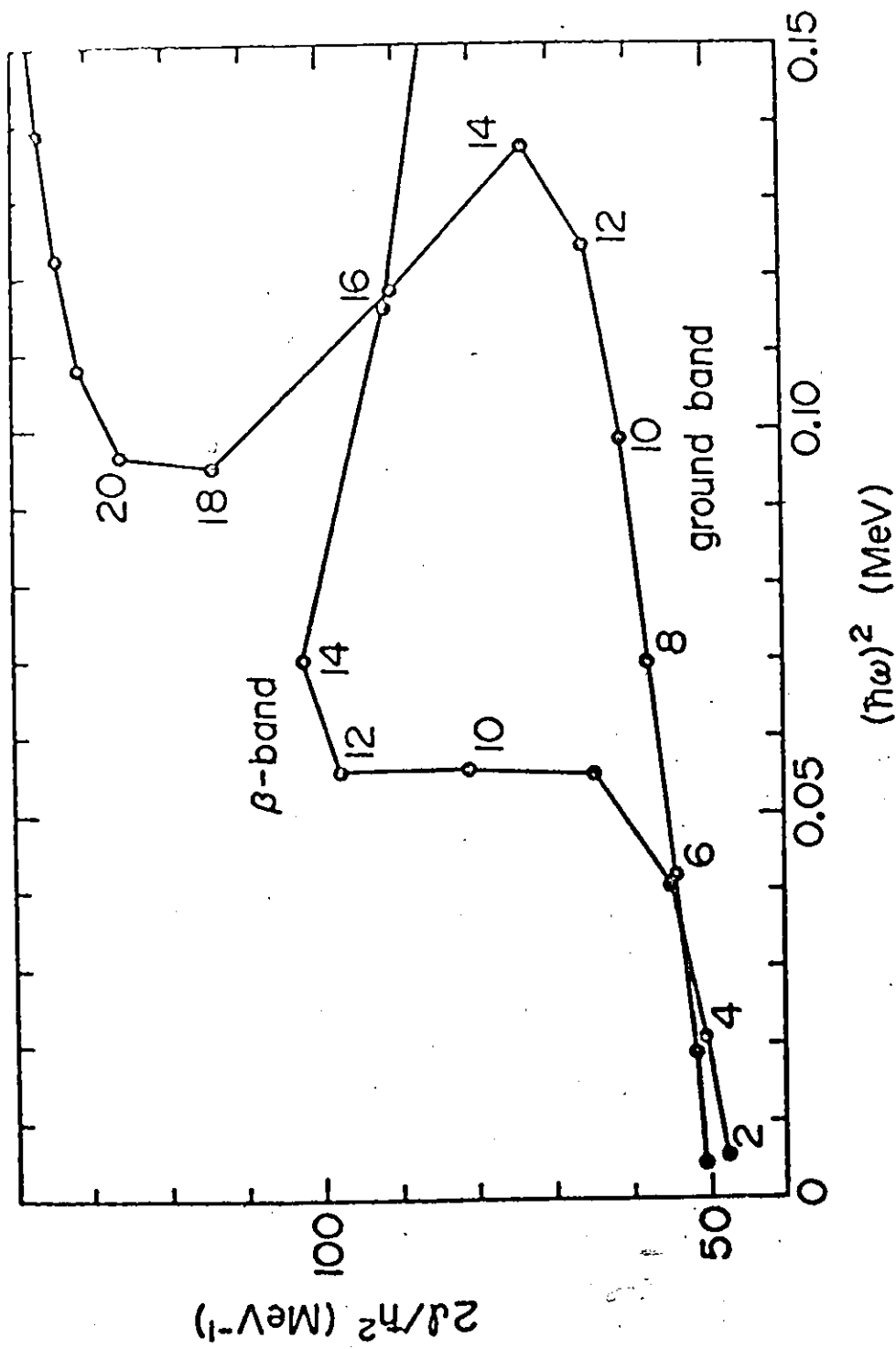


Fig. 20 Same as fig. 19, but for potential  $P_2$ .

the angular momentum can be related to the effect of the centrifugal barrier on the separation of the two masses in the rotor. For the two-particle system, this barrier is given by  $\frac{\hbar^2 J(J+1)}{2\mu r^2}$ , while the effective potential which controls vibrations of the coordinate  $r$  is given by

$$V_J(r) = V(r) + \frac{\hbar^2 J(J+1)}{2\mu r^2} \quad (18)$$

For small values of  $J$ , the first minimum of  $V_J(r)$  (the one nearest  $r=0$ ) will remain lower than the second. However, for a given  $J$ , the centrifugal barrier is largest for small values of  $r$ , and as a result, there exists some critical value of  $J$  at which the lowest minimum of  $V_J(r)$  shifts to the vicinity of the secondary minimum of  $V(r)$ . Under these circumstances, the (average) size of the rotor shifts to a value of  $r$  near this new minimum of  $V_J(r)$  and the moment of inertia undergoes a corresponding increase, leading to the observed backbending behaviour.

The major discrepancy between the results calculated from potentials  $P_1$  and  $P_2$  and those deduced from the experimental values of  $E_J$  is that the calculated moments of inertia are slightly too small. This can be remedied by allowing the rotor to stretch more easily (decrease  $a_2$ ) although the separation of the two particles then tends to become unrealistically large. However, a serious limitation of the rotor model is that the mass is fixed, while in the governor



model the amount of mass participating in the rotational motion increases with increasing  $J$ . If this effect could be incorporated into the rotor model, the moment of inertia could increase more rapidly with increasing angular momentum than is permitted with simple stretching.

Although backbending has been observed in a wide range of rare-earth nuclei, it is only recently that attempts have been made to measure the reduced transition probability  $B(E2, J \rightarrow J-2)$  for values of  $J$  lying in the backbending region. Measurements have been reported (Ward et al. 1973b) for several of the  $J \rightarrow (J-2)$  transitions in the ground state band of  $^{158}\text{Er}$ , and despite the fact that this nuclide shows extreme backbending (Davidson et al. 1972) the reduced transition probabilities are found to be consistent with those predicted by the simple rotational model. These results can be used as a further test of the stretching model proposed in this section, and in order to calculate  $B(E2)$  for the two-particle rotor, the assumption is made that each of the two masses has a charge  $ze$  where  $z$  is given by

$$z = (Z/A)a,$$

and  $a$  is the mass number of each of the particles in the rotor.

If  $|JM\rangle$  specifies a nuclear state with angular momentum  $J$  and  $z$ -component of  $J$  given by  $M$ , then the reduced

transition probability is defined by (Rowe 1970, p.21)

$$B(E2, J_i \rightarrow J_f) = \sum_{M_f} |\langle J_f M_f | Q_{2\mu} | J_i M_i \rangle|^2, \quad (19)$$

where  $M_i$  can take on any value consistent with  $-J_i \leq M_i \leq J_i$ .

The operator  $Q_{2\mu}$  is given by

$$Q_{2\mu} = e \sum_i r_i^2 Y_{2\mu}(\Omega_i), \quad (20)$$

where the sum is over all the protons in the nucleus. In the rotor model, only the protons in the two point masses are assumed to participate in the E2 transitions, and so eq. (20) simplifies to

$$Q_{2\mu} = 0.5 ze r^2 Y_{2\mu}(\Omega), \quad (21)$$

where the vector  $\underline{r}$  specifies the relative coordinates of the two-particle system. For the rotor, the wave function  $|JM\rangle$  is given by

$$|JM\rangle = R_{0J}(r) Y_{JM}(\Omega), \quad (22)$$

where  $R_{0J}(r)$  denotes the radial wave function with quantum numbers  $n=0$  and  $J$ , and so  $B(E2)$  becomes

$$B(E2, J \rightarrow J-2) = \frac{5 \cdot 10^{-4}}{16\pi} z^2 (2J-3) \begin{pmatrix} J & 2 & J-2 \\ 0 & 0 & 0 \end{pmatrix}^2$$

$$\times \left\{ \int_0^\infty R_{0(J-2)}(r) r^2 R_{0J}(r) r^2 dr \right\}^2 e^{2-b^2}, \quad (23)$$

where  $lb = 10^{-24} \text{ cm}^2$ . The corresponding result for a rigid rotor is

$$B(E2, J \rightarrow J-2) = \frac{5}{16\pi} (2J-3) \begin{pmatrix} J & 2 & J-2 \\ 0 & 0 & 0 \end{pmatrix}^2 Q_0^2 e^{2-b^2}, \quad (24)$$

where  $Q_0$  is the quadrupole moment of the ground state band.

The results obtained for  $^{162}\text{Er}$  using eqs. (23) and (24) are shown in fig. 21, where  $Q_0$  has been determined such that eq. (23) and (24) give the same value for  $B(E2, 2 \rightarrow 0)$ . This figure shows that a simple stretching model predicts that the transition probabilities in the backbending region should be greatly enhanced over the corresponding rigid rotor values. This result is in disagreement with the measurements of Ward et al. (1973b) and suggests that centrifugal stretching is not an important mechanism in the backbending region. However, the rotor model proposed in this section is only able to simulate stretching in the prolate direction, and does not include the possibility of more complicated stretching mechanisms such as a prolate-to-oblate shape transition. This possibility, as

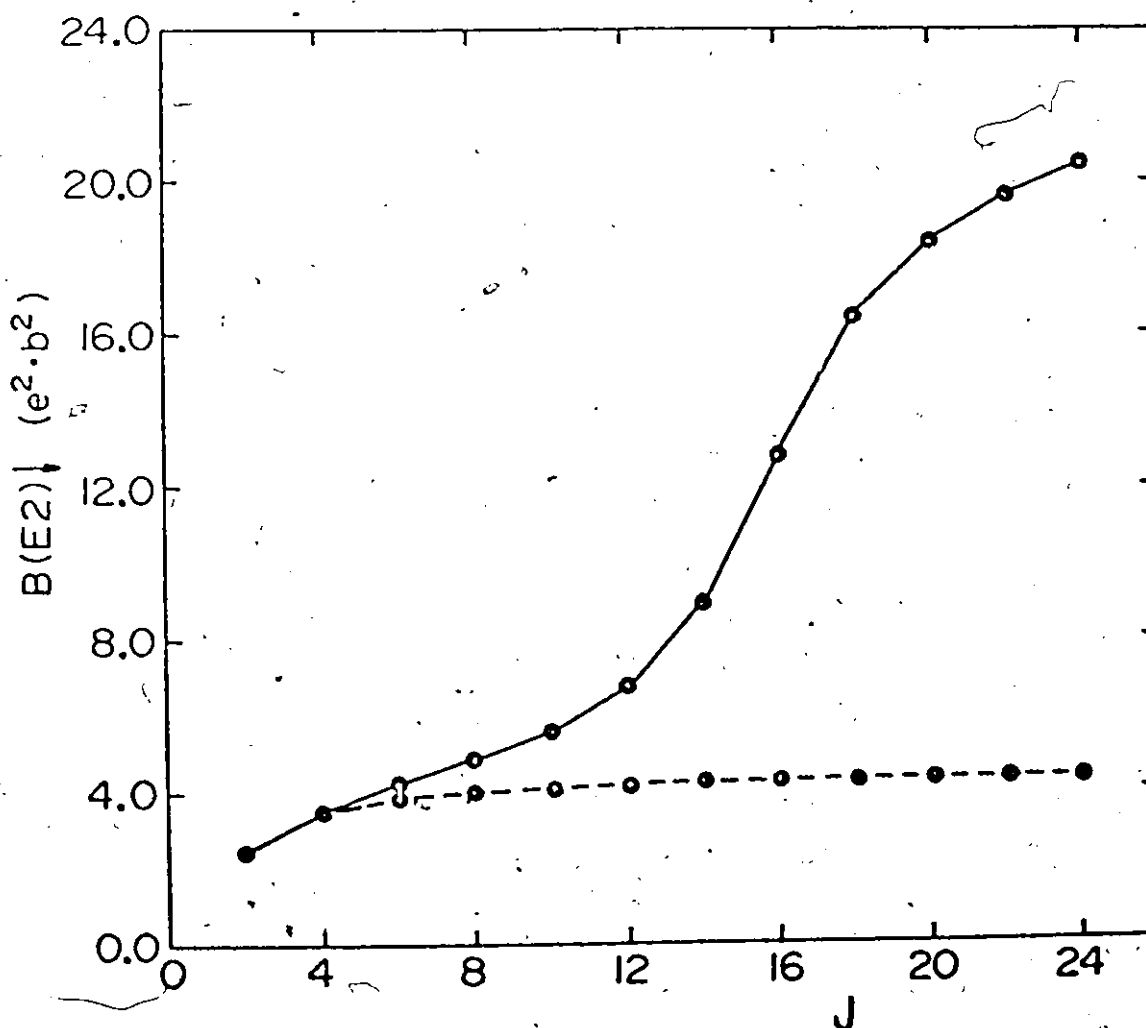


Fig. 21 The reduced transition probability  $B(E2)$  as a function of  $J$  for the transitions  $J \rightarrow J-2$  in the ground state band of potential  $P_1$ . The results from the exact calculation are shown by the solid line, while the values predicted by the rotational model are shown by the dashed line.

well as its effect on the reduced transition probability, will be examined qualitatively in the next section.

### V.3 Possible Effects of More Complicated Stretching.

The rotor model of the last section was constructed to simulate the possible effects of a secondary minimum in the nuclear deformation energy for prolate deformations considerably larger than the ground state minimum. Although this model is able to give backbending in the ground state band, and backbending and downbending in the  $\beta$ -band, it does not seem possible (at least with the form of  $V(r)$  given by eq. (15)) to obtain the downbending which has recently been observed experimentally (Davidson et al. 1972) for the ground state band. Another weakness of the model is that it predicts transition probabilities in the ground state band which are greatly enhanced over the rotational model values, in contrast to the recent measurements for  $^{158}\text{Er}$ . On the other hand, Gotz et al. (1972) have performed detailed calculations of the deformation energy for rare-earth nuclei using the Strutinsky method, and their calculations show that isotopes of Pt show a well-defined secondary minimum at large prolate deformations. Although backbending has not yet been observed for Pt, measurements have been reported for the nearby nuclide of  $^{182}\text{Os}$  and  $^{180}\text{W}$  (Warner and Bernthal 1972, Bethoux and Lindblad 1972) and it may be that stretching in the prolate direction is more important

in these cases than it is for the lighter rare-earth elements. Measurements of  $B(E2)$  for these isotopes should help to determine whether or not this is the case.

Another feature of the deformation energy which might be expected to lead to anomalous behaviour in rotational bands at high excitation energies is the existence of an oblate minimum slightly higher in energy than the prolate ground state minimum. Calculations of the deformation energy using the pairing-plus-quadrupole model (Kumar and Baranger, 1968) show that both minima are present for many of the isotopes of Er, and a secondary oblate minimum might be expected to have a similar influence on the spectra of the ground state band and  $\beta$ -band as the second prolate minimum discussed in the last section. However, a detailed examination of the effect of an oblate minimum must include the asymmetric degree of freedom  $\gamma$  as well as the quadrupole deformation  $\beta$ , since it is through a change in  $\gamma$  by  $60^\circ$  that any prolate-to-oblate shape transition will occur. Unfortunately, the rotor model is not able to simulate the effects of deviations from axial symmetry, and a detailed solution for the eigenvalues and eigenfunctions of the Bohr Hamiltonian for a given deformation energy  $V(\beta, \gamma)$  is quite complicated (Kumar and Baranger 1967). As a result, the present section is only a qualitative discussion of the possibility of a prolate-to-oblate shape transition at high excitation energies, and its effect on the ground state band and  $\beta$ -band spectra, and

on the reduced transition probabilities.

The solid line in fig. 22. is a schematic plot of the deformation energy  $V(\beta, \gamma)$  as a function of  $\beta$  for  $\gamma=0$ , and for simplicity it will be denoted by  $V(\beta)$ . Since  $\gamma=0$ , only axially symmetric shapes are represented in this figure, with positive and negative values of  $\beta$  leading respectively to prolate and oblate shapes. The essential features of  $V(\beta)$  as shown in fig. 22 is the existence of a prolate minimum at  $\beta_p$  and an oblate minimum at  $\beta_o$  with the following properties:

$$|\beta_o| > \beta_p \quad (25)$$

$$V(\beta_o) > V(\beta_p) \quad (26)$$

For a given angular momentum  $J$ , the effective potential for  $\beta$ -vibrations is given by

$$V_J(\beta) = V(\beta) + \frac{\hbar^2 J(J+1)}{2\mathcal{I}(\beta)} \quad (27)$$

where  $\mathcal{I}(\beta)$  is the moment of inertia. As the work of Chapter IV shows,  $\mathcal{I}(\beta)$  is in general a complicated function of  $\beta$ , but for the qualitative discussion in this section, it is sufficient to take the hydrodynamic estimate of  $\mathcal{I}(\beta)$  which gives (Rowe 1970, p.120)

$$\mathcal{I}(\beta) = 388\beta^2 \quad (28)$$

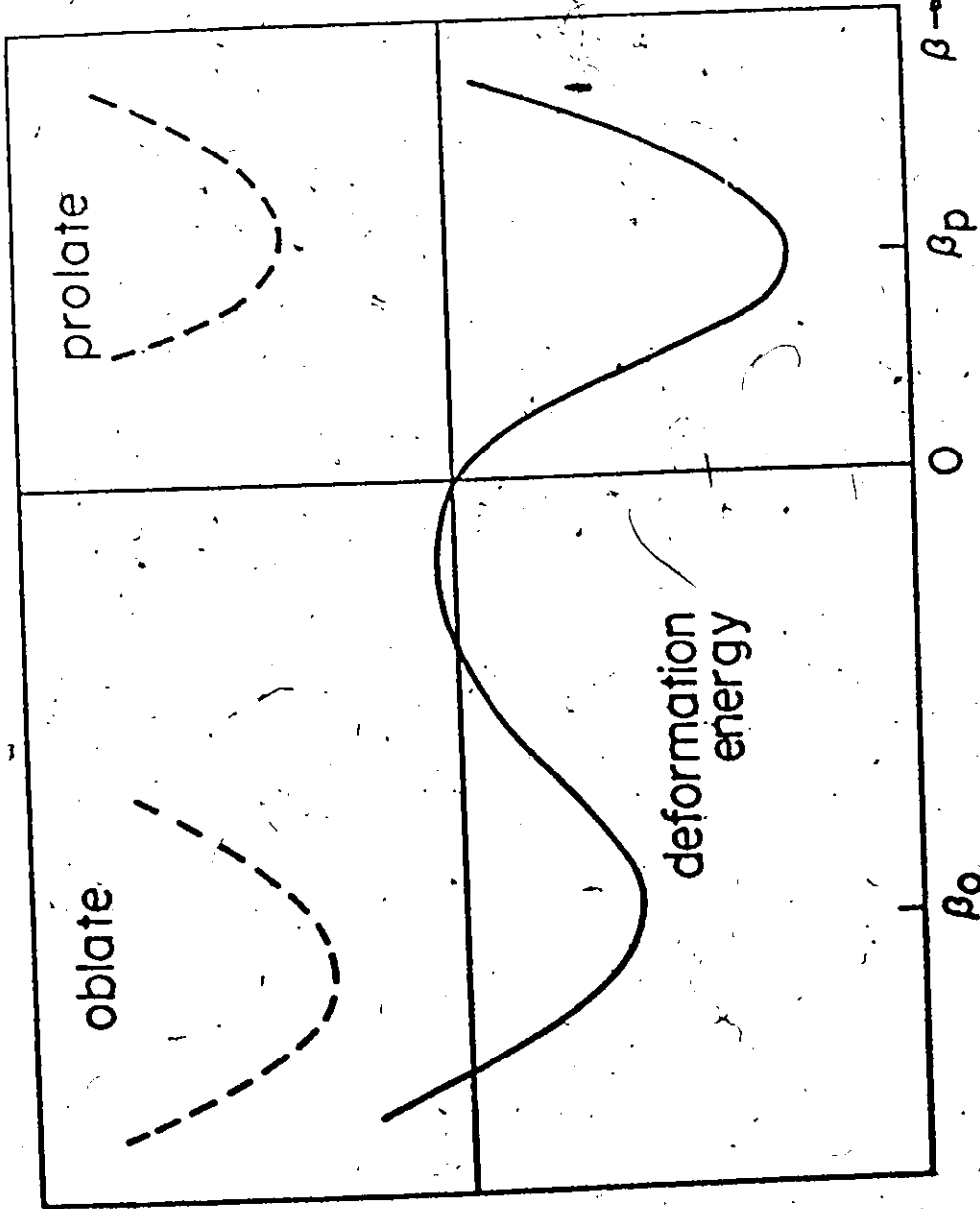


Fig. 22 Schematic of the possible dependence of the nuclear deformation energy on the deformation  $\beta$  (solid line). When the rotational kinetic energy is added to the deformation energy, the oblate minimum of the effective potential for  $\beta$ -vibrations becomes lower than the corresponding prolate minimum for some critical angular momentum, as shown by the dashed lines.



where  $B$  is the inertial mass for quadrupole deformations.

Then eq. (27) becomes

$$V_J(B) = V(B) + \frac{\hbar^2 J(J+1)}{6B^2} \quad (29)$$

and the argument now follows closely the discussion given in the last section on the reasons for backbending in the rotor model.

For small values of  $J$ , the prolate minimum of  $V_J(B)$  will be lower than the corresponding oblate minimum. However, because of eq. (25) there will exist some critical value of  $J$  given by  $J_c$  for which the oblate minimum of the effective potential becomes lower than the prolate minimum. (The dotted lines in fig. 22 illustrate this situation). Under these circumstances, the nucleus will undergo a prolate-to-oblate shape transition, and because of the larger moment of inertia associated with the oblate shape, a sudden change should occur in a plot of  $2J/\hbar^2$  versus  $(\hbar\omega)^2$  for values of  $J$  near  $J_c$ . Whether or not this shape transition will be sharp enough to lead to backbending will depend on how well defined the prolate and oblate minima are, and can only be determined by more detailed calculations.

The effect of a shape change on the reduced transition probability is more difficult to estimate because of the sensitive dependence of the  $B(E2)$  on the nuclear wave functions. However, the main reason for the enhancement of  $B(E2)$  in the

rotor model is that even as the equilibrium shape shifts toward the secondary prolate minimum, the overlap of the wave functions for the states specified by  $J$  and  $(J-2)$  remains large. As a result, the matrix element in eq. (23) is approximately  $\langle r^2 \rangle$ , and so the  $B(E2)$  will increase dramatically as the rotor stretches. On the other hand, a shape change involving a prolate-to-oblate transition involves not only an increase in  $|\beta|$ , but also a change of  $\gamma$  by  $60^\circ$ . Because of this sudden change in  $\gamma$ , the overlap of the wave functions before and after the transition may be rather small, and so the enhancement of  $B(E2)$  may be less than obtained using the rotor model.

Although the calculations of Kumar and Baranger (1968) show that the deformation energy for the Er isotopes has both a prolate and oblate minimum, the deformation of the oblate minimum is generally such that  $|\beta_o| < \beta_p$ . As a result, eq. (25) is not satisfied, and the arguments presented in this section would indicate that no shape transition should occur. However, a more detailed calculation including the  $\gamma$  degree of freedom in both the deformation energy and the moment of inertia will have to be performed before this possibility is completely ruled out.

The purpose of the present chapter has been to show that secondary minima in the nuclear deformation energy can lead to the backbending behaviour characteristic of many of the rare-earth nuclei. However, Varshni and Bose (1972, 1973)

have attempted to solve the inverse problem of extracting the deformation energy from the experimental energy levels by using a generalized variable moment of inertia model. Some of the difficulties and ambiguities of this approach have been discussed recently by Ross and Nogami (1973), and it is concluded that this approach cannot be used to reliably obtain information on the deformation energy.

APPENDIX A  
ELECTROMAGNETIC RADIATION IN A SMALL  
CUBIC CAVITY

As a further application of the partition function method of Chapter II, it will be used here to obtain corrections to Planck's radiation law for electromagnetic radiation confined to a small cubic cavity. Several discussions of this problem already exist in the literature (Case and Chiu 1970, Balian and Bloch 1971, Baltes and Kneubuhl 1971) and none of the results presented here are new. However, the corrections arise due to the effects of the finite size of the cavity on the density of photon states, and as the work of Chapter II indicates, the partition function method is particularly suited to this kind of problem. In addition, the application of this approach to a problem for which the solution is already known serves as a useful check on its accuracy and reliability.

Consider a gas of photons in thermal equilibrium within a cavity maintained at temperature  $T$ . If  $s$  denotes a photon state of energy

$$\epsilon_s = \hbar\omega_s \quad (1)$$

then the number of photons in state  $s$  is given by the Bose-Einstein distribution (Reif 1965, p.373)

$$n(\omega_s) = \frac{1}{\exp(\beta\hbar\omega_s) - 1} \quad (2)$$

where  $\beta = 1/kT$ . The total energy of the photons in state  $s$  is given by  $h\omega_s n(\omega_s)$ , and thus the energy of all the photons with frequency between  $\omega$  and  $\omega+d\omega$  is

$$u(\omega) d\omega = \frac{h\omega}{\exp(\beta h\omega) - 1} D(\omega) d\omega \quad (3)$$

where  $D(\omega)$  is the density of photon states. For a very large cavity of volume  $V$ ,  $D(\omega)$  is given by<sup>2</sup> (Reif 1965, p.375)

$$D(\omega) = \frac{V}{\pi^2 c^3} \omega^2 \quad (4)$$

and when eq. (4) is substituted in eq. (3), the well-known expression of Planck's radiation law is obtained. However, for a cavity of finite size  $D(\omega)$  will deviate from the result given by eq. (4), and the purpose of this appendix is to calculate the corrections to  $D(\omega)$  for a cubic cavity of length  $L$ .

In order to apply the partition function method to the calculation of  $D(\omega)$ , the photon energies  $\epsilon_s$  must be known for the cubic box. These are conveniently obtained by first placing one corner of the box at the origin of a Cartesian coordinate system such that the (positive)  $x$ ,  $y$  and  $z$  axes lie along the edges of the box. The electromagnetic field in the cavity can then be analysed in terms of the linearly independent transverse electric (TE) and transverse magnetic (TM) fields (Elliott 1966, p.300). If the quantum numbers  $l$ ,  $m$  and  $n$  refer

respectively to the x, y and z axes, then for both the TE and TM modes the eigen-energies are given by (Argence and Kahan 1967, p.363)

$$\epsilon_{lmn} = \kappa [l^2 + m^2 + n^2]^{1/2}, \quad (5)$$

where  $\kappa = \hbar\pi c/L$ . However, the following restrictions must be imposed on the integers  $l$ ,  $m$  and  $n$ :

- a) Neither  $l$ ,  $m$  nor  $n$  can be negative.
- b) If all of  $l$ ,  $m$  and  $n$  are positive, both TE and TM modes can exist in the cavity.
- c) For the TE mode to exist,  $n$  must be nonzero, but either  $l$  or  $m$  may be zero.
- d) For the TM mode to exist,  $l$  and  $m$  must be non-zero, but  $n$  may be zero.

With  $l$ ,  $m$  and  $n$  subject to these restrictions, the exact single-particle partition function is given by

$$Z(\beta) = 2 \sum_{l,m,n=1}^{\infty} \exp[-\beta\kappa(l^2+m^2+n^2)^{1/2}] + 3 \sum_{l,m=1}^{\infty} \exp[-\beta\kappa(l^2+m^2)^{1/2}]. \quad (6)$$

The small  $\beta$  expansion of  $Z(\beta)$  may be obtained by evaluating the sums in eq. (6) using the Euler-Maclaurin summation formula, with the result that

$$Z_{sc}(\beta) = \frac{2\pi}{(\beta\kappa)^{3/2}} - \frac{3}{2} \frac{1}{(\beta\kappa)} + \frac{1}{2} + \dots \quad (7)$$

The corresponding density of states  $g_{sc}(\epsilon)$  is given by the Laplace inverse of  $\beta Z_{sc}(\beta)$  so that

$$g_{sc}(\epsilon) = \left[ \pi \left( \frac{\epsilon}{\kappa} \right)^2 - \frac{3}{2} \right] \frac{\theta(\epsilon)}{\kappa} + \frac{\delta(\epsilon)}{2} + \dots \quad (8)$$

Once  $g_{sc}(\epsilon)$  is known,  $D(\omega)$  may easily be obtained, since

$$g_{sc}(\epsilon) d\epsilon = g_{sc}(\hbar\omega) \hbar d\omega = D(\omega) d\omega,$$

and so

$$D(\omega) = \left[ \pi \left( \frac{\hbar}{\kappa} \right)^3 \omega^2 - \frac{3}{2} \left( \frac{\hbar}{\kappa} \right) \right] \theta(\omega) + \frac{\delta(\omega)}{2} + \dots \quad (9)$$

Substituting in eq. (3) gives the energy density  $u(\omega)$  to be

$$u(\omega) = \frac{\hbar\omega}{(\exp(\beta\hbar\omega) - 1)} \left[ \frac{1}{\pi} \left( \frac{L}{c} \right)^3 \omega^2 - \frac{3}{2\pi} \left( \frac{L}{c} \right) + \frac{\delta(\omega)}{2} + \dots \right], \quad (10)$$

where the first term is the result discussed earlier for a very large enclosure, while the additional terms are corrections for a cavity of finite size.

The total energy content of the cavity is given by

$$U(T) = \int_0^{\infty} u(\omega) d\omega, \quad (11)$$

and the integral may easily be evaluated to give

$$U(T) = \frac{\pi^2}{15} \left(\frac{L}{hc}\right)^3 (kT)^4 - \frac{\pi(L)}{4(hc)} (kT)^2 + \frac{kT}{2} + \dots \quad (12)$$

The first term in eq. (12) is the usual expression of the Stefan-Boltzmann law (Reif 1965, p.376) while the additional terms are corrections for a cavity of finite size. The correction terms in eq. (12) are in agreement with those obtained by Case and Chiu (1970) using a different approach, and this lends further support to the partition function method.



APPENDIX B  
CONTINUUM CONTRIBUTIONS IN THE STRUTINSKY PROCEDURE

According to eq. (III.7) the contribution of the continuum resonances to the smooth density of states is given by

$$\bar{g}_c(\epsilon) = \frac{1}{\gamma\pi^{3/2}} \sum_j \Sigma(2j+1) \times \sum_{\ell=j-1/2}^{\ell=j+1/2} \int_0^{\infty} \frac{d\delta_{\ell,j}(\epsilon')}{d\epsilon'} L_k^{1/2}(u'^2) e^{-u'^2} du' \quad (1)$$

where  $u' = (\epsilon - \epsilon')/\gamma$ . In order to avoid having to take the derivative of the phase shifts, it is desirable to first integrate eq. (1) by parts. For a given  $\ell$  and  $j$ , the integral becomes

$$-L_k^{1/2}(\epsilon^2/\gamma^2) \exp(-\epsilon^2/\gamma^2) \delta_{\ell,j}(0) - \int_0^{\infty} \frac{d}{d\epsilon'} \left[ L_k^{1/2}(u'^2) e^{-u'^2} \right] \delta_{\ell,j}(\epsilon') d\epsilon' \quad (2)$$

where

$$\frac{d}{d\epsilon'} \left[ L_k^{1/2}(u'^2) e^{-u'^2} \right] = -\frac{2u'}{\gamma} \frac{d}{du'^2} \left[ L_k^{1/2}(u'^2) e^{-u'^2} \right] \quad (3)$$

Using the result (Abramowitz and Stegun 1965, p.783)

$$\frac{d}{dx} L_k^{1/2}(x) = \frac{1}{x} \left[ k L_k^{1/2}(x) - (k+1/2) L_{k-1}^{1/2}(x) \right], \quad (4)$$

eq. (3) may be further expanded to give

$$- \frac{2}{\gamma} e^{-u'^2} \left[ (k/u' - u') L_k^{1/2}(u'^2) - (k+1/2) L_{k-1}^{1/2}(u'^2)/u' \right]. \quad (5)$$

Eqs. (1), (2) and (5) may be combined to give

$$\begin{aligned} \bar{g}_c(\epsilon) = & \frac{1}{\gamma \pi^{3/2}} \left[ -L_k^{1/2}(\epsilon^2/\gamma^2) \exp(-\epsilon^2/\gamma^2) G(0) \right. \\ & + \frac{2}{\gamma} \int_0^\infty e^{-u'^2} \left\{ (k/u' - u') L_k^{1/2}(u'^2) - \right. \\ & \left. \left. (k+1/2) L_{k-1}^{1/2}(u'^2)/u' \right\} G(\epsilon') d\epsilon' \right], \quad (6) \end{aligned}$$

where

$$G(\epsilon') = \sum_j^{j+1/2} \sum_{l=j-1/2} \delta_{l,j}(\epsilon'). \quad (7)$$

In performing the integral in eq. (6) special care must be taken in the neighbourhood of the resonances where  $G(\epsilon')$  is changing rapidly, but otherwise the integral gives no special difficulties. It should be noted that since  $\bar{g}_c(c)$  is only required for  $c < 0$ , there is no problem with singularities in the integrand for  $u'=0$ .

## APPENDIX C

### THE NILSSON MODEL POTENTIAL

The Nilsson model Hamiltonian used in Chapter IV has been taken from Gustafsson et al. (1967) and is given by

$$H = -\frac{\hbar^2}{2m} \nabla^2 + \frac{1}{2} m \omega^2(\epsilon) \left[ x^2 \left(1 + \frac{\epsilon}{3}\right)^2 + y^2 \left(1 + \frac{\epsilon}{3}\right)^2 + z^2 \left(1 - \frac{2}{3} \epsilon\right)^2 \right] - \hbar \omega_0 \kappa \left[ 2 \underline{l} \cdot \underline{s} + \mu (\underline{l}^2 - N(N+3)) / 2 \right] \quad (1)$$

where  $\epsilon$  specifies the quadrupole deformation,  $N$  is the principal quantum number given by

$$N = 2n + l \quad (2)$$

and  $\kappa$ ,  $\mu$  and  $\omega_0$  are adjustable parameters. The volume enclosed by equipotential surfaces is required to be constant in order to guarantee the approximate incompressibility of nuclear matter, and this gives

$$\omega(\epsilon) = \omega_0 \left[ 1 - \frac{1}{3} \epsilon - \frac{2}{27} \epsilon^2 \right]^{-1/3} \quad (3)$$

Apart from a slight modification of the  $\underline{l}^2$  term, this Hamiltonian is identical in form to that originally proposed

by Nilsson (1955) and it has been extensively used, particularly in calculating the deformation energy of heavy and superheavy elements (Nilsson et al. 1969).

Various sets of parameters have been proposed for use in eq. (1), but the one chosen here is from Seeger (1967). It has the advantage that  $\kappa$  and  $\mu$  are allowed to vary from one major oscillator shell to another, and no readjustment of parameters from one region of  $A$  to another is required. According to Seeger, a reasonable parameter set is :

neutrons

$$\hbar\omega_0 = 44/A^{1/3},$$

$$\kappa_0 = 0.21,$$

$$\mu_0 = 0.308,$$

protons

$$\hbar\omega_0 = 38/A^{1/3},$$

$$\kappa_0 = 0.18,$$

$$\mu_0 = 0.62, \quad (4)$$

where

$$\mu = \mu_0, \quad (5)$$

and

$$\kappa = \kappa_0 / [(N+1)(N+2)/2]^{1/3}. \quad (6)$$

In Chapter IV the Nilsson model wave functions have been labeled by  $\mu$  and  $\nu$ , and these indices stand for the quantum numbers  $N$ ,  $\Omega$  and  $\alpha$ , where  $\Omega$  is the projection of  $j$  on the axis of symmetry and  $\alpha$  labels the  $(N-\Omega+3/2)$  states allowed for each set of  $N$  and  $\Omega$ . The eigenfunctions and eigenvalues are obtained by first transforming the Hamiltonian

given by eq. (1) to "stretched" coordinates (Nilsson 1955) and expanding the wave functions as

$$|N\Omega\alpha\rangle = \sum_{\ell j} C_{\ell j}(N\Omega\alpha) |n\ell j\Omega\rangle, \quad (7)$$

where  $|n\ell j\Omega\rangle$  specifies the spherical oscillator basis, and the  $C_{\ell j}(N\Omega\alpha)$  are expansion coefficients. The diagonalization of the Hamiltonian in the basis specified by  $|n\ell j\Omega\rangle$  follows closely the method discussed by Nilsson (1955) and the details will not be repeated here.

In the evaluation of  $\langle J^2 \rangle$  and  $\mathcal{G}$  in Chapter IV the time-reversed state of  $|N\Omega\alpha\rangle$  is required, and it is given by

$$T|N\Omega\alpha\rangle = \sum_{\ell j} (-1)^{j+\Omega} C_{\ell j}(N\Omega\alpha) |n\ell j-\Omega\rangle, \quad (8)$$

where  $T$  is the time-reversal operator.

## APPENDIX D

### DETAILS OF THE PAIRING CALCULATION

The Fermi energy  $\lambda$ , and the gap parameter  $\Delta$  for either neutrons or protons are given by the simultaneous solution of (Rowe 1970, p.189)

$$\frac{G}{2} \sum_{\mu > 0} \frac{1}{[(\epsilon_{\mu} - \lambda)^2 + \Delta^2]^{1/2}} = 1 \quad (1)$$

and

$$\sum_{\mu > 0} \left\{ 1 - \frac{(\epsilon_{\mu} - \lambda)}{[(\epsilon_{\mu} - \lambda)^2 + \Delta^2]^{1/2}} \right\} = N_p \quad (2)$$

where  $G$  is the strength of the pairing interaction. The sums over single-particle levels include only a limited number of levels near the Fermi energy, and  $N_p$  is the number of particles which occupy these levels. The value of  $G$ , and the number of levels to be summed over are closely related, and Nilsson et al. (1969) have obtained these quantities by fitting the experimentally determined gap parameters of the rare-earth nuclei. The pairing strength is allowed to be different for neutrons and protons, and is given by

$$G = \frac{1}{\lambda} \left[ g_0 \pm g_1 \frac{(N-Z)}{\lambda} \right] \quad (3)$$

where the plus sign is for protons, the minus sign for neutrons, and  $g_0 = 19.2$  and  $g_1 = 7.4$ . With  $G$  as given by eq. (3),  $\sqrt{15N}$  (or  $\sqrt{15Z}$ ) levels above and below the last filled level should be included in the pairing calculation. Once this number of levels is specified,  $N_p$  can be determined, and eqs. (1) and (2) solved for  $\lambda$  and  $\Delta$ .

The pairing equations have been solved by defining

$$S(\lambda, \Delta) = \left[ 1 - \frac{G}{2} \sum_{\mu > 0} \frac{1}{[(\epsilon_{\mu} - \lambda)^2 + \Delta^2]^{1/2}} \right]^2 + \frac{1}{N_p^2} \left[ N_p - \sum_{\mu > 0} \left\{ 1 - \frac{\epsilon_{\mu} - \lambda}{[(\epsilon_{\mu} - \lambda)^2 + \Delta^2]^{1/2}} \right\} \right]^2, \quad (4)$$

and minimizing  $S(\lambda, \Delta)$  with respect to  $\lambda$  and  $\Delta$ .

## REFERENCES

- Abramowitz, M. and Stegun, I.A. 1965, Handbook of Mathematical Functions (Dover, New York)
- Argence, E. and Kahan, T. 1967, Theory of Waveguides and Cavity Resonators (Blackie and Son, London)
- Balian, R. and Bloch, C. 1970, Ann. Phys. (New York) 60, 401
- Balian, R. and Bloch, C. 1971, Ann. Phys. (New York) 64, 271
- Baltes, H.P. and Kneubuhl, F.K. 1971, Optics Communications 4, 9
- Baranger, M. 1961, Phys. Rev. 122, 992
- Bassichis, W.H., Tsang, C.F., Tuerpe, D.R. and Willets, L. 1973, Phys. Rev. Lett. 30, 294
- Bengtsson, R. 1972, Nucl. Phys. A198, 591
- Bes, D.R., Landowne, S. and Mariscotti, M.A.J. 1968, Phys. Rev. 166, 1045
- Beth, E. and Uhlenbeck, G.E. 1937, Physica 4, 915
- Bethe, H.A. and Bacher, R.F. 1936, Rev. Mod. Phys. 8, 82
- Bethe, H.A. 1971, Ann. Rev. Nucl. Sci. 21, 93
- Bethoux, R. and Lindblad, Th. 1972, Research Institute for Physics, Stockholm, Annual Report, p.19
- Bhaduri, R.K. and Ross, C.K. 1971, Phys. Rev. Lett. 27, 606
- Bjornholm, S. and Strutinsky, V.M. 1969, Nucl. Phys. A136,



- Blatt, J.M. 1967, J. Comp. Phys. 1, 382
- Blomqvist, J. and Wahlborn, S. 1960, Ark. Fys. 16, 545
- Bohr, A. 1952, Kgl. Dan. Selsk., Mat. Fys. Medd. 26, No. 14
- Bohr, N. and Wheeler, J. 1939, Phys. Rev. 56, 426
- Bolsterli, M., Fiset, E.O., Nix, J.R. and Norton, J.L. 1972,  
Phys. Rev. C5, 1050
- Brack, M., Damgaard, J., Jensen, A.S., Pauli, H.C., Strutinsky,  
V.M. and Wong, C.Y. 1972, Rev. Mod. Phys. 44, 320
- Bunatian, G.G., Kolomiets, V.M. and Strutinsky, V.M. 1972,  
Nucl. Phys. A188, 225
- Case, K.M. and Chiu, S.C. 1970, Physics Rev. A1, 1170
- Clark, D.D. 1971, Physics Today 24, No. 12, 23
- Damgaard, J. and Faessler, A. 1973, Phys. Lett. 43B, 157
- Davidson, W.F., Lieder, R.M., Beuscher, G. and Mayer-Boricke,  
C. 1972, Physica Scripta 6, 251
- Elliott, R.S. 1966, Electromagnetics (McGraw-Hill, New York)
- Faessler, A., Lin, L. and Wittmann, F. 1973, Phys. Lett. 44B,  
127
- Fiset, E.O. and Nix, J.R. 1972, Nucl. Phys. A193, 647
- Fowler, R.H. 1936, Statistical Mechanics (University Press,  
Cambridge)
- Goetze, K., Faessler, A. and Wolter, H.H. 1972, Nucl. Phys.  
A183, 352
- Goetze, K., Muther, H. and Faessler, A. 1973, Nucl. Phys. A201,  
49
- Gots, U., Pauli, H.C., Alder, K. and Junker K. 1972, Nucl.  
Phys. A192, 1

- Gunye, M.R. and Khadkikar, S.B. 1970, Phys. Rev. Lett. 24,  
910
- Gustafson, C., Lamm, I.L., Nilsson, B. and Nilsson, S.G.  
1967, Ark. Fys. 36, 613.
- Hill, D. L. and Wheeler, J.A. 1953, Phys. Rev. 89, 1102
- Huangy K. 1963, Statistical Mechanics (John Wiley and Sons,  
New York)
- Inglis, D.R. 1954, Phys. Rev. 96, 1059
- Jennings, B.K. 1973, Nucl. Phys. A207, 538
- Johnson, A., Ryde, H. and Hjorth, S.A. 1972, Nucl. Phys. A179,  
753
- Johnson, A. and Szymanski, Z. 1973, Physics Reports 7C, 182
- Kelson, I. and Shoshani, Y. 1972, Phys. Lett. 40B, 58
- Khoo, T., Bernthal, F.M., Boyno, J.S. and Warner, R.A. 1973,  
Bull. Am. Phys. Soc. 18, 630 and private communication
- Krumlinde, J. 1968, Nucl. Phys. A121, 306
- Krumlinde, J. 1971, Nucl. Phys. A160, 471
- Krumlinde, J. and Szymanski, Z. 1971, Phys. Lett. 36B, 157
- Kumar, K. 1972, Physica Scripta 6, 270
- Kumar, K. and Baranger, M. 1967, Nucl. Phys. A92, 608
- Kumar, K. and Baranger, M. 1968, Nucl. Phys. A110, 529
- Lin, W.F. 1970, Phys. Rev. C2, 871
- Mariscotti, M.A.J., Scharff-Goldhaber, G. and Buck, B. 1969,  
Phys. Rev. 178, 1864
- Messiah, A. 1965, Quantum Mechanics (North-Holland, Amsterdam)
- Moller, P. 1970, Nucl. Phys. A142, 1

- Mottelson, B.R. and Nilsson, S.G. 1959, Mat. Fys. Skr. Dan. Vid. Selsk 1, No. 8
- Mottelson, B.R. and Valatin, J.G. 1960, Phys. Rev. Lett. 5, 511
- Myers, W.D. and Swiatecki, W.J. 1966, Nucl. Phys. 81, 1
- Myers, W.D. and Swiatecki, W.J. 1967, Ark. Fys. 36, 343
- Nathan, O. and Nilsson, S.G. 1965, Alpha-, Beta- and Gamma-Ray Spectroscopy, ed. K. Siegbahn (North-Holland Pub. Co., Amsterdam), Vol. I, p.601
- Nilsson, S.G. 1955, Mat. Fys. Medd. Dan. Vid. Selsk. 29, No. 16
- Nilsson, S.G., Tsang, C.F., Sobiczewski, A., Szymanski, Z., Wycech, S., Gustafson, C., Lamm, I.L., Moller, P. and Nilsson, B. 1969, Nucl. Phys. A131, 1
- Nix, J.R. 1972, Ann. Rev. Nucl. Sci. 22, 65
- Onishi, N. and Yoshida, S. 1966, Nucl. Phys. 80, 367
- Pauli, H.C. 1971, private communication
- Ramamurthy, V.S. and Kapoor, S.S. 1972, Phys. Lett. 42B, 399
- Reif, F. 1965, Fundamentals of Statistical and Thermal Physics (McGraw-Hill, New York)
- Ripka, G. 1968, Adv. Nucl. Phys. 1, 183
- Ross, C.K. and Bhaduri, R.K. 1972, Nucl. Phys. A188, 566
- Ross, C.K. and Nogami, Y. 1973, Nucl. Phys., in press
- Ross, C.K. and Warke, C.S. 1973, Phys. Rev. Lett. 30, 55
- Rowe, D.J. 1970, Nuclear Collective Motion (Methuen and Co. Ltd. London)
- Roy, R.R. and Nigam, B.P. 1967, Nuclear Physics, (John Wiley and Sons, New York)

- Satpathy, L., Goss, D. and Banerjee, M.K. 1969, Phys. Rev. 183, 887
- Seeger, P.A. 1967, Proc. Int. Conf. Atomic Masses, ed. R.C. Barber (Univ. of Manitoba Press), p.85
- Sheline, R.K., Ragnarsson, I. and Nilsson, S.G. 1972, Phys. Lett. 41B, 115
- Sobiczewski, A., Bjornholm, S. and Pomorski, K. 1973, Nucl. Phys. A202, 274
- Sobizewski, A., Krogulski, T., Blocki, J. and Szymanski, Z. 1971, Nucl. Phys. A168, 519
- Sorensen, R.A. 1971, Proc. Orsay Colloquium on Intermediate Nuclei (Orsay), p.70
- Stephens, F.S., Lark, N. and Diamond, R.M. 1964, Phys. Lett. 12, 225
- Stephens, F.S. and Simon, R.S. 1972, Nucl. Phys. A183, 257
- Strutinsky, V.M. 1967, Nucl. Phys. A95, 420
- Strutinsky, V.M. 1968, Nucl. Phys. A122, 1
- Strutinsky, V.M. 1972, private communication
- Trainor, L.E.H. and Gupta, R.K. 1971, Can. J. Phys. 49, 193
- Valatin, J.G. 1961, Phys. Rev. 122, 1012
- Vallieres, M., Klein, A. and Dreizler, R.M. 1972, Phys. Lett. 41B, 125
- van der Pol, B. and Bremner, H. 1955, Operational Calculus (University Press, Cambridge)
- von Weizsacker, C.F. 1935, Z. Phys. 96, 431
- Varshni, Y.P. and Bose, S. 1972, Phys. Rev. C6, 1770

Varshni, Y.P. and Bose, S. 1973, Bull. Am. Phys. Soc. 18,

646

Ward, D., Graham, R.L., Geiger, J.S. and Andrews, H.R. 1973a,

Phys. Lett. 44B, 39

Ward, D., Andrews, H.R., Geiger, J.S., Graham, R.L. and

Sharpey-Schaefer, J.F., 1973b, Phys. Rev. Lett. 30,

493

Warner, R.A. and Bernthal, F.M. 1972, Michigan State University

Cyclotron Laboratory Annual Report, p.68